Zinc Bromide: A General Mediator for the Ionothermal Synthesis of Microporous Polymers via Cyclotrimerization Reactions

Jaehwan Kim,[a,‡] Minh H. Le,[a,‡] Makayla C. Spicer,[a] Casandra M. Moisanu,[a] Suzi M. Pugh,[b] Phillip J. Milner[a,*]

[a]Department of Chemistry and Chemical Biology, Cornell University, Ithaca, NY, 14853, United States
[b]Yusuf Hamied Department of Chemistry, University of Cambridge, Cambridge, CB2 1EW, United Kingdom

*pjm347@cornell.edu
‡These authors contributed equally.

Supporting Information

Table of Contents

1. General procedures.

The reagents 1,4-diacetylbenzene (**DAB**, 97%, Alfa Aesar), 1,3,5-triacetylbenzene (**TAB**, 96%, Tokyo Chemical), 4,4′-diacetylbiphenyl (**DABP**, 98%, Alfa Aesar), 2,7-diacetylfluorene (**DAF**, >98%, Oakwood), 1,4-dicyanobenzene (**DCNB**, 98%, Fluka Chemical), 4-methylacetophenone (97%, Lancaster Synthesis), acetyl chloride (98%, Aldrich), aniline (99%, Fluka Chemical), aqueous hypophosphorous acid (H_3PO_2, 50 w/w%, Alfa Aesar), isoamyl nitrite (96%, Aldrich), hydrochloric acid (37%, Aldrich), pivalic acid (99%, TCI), sodium bicarbonate ($NaHCO_3$, 99%, Fluka), anhydrous sodium sulfate (Na_2SO_4, 99%, Aesar), triflic acid (TfOH, 98%, Aldrich), triphenylphosphine (PPh_3, 99.0%, Aldrich), triphenylphosphine oxide (PPh_3O, 98%, Aldrich), anhydrous aluminum bromide ($AlBr_3$, 99%, Aldrich), anhydrous aluminum chloride ($AlCl_3$, 99%, Acros), aluminum nitrate ($Al(NO_3)_3$, 98%, Aldrich), aluminum triflate ($Al(SO_3CF_3)_3$, 99%, Lancaster Synthesis), antimony (V) chloride ($SbCl_5$, 99%, Aldrich), anhydrous bismuth chloride ($BiCl_3$, 97%, TCI), iron(III) bromide ($FeBr_3$, 95%, Aldrich), iron(III) chloride ($FeCl_3$ 98%, Alfa Aesar), potassium chloride (KCl, 99%, VWR), silicon chloride ($SiCl_4$, 99%, Alfa Aesar), sodium chloride (NaCl, 99.5%, Fluka), tin(II) chloride ($SnCl_2$, 98%, Alfa Aesar), titanium(IV) bromide ($TiBr_4$, 98%, Santa Cruz Biotech. Inc.), titanium(IV) chloride ($TiCl_4$, 99.9%, Aldrich), zinc acetate dihydrate ($Zn(OAc)_2•2H_2O$, 99%, J.T. Baker), anhydrous zinc bromide ($ZnBr_2$, 99.9%, Aldrich), anhydrous zinc chloride ($ZnCl_2$, 99.9%, Aldrich), zinc nitrate hexahydrate ($Zn(NO_3)_2•6H_2O$, 99%, Lancaster), zinc triflate ($Zn(SO_3CF_3)_2$, 99%, Fluka), acetic acid (AcOH, 99.7%, Fisher Scientific), benzenesulfonic acid ($PhSO_3H$, 98.0%, Fluka), bistosylimide ($(MePhSO_2)_2NH$, 98%, TCI), dibenzenesulfonimide ($(PhSO_2)_2NH$, 95%, Fisher Scientific), diphenyl phosphate ($(PhO)_2P(O)OH$, 98%, Oakwood), diphenylphosphinic acid ($Ph_2P(O)OH$, 99%, Oakwood), methanesulfonic acid (MsOH, 98%, Alfa-Aesar), pyridinium hydrochloride (Py•HCl, 98%, Aldrich), p-toluenesulfonic acid monohydrate ($TsOH•H_2O$, 98.5%, Aldrich), trifluoroacetic acid (TFA, 99%, Oakwood), trifluoromethanesulfonimide ($(TfO_2)NH$, 95%, Oakwood), dichloromethane (CH_2Cl_2, 99.5%, J.T. Baker), anhydrous diglyme (99%, Aldrich), ethanol (EtOH, 95%, Fisher Scientific), ethyl acetate (EtOAc, 99.5% Fisher Scientific), hexanes (98.5%, Fisher scientific), mesitylene (99%, Fluka), methanol (MeOH, 99.8%, Fisher Scientific), *N*,*N*-dimethylformamide (DMF, 99.8%, Sigma), and toluene (99.5%, Fisher Scientific) were purchased from commercial vendors and used without additional purification unless specified otherwise.

Infrared (IR) spectra were collected on a Bruker Tensor II IR spectrometer with a diamond Attenuated Total Reflectance (ATR) attachment. Raman scattering was taken with a Renishaw Invia confocal Raman microscope at an excitation wavelength of 785 nm. Surface area data were collected on a Micromeritics 3-flex gas sorption analyzer using ultrapure N_2 (99.999%) and a liquid N_2 bath. Brunauer-Emmett-Teller (BET) and Langmuir surface areas were determined by linear least squares regression analysis using the linearized forms of the BET and Langmuir equations, respectively. Powder X-ray diffraction (PXRD) patterns were collected on a Rigaku Ultima IV diffractometer or a Bruker D8 Advance ECO powder diffractometer equipped with a Cu K_α source (λ = 1.5406 Å) and were baseline-corrected using OriginPro. Solution-state NMR

data were collected on a Bruker INOVA 500 MHz spectrometer and are referenced to residual solvent. Magic angle spinning solid-state NMR (MAS SSNMR) measurements at Cornell University were carried out using a Phoenix NMR HX NB Probe (3.2 mm) located within a Varian INOVA 500 MHz spectrometer. MAS SSNMR experiments at Cornell University were carried out using samples packed within 35 μL rotors at a spinning speed of 20 kHz. Solid-state NMR experiments at the University of Cambridge were performed using a Bruker Avance I 400 MHz spectrometer, using a Bruker 3.2 mm HFXY triple resonance probe at a spinning speed of 20 kHz. ^{1}H–^{13}C cross polarization (CP) MAS experiments were performed using a contact pulse of 1 ms duration (ramped for ^{1}H) and a recycle delay of 1 s. Continuous wave (cw) ^{1}H decoupling was applied during acquisition. ^{13}C chemical shifts were referenced to TMS at 0 ppm using adamantane as a secondary reference (left hand peak at 38.5 ppm). Solid-state diffuse reflectance UV-Vis absorption spectra were collected using a Shimadzu UV-2600i UV-Vis Spectrometer equipped with an ISR-2600 Plus Integrating Sphere. Decomposition profiles were collected on a TA Instruments Q500 V6.7 thermogravimetric analyzer using a temperature ramp of 3.00 °C/min from room temperature to 600.00 °C or 900.00 °C under N_2, unless specified otherwise. Scanning electron microscopy images were taken at 5.0–10 kV using a Zeiss Gemini 500 scanning electron microscope. The powder samples were immobilized on carbon tape mounted on an aluminum stub. The samples were blown using compressed air to remove excess material not stuck to the tape and then coated with a carbon layer. Energy dispersive X-ray scattering (EDS) data were collected at 30.0 kV using a Zeiss Gemini 500 scanning electron microscope equipped with an Oxford Instruments Ultima Max 170 detector (detector type X-max) and processed using the AZtec software. X-ray photoelectron spectroscopy (XPS) samples were analyzed using a Scienta Omicron ESCA-2SR with operating pressure ca. 1×10^{-9} Torr. Monochromatic Al K_α X-rays (1486.6 eV) were generated at 250W (15 kV; 20mA) with photoelectrons collected from a 2 mm diameter analysis spot. Photoelectrons were collected at a 0° emission angle with source to analyzer angle of 54.7° A hemispherical analyzer determined electron kinetic energy, using a pass energy of 200 eV for wide/survey scans, and 50 eV for high resolution scans. A flood gun was used for charge neutralization of non-conductive samples. The data was then processed with CasaXPS. Combustion C/H/N elemental analysis and Cl/Br ion chromatography measurements were carried out by Atlantic Microlabs Inc. Owing to their porosity, the samples for combustion analysis likely contain significant amounts of adsorbed water, which limits the accuracy of combustion analysis for determining their elemental composition.

Idealized structural models were constructed using BIOVIA Materials Studio 2020, and individual pores were optimized with density functional theory (DFT) calculations at the ωB97XD level of theory using Gaussian16.[1,2] The standard Def2-SVP basis set was used for geometry optimizations,[3] and the calculated structures were then depicted using Diamond or CYLview20.[4]

2. Synthesis and characterization of monomers.

a. Tetraphenylmethane.

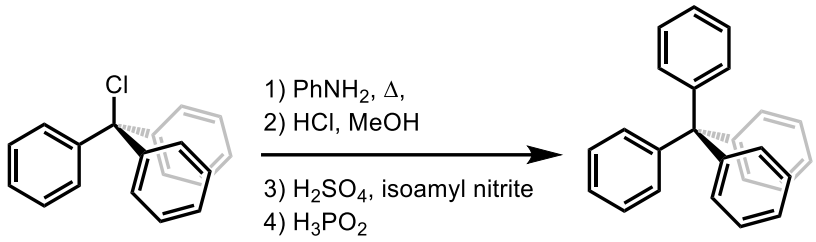

Figure S1. Synthesis of tetraphenylmethane.

Tetraphenylmethane was prepared according to the literature procedure.[5] A mixture of trityl chloride (25 g, 0.089 mol, 1.0 equiv) and aniline (22 mL, 0.23 mol, 2.8 equiv) was stirred for 15 min at 190 °C in a 500 mL round bottom flask. The mixture was cooled to room temperature, at which time 2 M HCl (100 mL) and MeOH (150 mL) were added. The addition of solvents resulted in precipitation of a purple solid from solution. The solid was broken up into smaller pieces using a spatula. The mixture was heated for 30 min at 80 °C and again allowed to cool to room temperature. The heterogeneous mixture was filtered, and the resulting light purple solid was rinsed with water (250 mL) before being dried under reduced pressure (<100 mTorr, 70 °C) for 16 h. The solid was then suspended in DMF (250 mL), and this mixture was cooled to −20 °C using an ice water bath containing NaCl. Concentrated H_2SO_4 (27.5 mL) and isoamyl nitrite (19.9 mL) were added to the reaction mixture slowly. The reaction mixture was then stirred for 1 h at 0 °C. At this time, 30% aqueous H_3PO_2 (75 mL, prepared by diluting 50% H_3PO_2 in water) was added dropwise, causing the solution to bubble. The mixture was heated to 50 °C until gas evolution ceased. The reaction mixture was cooled to room temperature and filtered. The solid was rinsed with DMF (2 × 250 mL), water (2 × 250 mL), and EtOH (2 × 250 mL). The resulting light brown solid was dried under reduced pressure (<100 mTorr, 80 °C) overnight to afford the final product (24.0 g, 83% yield) as a light brown solid. ^{1}H NMR (500 MHz, $CDCl_3$): δ 7.19–7.30 (m, 20H) ppm. ^{13}C NMR (125 MHz, $CDCl_3$): δ 146.8, 131.2, 127.5, 125.9, 65.0 ppm. These spectra are consistent with those reported in the literature.[5]

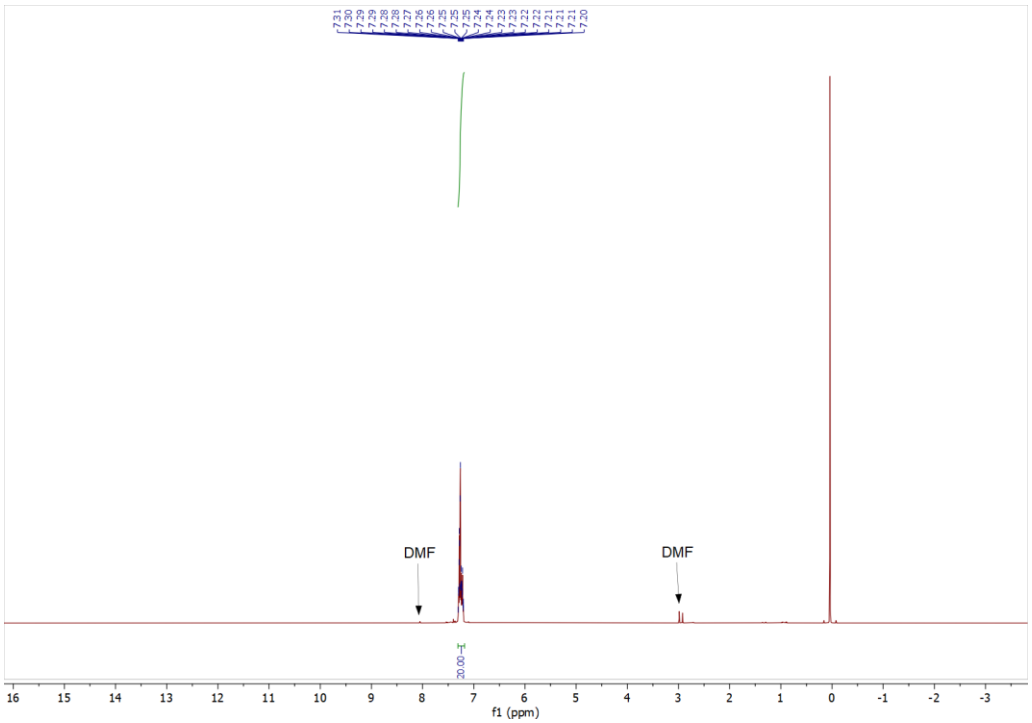

Figure S2. ^{1}H NMR (500 MHz, $CDCl_3$) spectrum of tetraphenylmethane used in this work.

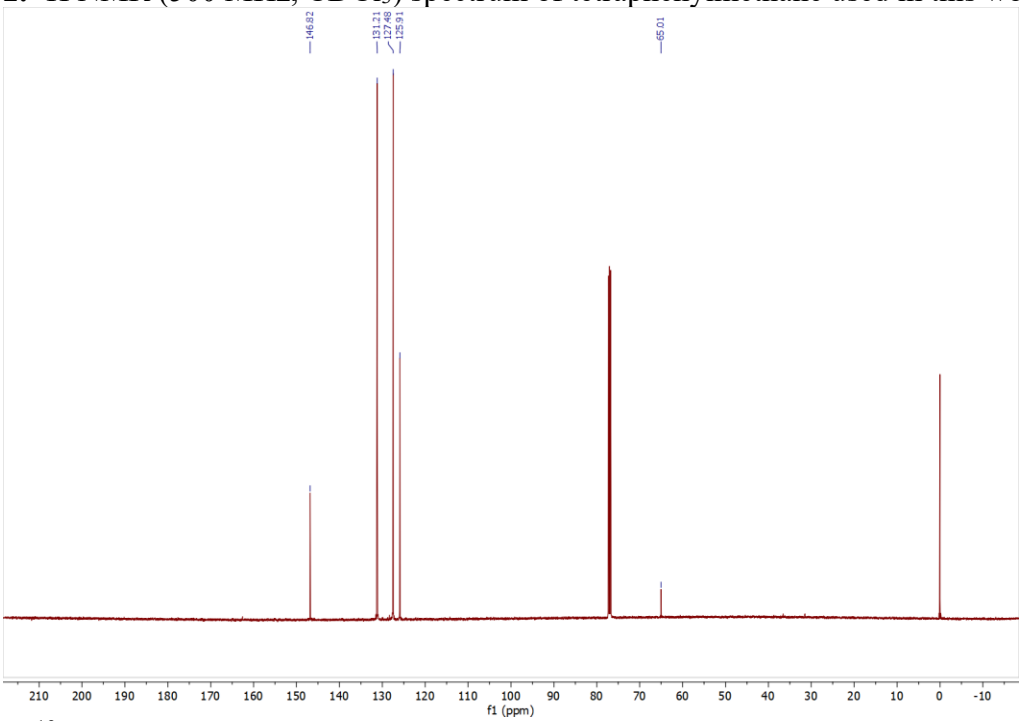

Figure S3. ^{13}C NMR (125 MHz, $CDCl_3$) spectrum of tetraphenylmethane used in this work.

b. Tetrakis(4-acetylphenyl)methane (TAPM).

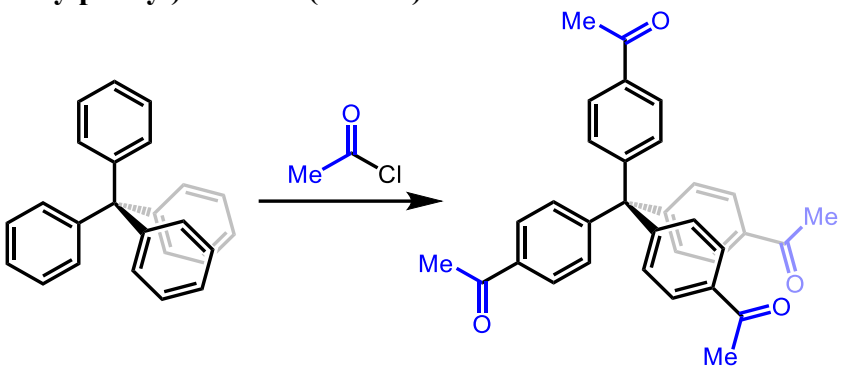

Figure S4. Synthesis of tetrakis(4-acetylphenyl)methane (**TAPM**).

Solid $AlCl_3$ (4.00 g, 18.0 mmol, 10 equiv) was added portion-wise to a stirred solution of tetraphenylmethane (1.00 g, 3.12 mmol, 1.0 equiv) and distilled acetyl chloride (2.23 mL, 31.2 mmol, 10.0 equiv) dissolved in anhydrous CH_2Cl_2 (30 mL) under N_2. The reddish-brown mixture was heated to reflux for 48 h. At this time, the reaction mixture was allowed to cool to room temperature, and then water was added dropwise to the three-neck flask until gas evolution ceased. The aqueous layer was then extracted with CH_2Cl_2 (3 × 10 mL). The combined organic extracts were neutralized with saturated aqueous $NaHCO_3$ (30 mL), washed with brine (30 mL), dried over Na_2SO_4, and filtered. The solvent was removed under reduced pressure and the resulting dark brown oily residue was purified by column chromatography (SiO_2, gradient of 0% → 20% → 25% → 30% → 40% → 50% → 100% ethyl acetate/hexanes) to afford **TAPM** (0.501 g, 33% yield) as a fluffy, pale-yellow solid. ^{1}H NMR (500 MHz, $CDCl_3$): δ 7.89 (d, J = 8.3 Hz, 8H), 7.35 (d, J = 8.6 Hz, 8H), 2.59 (s, 12H) ppm. ^{13}C NMR (125 MHz, $CDCl_3$) δ 197.4, 150.1, 135.5, 130.9, 128.2, 65.6, 26.6 ppm. These spectra are consistent with those reported in the literature.[6]

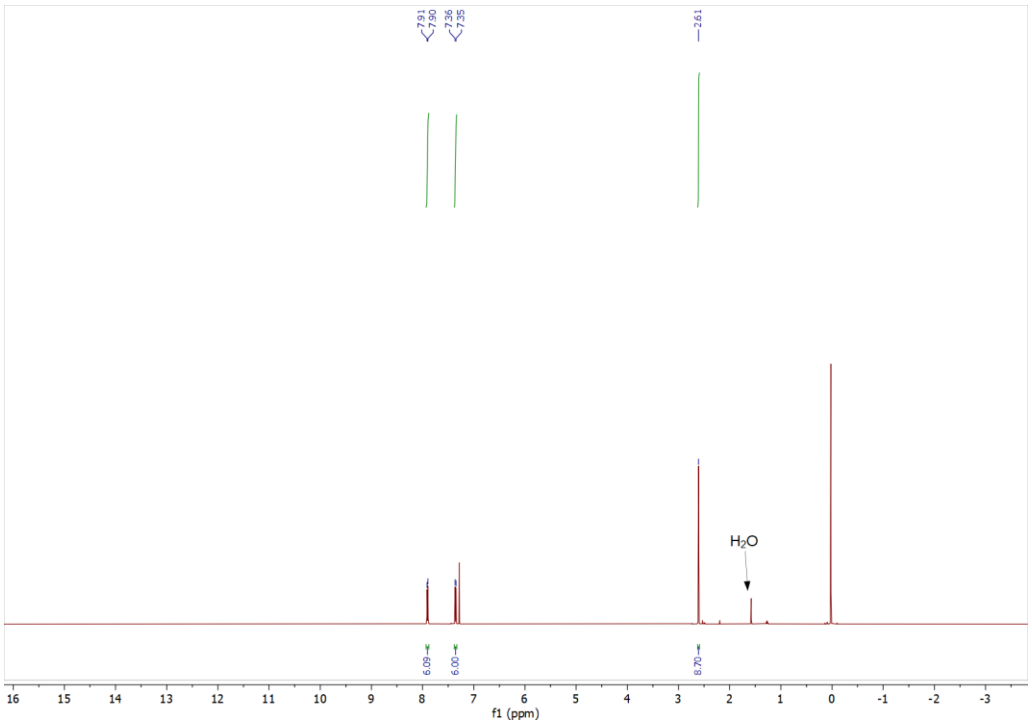

Figure S5. ^{1}H NMR (500 MHz, $CDCl_3$) spectrum of **TAPM** used in this work.

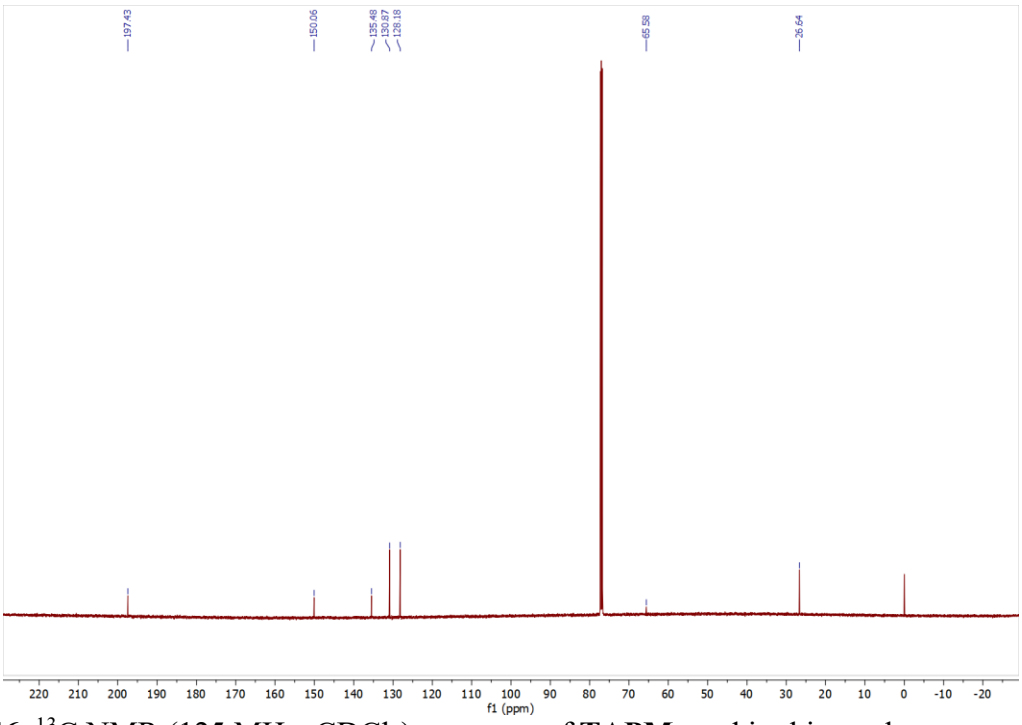

Figure S6. ^{13}C NMR (125 MHz, $CDCl_3$) spectrum of **TAPM** used in this work.

3. General procedure for the synthesis of polymeric materials with $ZnBr_2$.

This procedure was adapted from the literature.[7] Three 10 mm diameter borosilicate glass tubes were each charged with monomer (40.0 mg) and anhydrous zinc bromide (1−10 molar equiv.) in a N_2-filled glovebox. The tubes were evacuated (<100 mTorr) and then flame-sealed under high vacuum using a natural gas torch and a custom-built apparatus (**Figure S7**). The tubes were placed in a furnace and heated at 400 °C for 72 h (temperature sequence: ramp up to 400 °C over 6 h from room temperature, hold at 400 °C for 72 h, cool down to 25 °C over 6 h), unless specified otherwise. The tubes were allowed to cool to room temperature and snapped using a glass tube cutter. The black reaction mixture was scraped out of the tubes with a spatula, using water (10 mL) to help remove the mixture from the tube walls. The reaction mixtures from all three tubes were combined in a 24 mL scintillation vial and suspended in 3 M HCl (20 mL). The suspension was allowed to stir for 24 h. The heterogeneous mixture was filtered, and the resulting shiny black solid was rinsed with water (3 × 5 mL) and then THF (3 × 5 mL). The solid was transferred to a 20 mL scintillation vial filled with THF and allowed to stand for 24 h at room temperature, after which the THF was decanted and replaced with fresh THF. This soaking process was repeated two more times for a total of three THF soaks. After the third THF soak, the THF was decanted from the solid and replaced with acetone. The vial was allowed to stand for 24 h at room temperature, after which the acetone was decanted from the solid and replaced with fresh acetone. This soaking process was repeated two more times for a total of three acetone soaks. The acetone was decanted, and the solid was oven-dried under vacuum at 120 °C overnight prior to characterization.

Figure S7. A custom-built apparatus for flame-sealing tubes shown with three empty 10 mm tubes.

4. Synthesis and characterization of trimerized materials.

a. 1,4-diacetylbenzene trimerization.

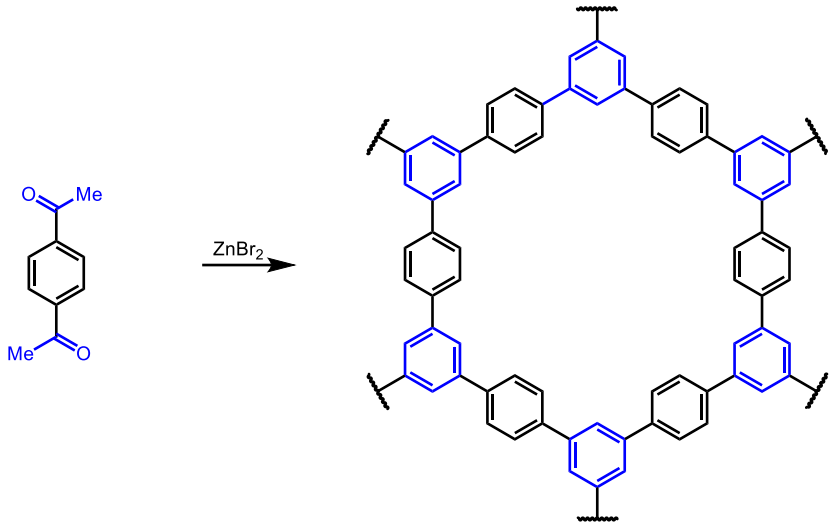

Figure S8. Synthesis of the **DAB-CMP** series from 1,4-diacetylbenzene (**DAB**) using $ZnBr_2$.

Following the general procedure, the **DAB-CMP** series was synthesized using **DAB** (40.0 mg) and varying amounts of $ZnBr_2$ (**Table S1**) to yield shiny black solids. The highest surface area material was made with 5.00 equivalents of $ZnBr_2$ in 72 h. This material was used for further characterization.

Table S1. List of conditions for the synthesis of **DAB-CMP** using $ZnBr_2$. The condition that yielded the highest surface area material is highlighted in yellow.

DAB-CMP	Mass of $ZnBr_2$ per Tube (mg)	Total Mass of $ZnBr_2$ (mg)	Equivalents of $ZnBr_2$ (equiv)	Time (h)	Yield (mg (%))	BET Surface Area (m^2/g)
1.00 equiv, 24 h	55.5	167	1.00	24	95.3 (102)	399 ± 1
1.00 equiv, 72 h	55.5	167	1.00	72	96.1 (103)	584 ± 2
5.00 equiv, 24 h	278	834	5.00	24	87.2 (93)	581 ± 1
5.00 equiv, 72 h	278	834	5.00	72	95.8 (102)	651 ± 2
10.0 equiv, 24 h	555	1670	10.0	24	90.7 (97)	571 ± 1
10.0 equiv, 72 h	555	1670	10.0	72	74.0 (79)	599 ± 1

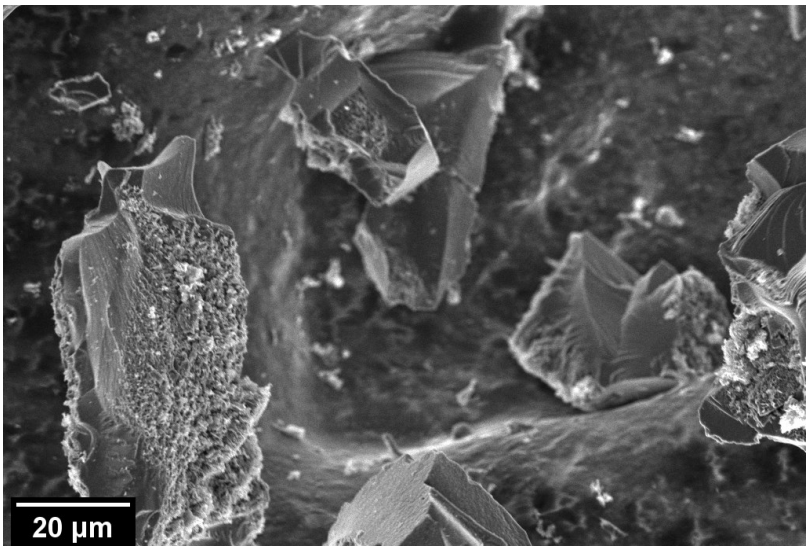

Figure S9. SEM image of **DAB-CMP** synthesized at 400 °C with 5.00 equivalents of $ZnBr_2$ for 72 h.

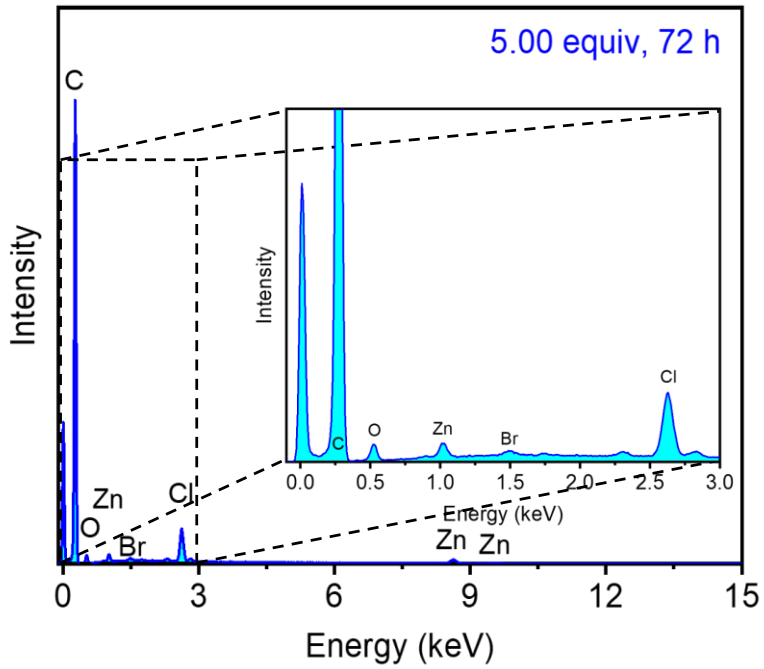

Figure S10. EDS spectrum of **DAB-CMP** synthesized with 5.00 equivalents of $ZnBr_2$ for 72 h. The residual Cl likely arises from the HCl wash used to remove zinc salts.

Table S2. Tabulated EDS data averages for **DAB-CMP** synthesized with 5.00 equivalents of $ZnBr_2$ for 72 h.

Element	Line Type	Wt %	Atomic %	Theoretical Atomic %[1]
C	K series	95.95	98.35	100.00
O	K series	1.03	0.80	0.00
Cl	K series	1.78	0.62	0.00
Zn	K series	1.19	0.22	0.00
Br	K series	0.05	0.01	0.00
Total:		100.00	100.00	100.00

[1]Excludes hydrogen.

Table S3. Tabulated elemental analysis data through combustion and ion chromatography for **DAB-CMP** synthesized with 5.00 equivalents of $ZnBr_2$ for 72 h.

Element	Wt %	Theoretical Wt %
C	87.38	95.21
H	4.15	4.79
Cl	1.55	0.00
N	0.22	0.00
Br	0.00	0.00
O and Zn	6.70[1]	0.00
Total:	100.00	100.00

[1]The remaining mass not attributed to C, H, Cl, and Br was assumed to come from Zn and O, as they were not directly analyzed during combustion analysis.

Table S4. Tabulated XPS data for **DAB-CMP** synthesized with 5.00 equivalents of $ZnBr_2$ for 72 h.

Element	Peak label	Position	Atomic %
C	C 1s	533.13	95.04
O	O 1s	285.13	4.19
Cl	Cl 2p	199.127	0.66
Zn	Zn 2p	1022.73	0.07
Br	Br 3d	69.53	0.04
Total:			100.00

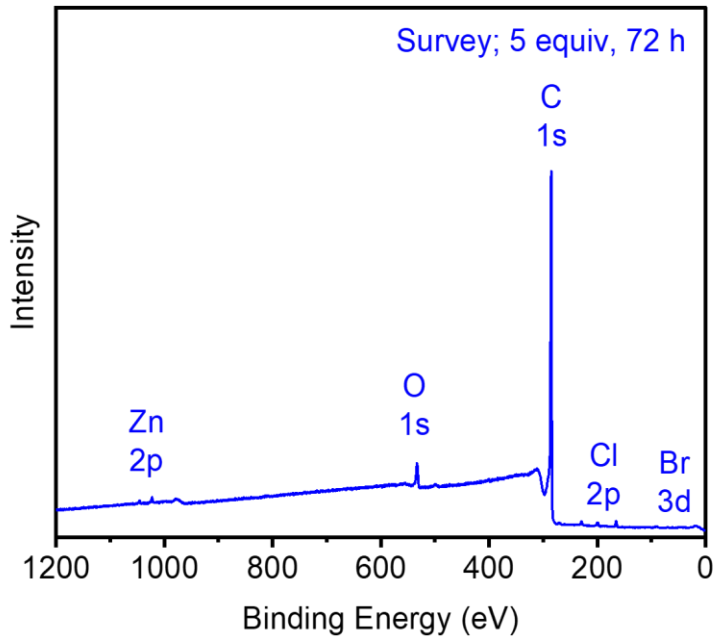

Figure S11. XPS spectrum for **DAB-CMP** synthesized with 5.00 equivalents of $ZnBr_2$ for 72 h. The relevant energies and transitions are labeled at the expected energies.

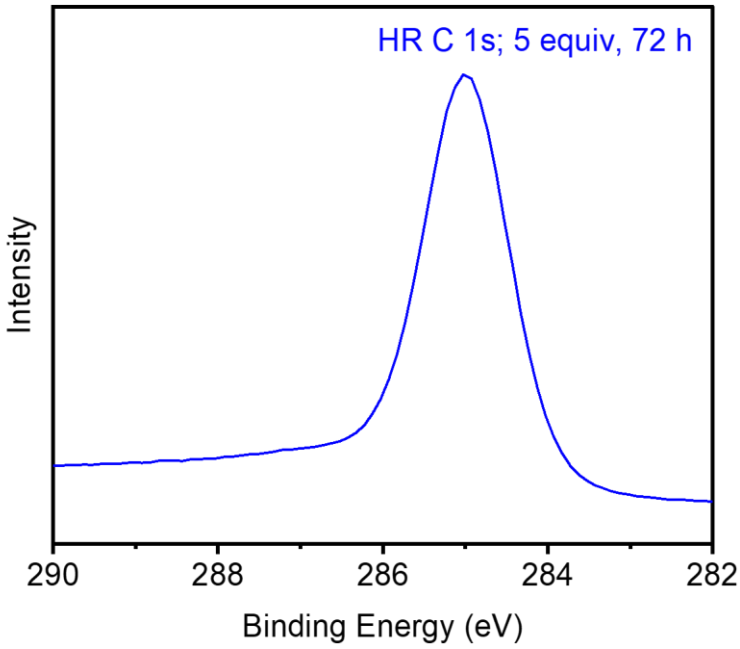

Figure S12. High-resolution (HR) C 1s XPS spectrum of **DAB-CMP** synthesized with 5.00 equivalents of $ZnBr_2$ for 72 h.

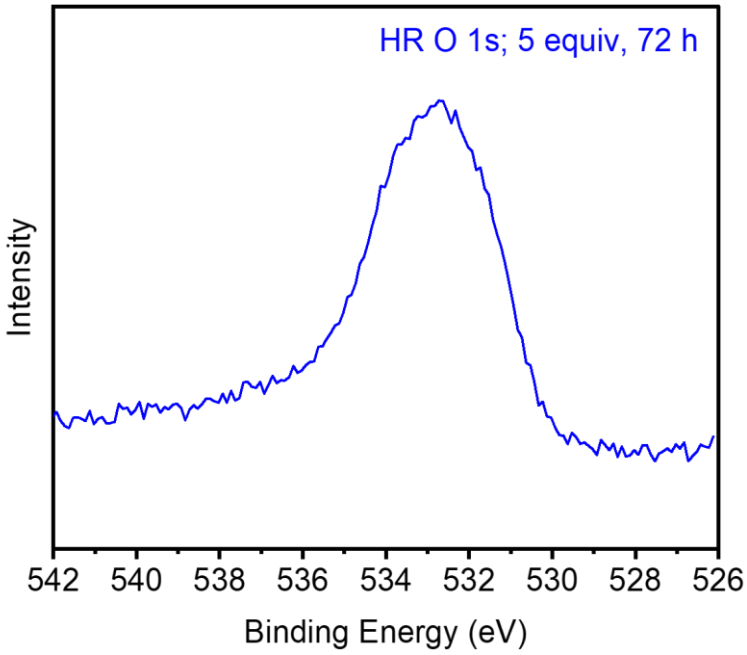

Figure S13. HR O 1s XPS spectrum of **DAB-CMP** synthesized with 5.00 equivalents of $ZnBr_2$ for 72 h.

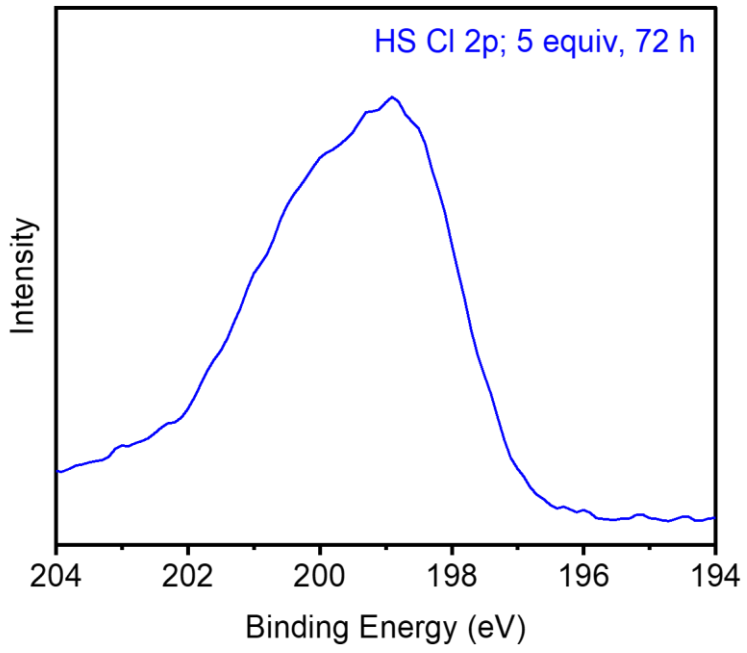

Figure S14. High-sensitivity (HS) Cl 2p XPS spectrum of **DAB-CMP** synthesized with 5.00 equivalents of $ZnBr_2$ for 72 h.

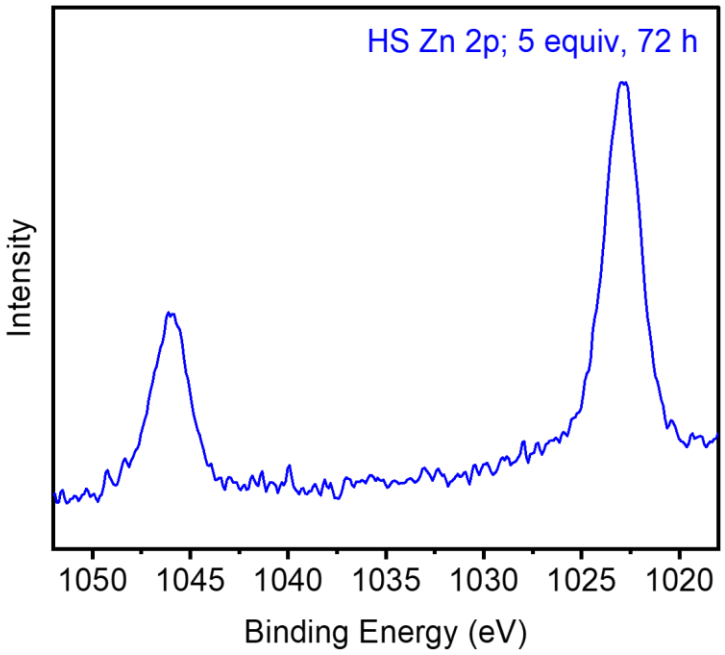

Figure S15. HS Zn 2p XPS spectrum of **DAB-CMP** synthesized with 5.00 equivalents of $ZnBr_2$ for 72 h.

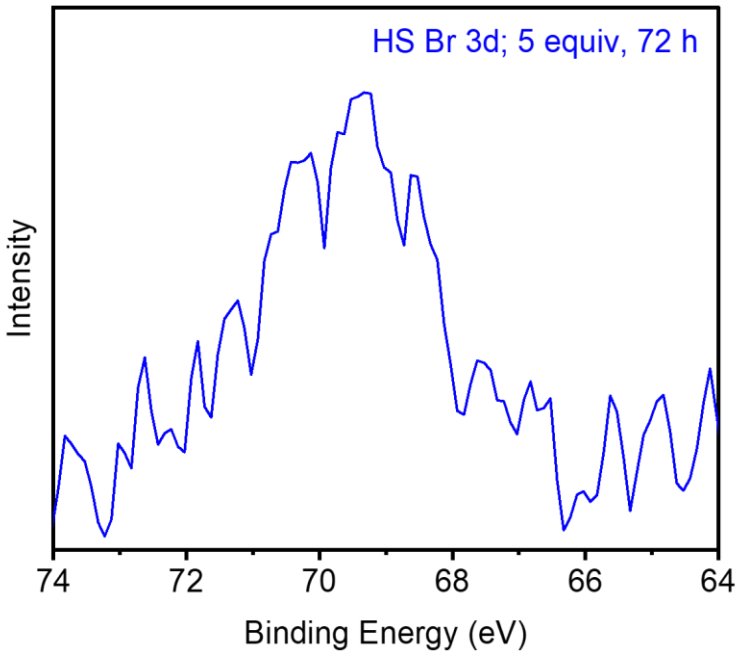

Figure S16. HS Br 3d XPS spectrum of **DAB-CMP** synthesized with 5.00 equivalents of $ZnBr_2$ for 72 h.

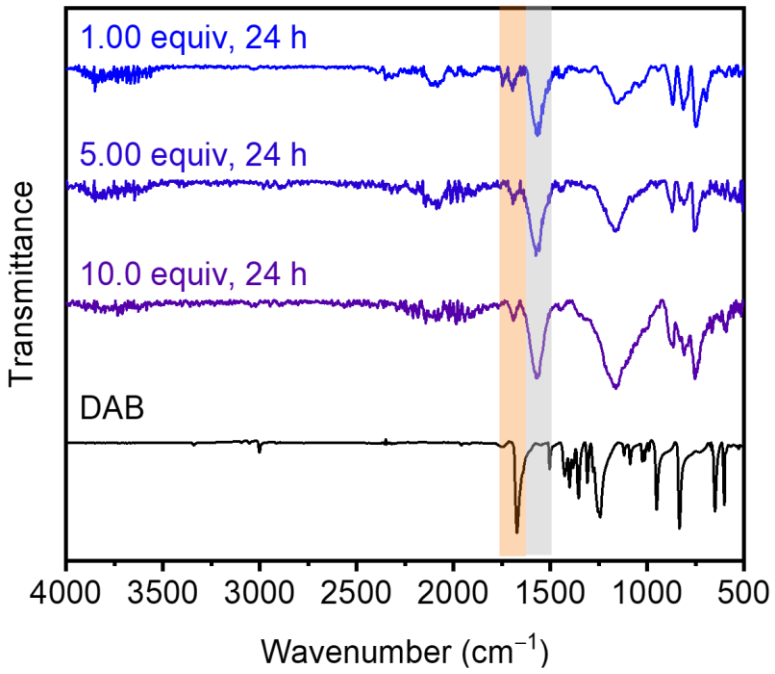

Figure S17. ATR-IR spectra of **DAB** and **DAB-CMP** synthesized with various equivalents of $ZnBr_2$ for 24 h. The indicated peaks correspond to carbonyl C=O (orange) and aromatic C=C (gray) stretches.

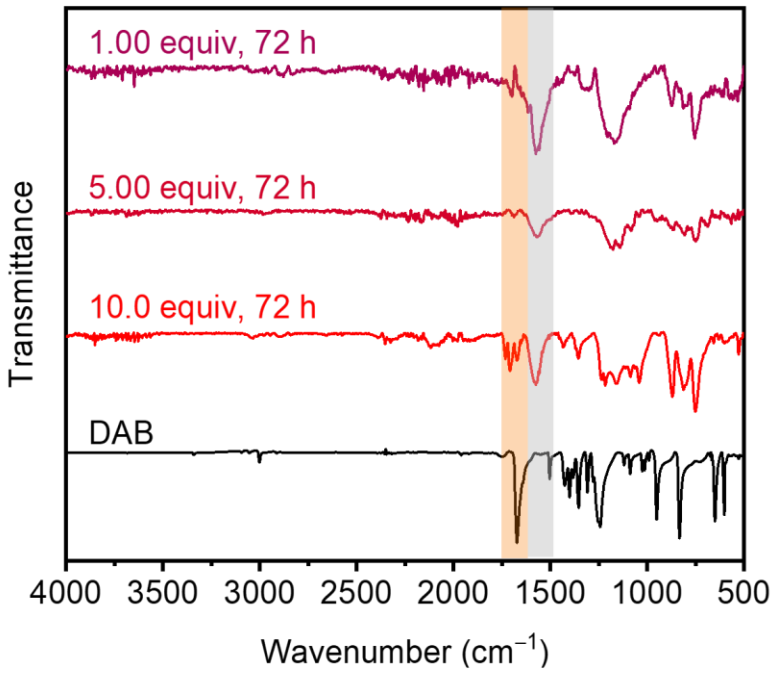

Figure S18. ATR-IR spectra of **DAB** and **DAB-CMP** synthesized with various equivalents of $ZnBr_2$ for 72 h. The indicated peaks correspond to carbonyl C=O (orange) and aromatic C=C (gray) stretches.

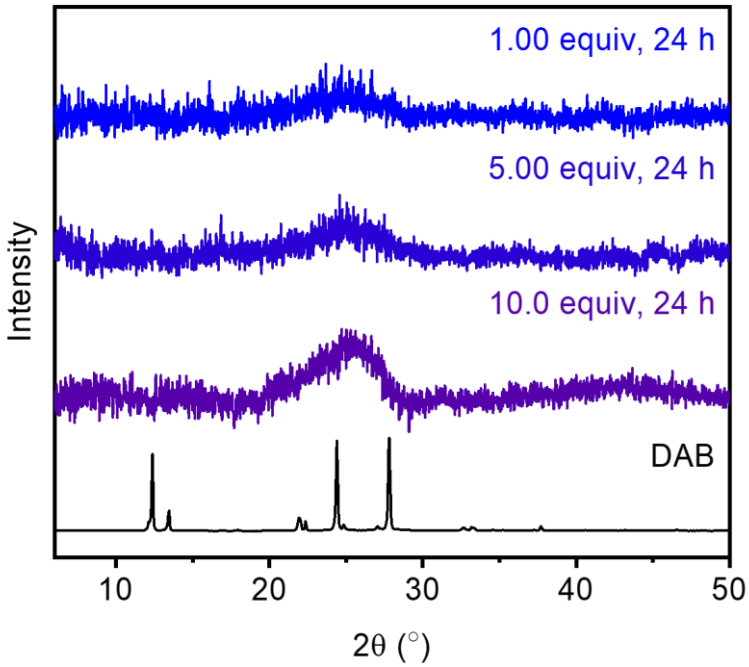

Figure S19. PXRD (λ = 1.5406 Å) patterns of **DAB** and **DAB-CMP** synthesized with various equivalents of $ZnBr_2$ for 24 h, indicating that **DAB-CMP** is an amorphous polymeric material.

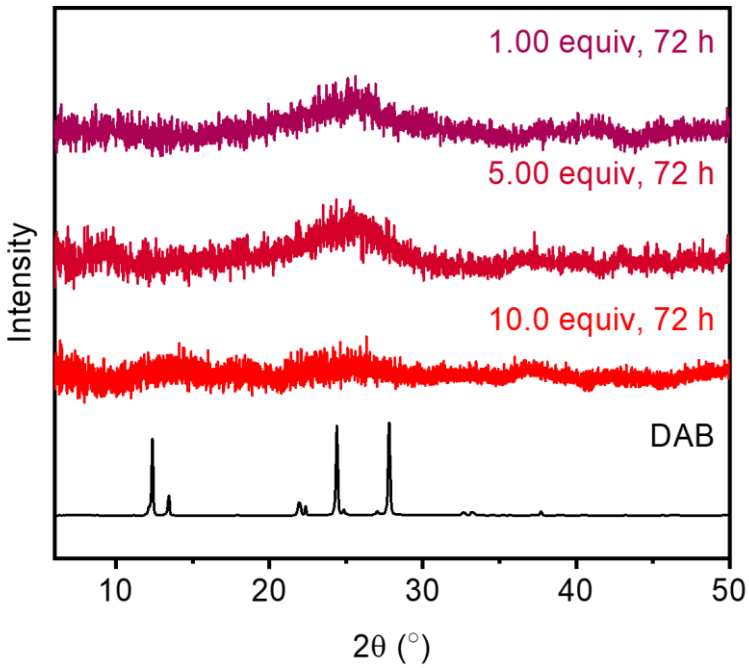

Figure S20. PXRD (λ = 1.5406 Å) patterns of **DAB** and **DAB-CMP** synthesized with various equivalents of $ZnBr_2$ for 72 h, indicating that **DAB-CMP** is an amorphous polymeric material.

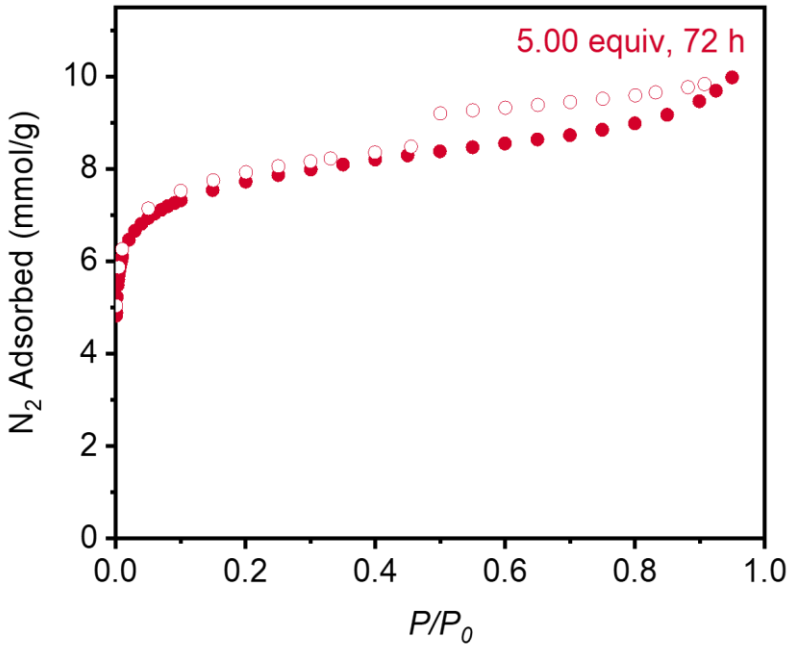

Figure S21. 77 K N_2 adsorption (filled circles) and desorption (open circles) isotherms of **DAB-CMP** synthesized with 5.00 equivalents of $ZnBr_2$ for 72 h. The Brunauer-Emmett-Teller (BET) and Langmuir surface areas were determined to be 651 ± 2 m^2/g and 906 ± 12 m^2/g, respectively.

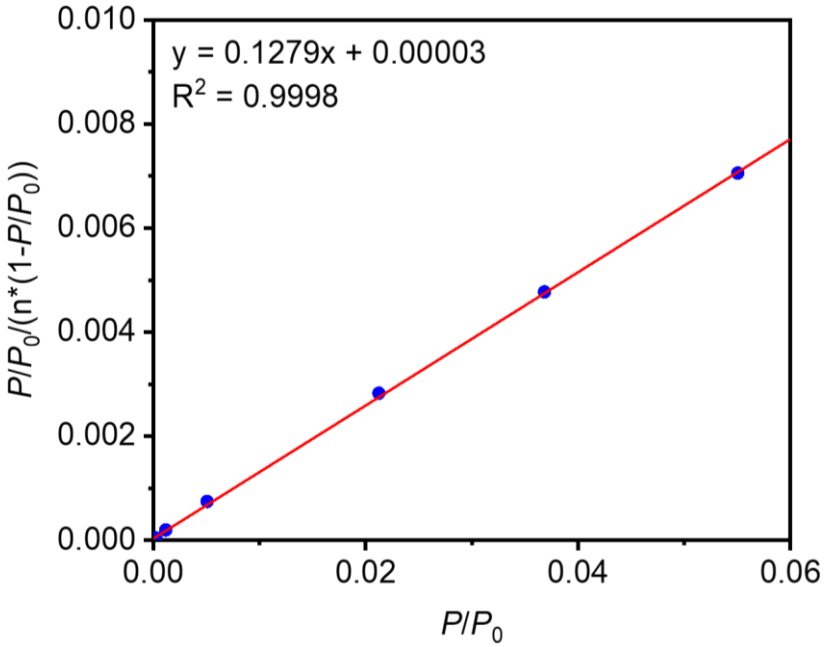

Figure S22. Linearized BET plot of **DAB-CMP** synthesized with 5.00 equivalents of $ZnBr_2$ for 72 h.

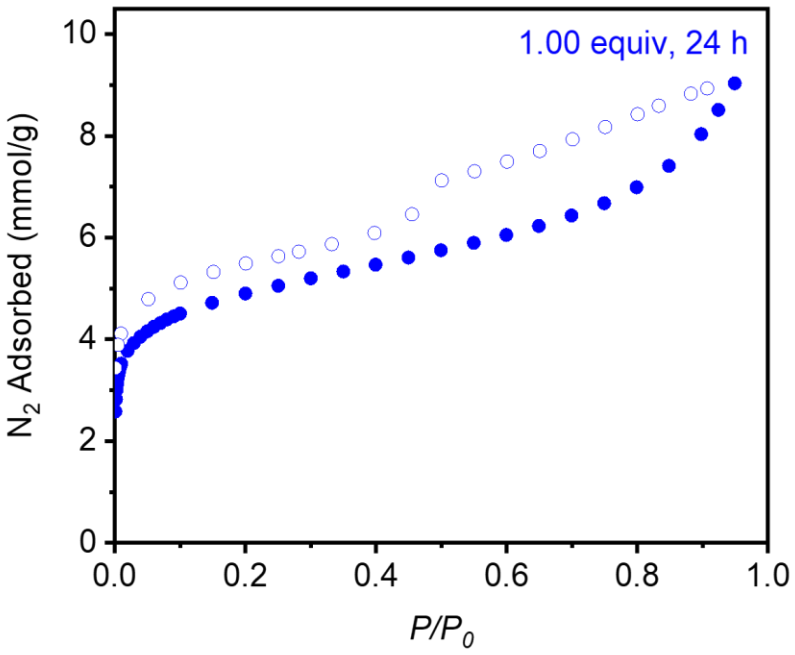

Figure S23. 77 K N_2 adsorption (filled circles) and desorption (open circles) isotherms for **DAB-CMP** made with 1.00 equivalent of $ZnBr_2$ for 24 h. The Brunauer-Emmett-Teller (BET) and Langmuir surface areas were determined to be 399 ± 1 m^2/g and 734 ± 28 m^2/g, respectively.

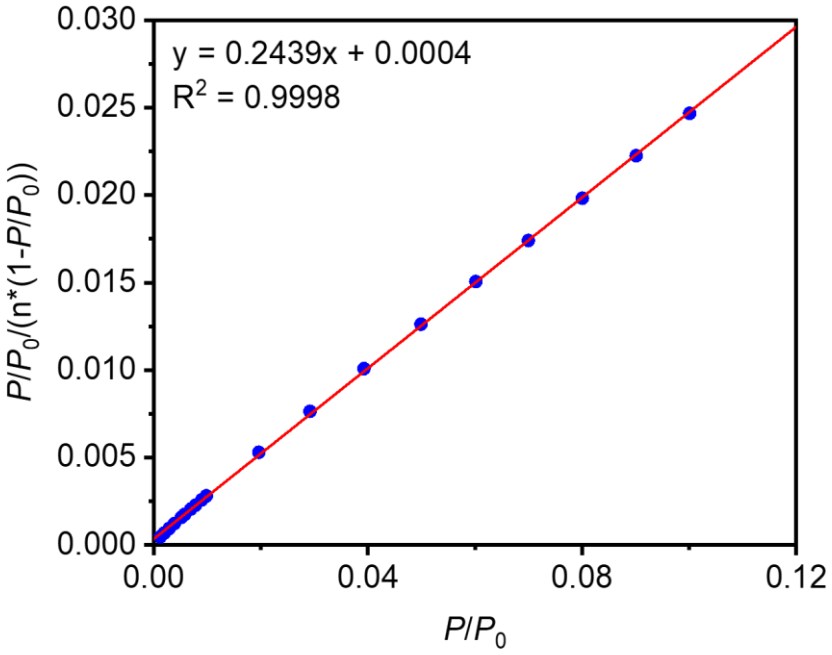

Figure S24. Linearized BET plot of **DAB-CMP** made with 1.00 equivalent of $ZnBr_2$ for 24 h.

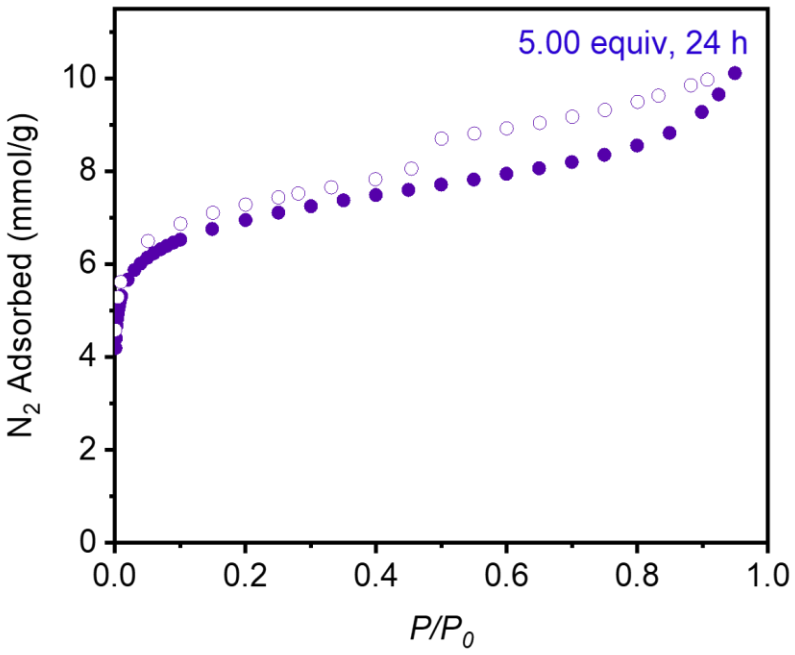

Figure S25. 77 K N_2 adsorption (filled circles) and desorption (open circles) isotherms for **DAB-CMP** made with 5.00 equivalents of $ZnBr_2$ for 24 h. The Brunauer-Emmett-Teller (BET) and Langmuir surface areas were determined to be 581 ± 1 m^2/g and 879 ± 44 m^2/g, respectively.

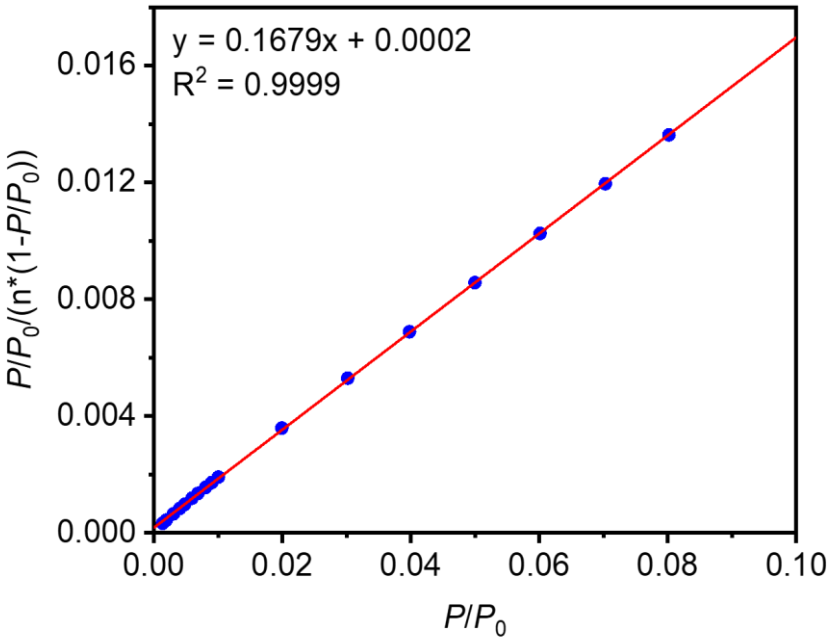

Figure S26. Linearized BET plot of **DAB-CMP** made with 5.00 equivalents of $ZnBr_2$ for 24 h.

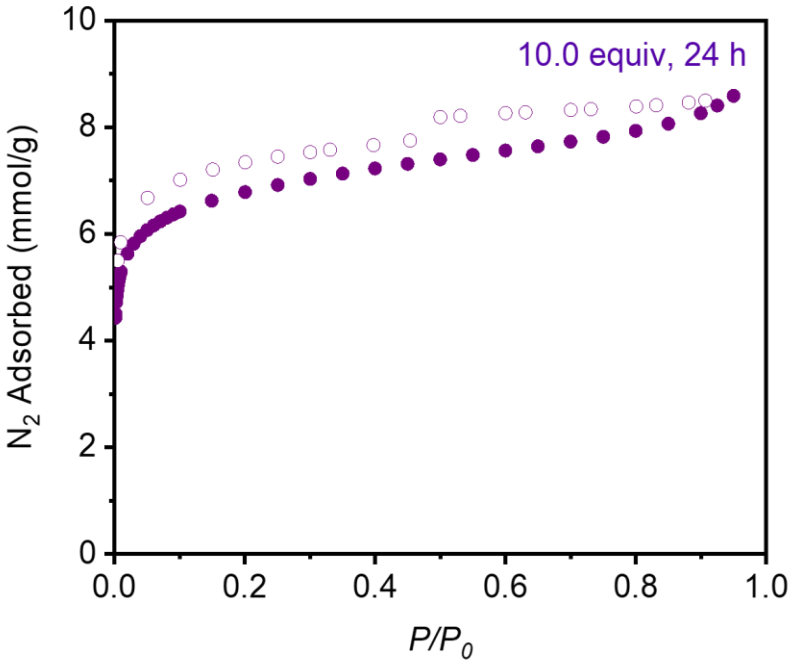

Figure S27. 77 K N_2 adsorption (filled circles) and desorption (open circles) isotherms for **DAB-CMP** made with 10.0 equivalents of $ZnBr_2$ for 24 h. The Brunauer-Emmett-Teller (BET) and Langmuir surface areas were determined to be 571 ± 1 m^2/g and 795 ± 10 m^2/g, respectively.

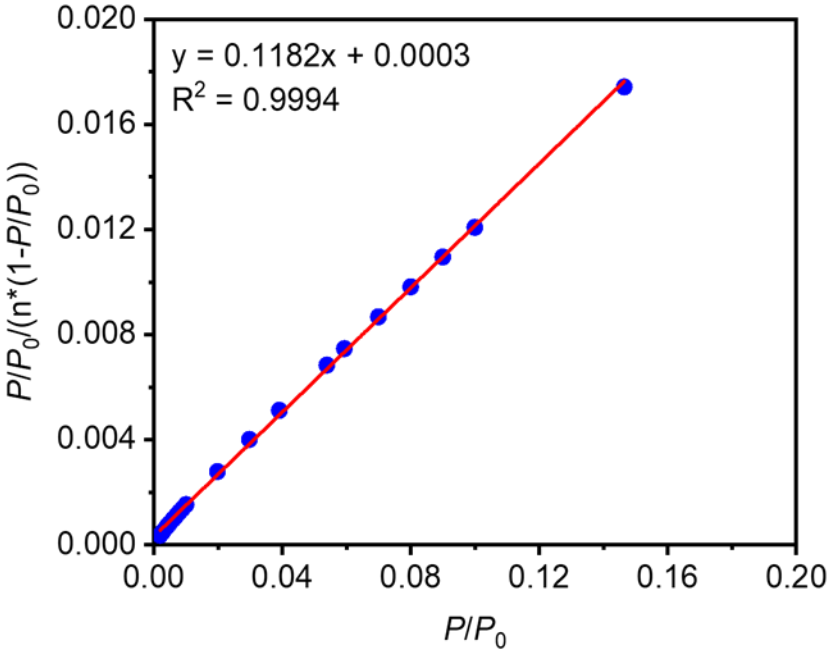

Figure S28. Linearized BET plot of **DAB-CMP** made with 10.0 equivalents of $ZnBr_2$ for 24 h.

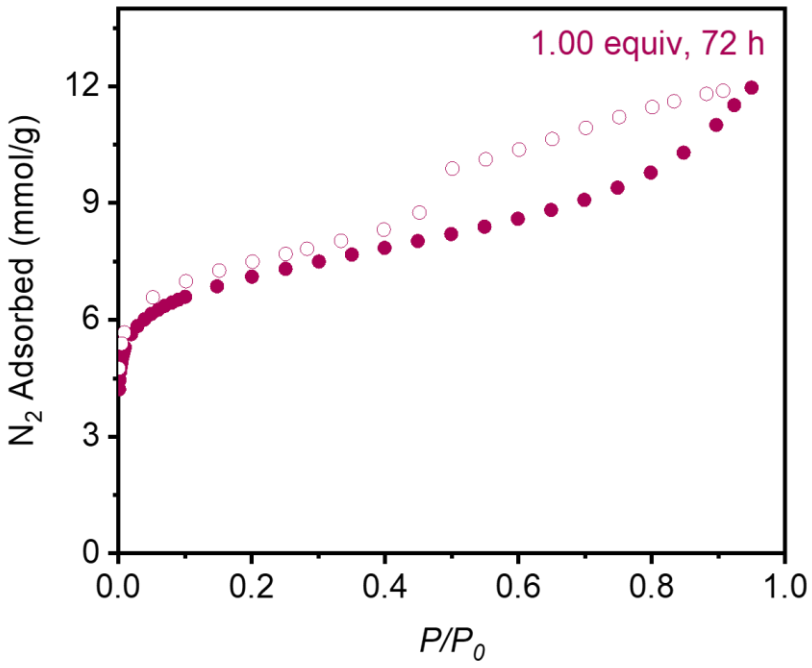

Figure S29. 77 K N_2 adsorption (filled circles) and desorption (open circles) isotherm for **DAB-CMP** made with 1.00 equivalent of $ZnBr_2$ for 72 h. The Brunauer-Emmett-Teller (BET) and Langmuir surface areas were determined to be 584 ± 2 m^2/g and 1013 ± 32 m^2/g, respectively.

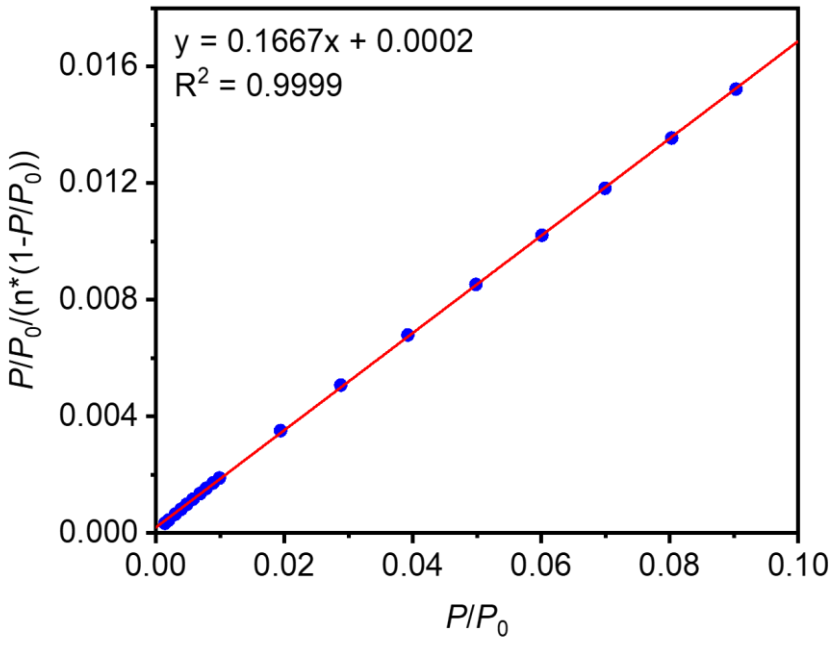

Figure S30. Linearized BET plot of **DAB-CMP** made with 1.00 equivalent of $ZnBr_2$ for 72 h.

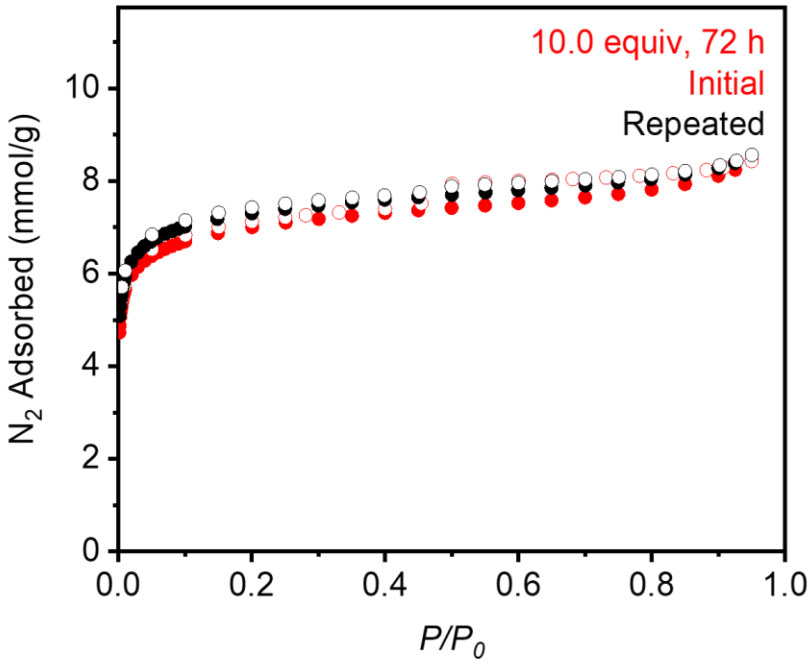

Figure S31. 77 K N_2 adsorption (filled circles) and desorption (open circles) isotherm for **DAB-CMP** made with 10.0 equivalents of $ZnBr_2$ for 72 h. The Brunauer-Emmett-Teller (BET) and Langmuir surface areas were determined to be 599 ± 1 m^2/g and 782 ± 8 m^2/g respectively. The synthesis was reproduced with a Langmuir surface area of 791 ± 3 m^2/g.

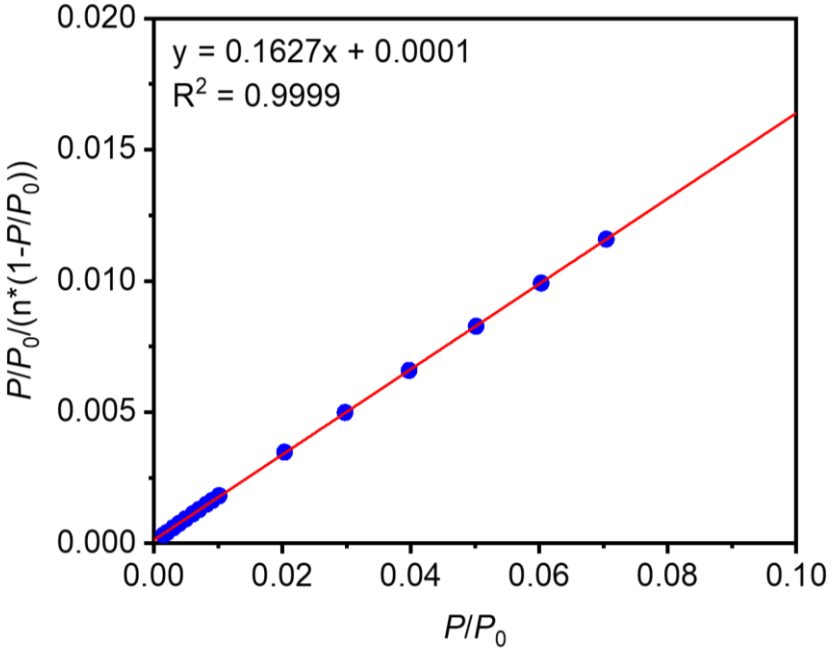

Figure S32. Linearized BET plot of **DAB-CMP** made with 10.0 equivalents of $ZnBr_2$ for 72 h.

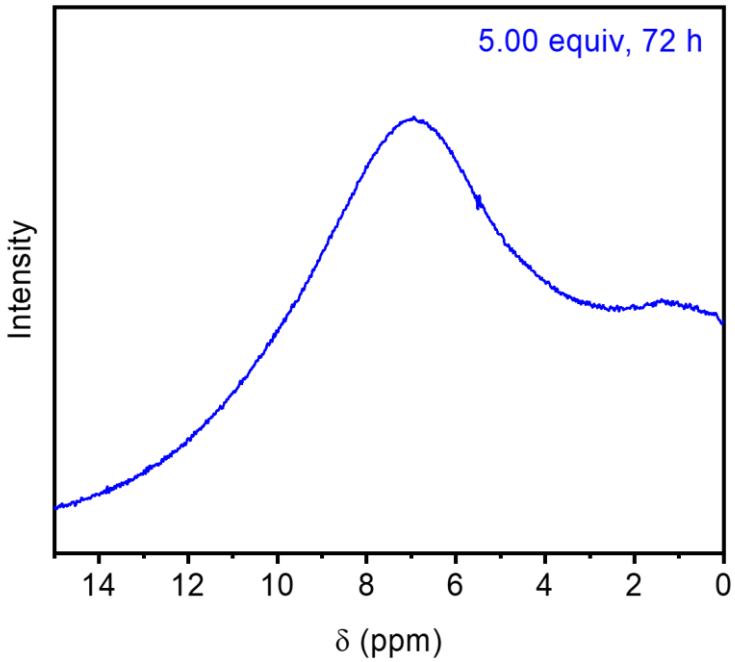

Figure S33. MAS ^{1}H SSNMR (500 MHz) spectrum of **DAB-CMP** synthesized with 5.00 equivalents of $ZnBr_2$ for 72 h, collected at a spinning speed of 20 kHz.

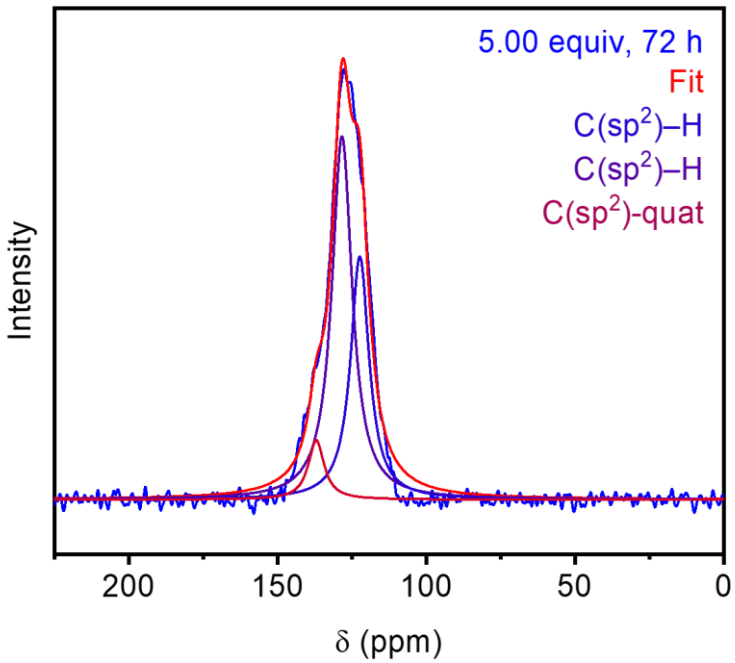

Figure S34. CP MAS ^{13}C SSNMR (125 MHz) spectrum of **DAB-CMP** synthesized with 5.00 equivalents of $ZnBr_2$ for 72 h with a ^{1}H–^{13}C contact time of 2 ms, collected at a spinning speed of 20 kHz. Deconvolution fits to the spectrum are shown.

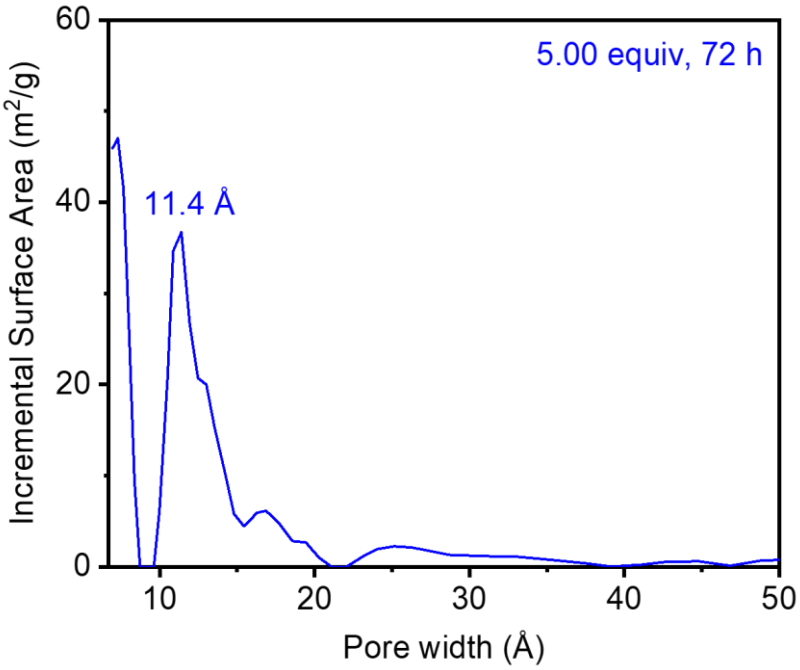

Figure S35. DFT-calculated pore size distribution of **DAB-CMP** synthesized with 5.00 equivalents of $ZnBr_2$ for 72 h, assuming a carbon slit pore geometry.

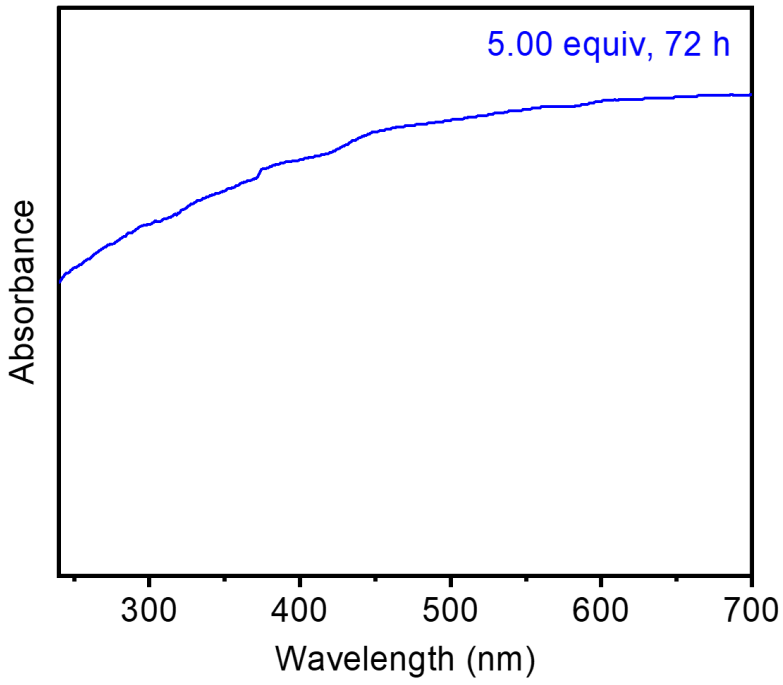

Figure S36. Diffuse reflectance UV-Vis absorbance spectrum of **DAB-CMP** synthesized with 5.00 equivalents of $ZnBr_2$ for 72 h.

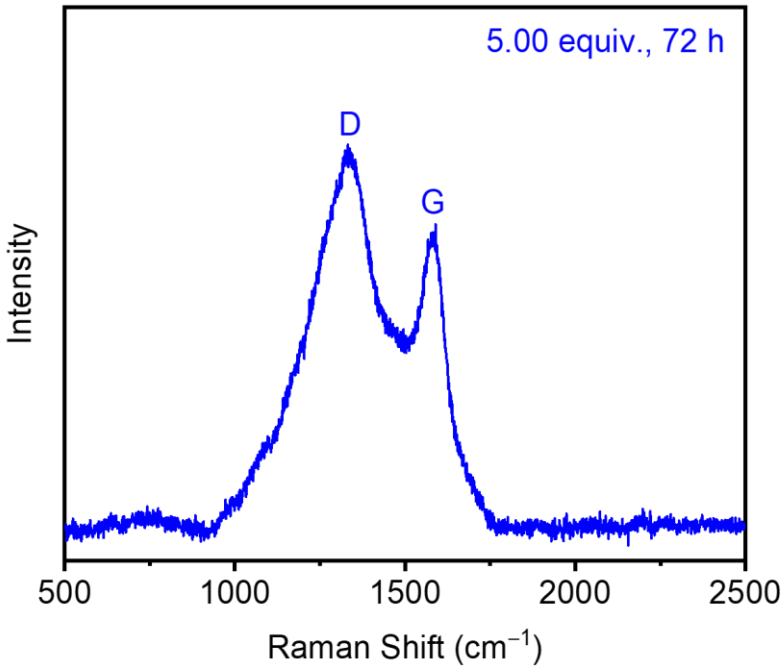

Figure S37. Raman spectrum of **DAB-CMP** synthesized with 5.00 equivalents of $ZnBr_2$ for 72 h. D and G bands resembling those of graphene are labeled.[7]

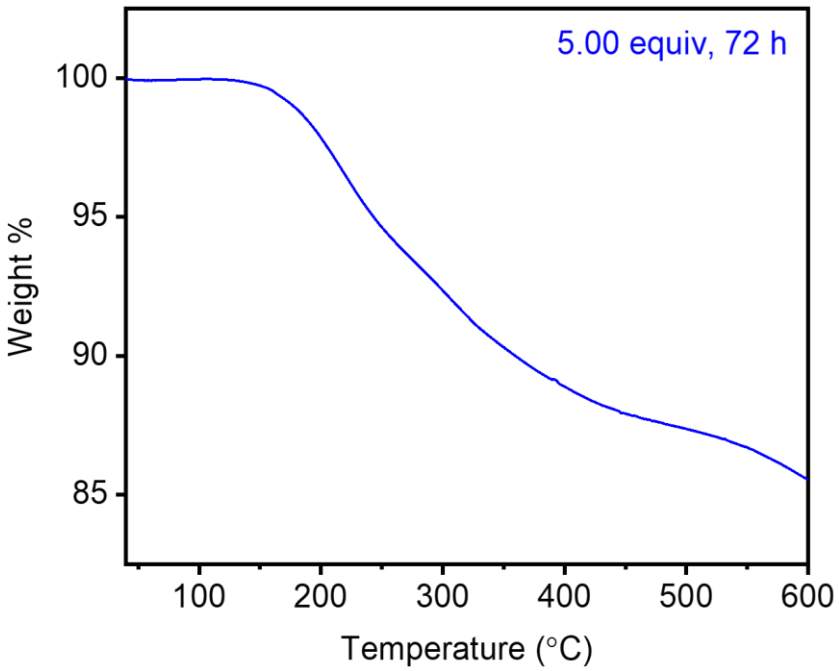

Figure S38. Thermogravimetric decomposition profile of **DAB-CMP** synthesized with 5.00 equivalents of $ZnBr_2$ for 72 h.

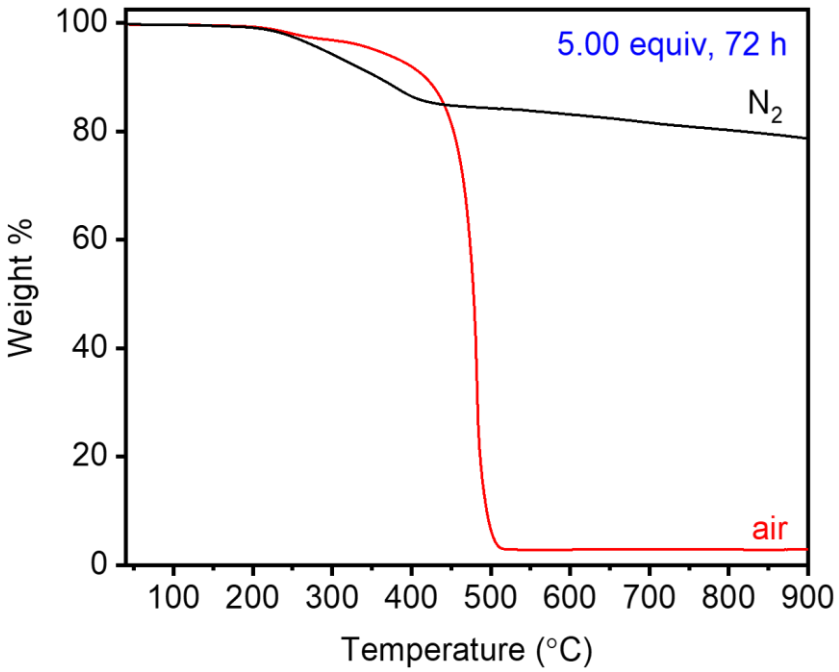

Figure S39. Extended thermogravimetric decomposition profile of **DAB-CMP** synthesized with 5.00 equivalents of $ZnBr_2$ for 72 h under both air and N_2. <3% of the initial mass was present after heating at 900 °C under air, indicating that the vast majority of the solid was organic matter. Under N_2, the total mass present still remained >80%, consistent with solvent desorption followed by slow carbonization under N_2.

b. 4,4′-diacetylbiphenyl trimerization.

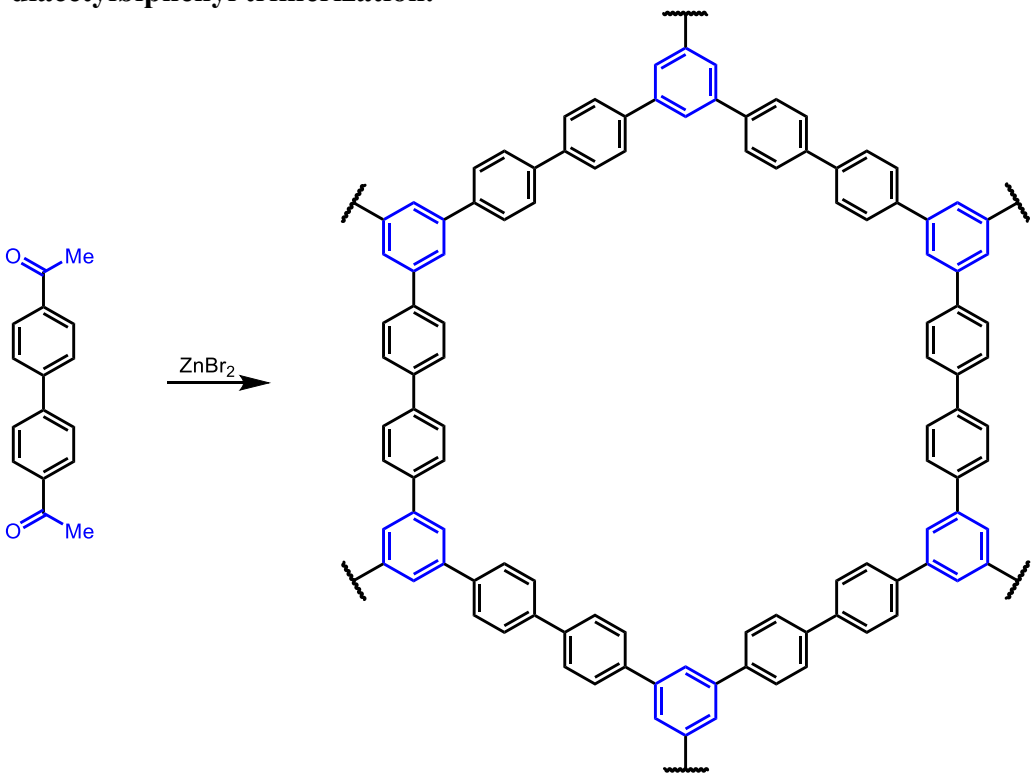

Figure S40. Synthesis of DABP-CMP from 4,4′-diacetylbiphenyl (**DABP**).

Following the general procedure, three tubes were charged with 4,4′-diacetylbiphenyl (**DABP**) (40.0 mg, 0.168 mmol, 1.00 equiv) and $ZnBr_2$ (189 mg, 0.0840 mmol, 5.00 equiv), and the products were combined to yield **DABP-CMP** as a shiny black solid (96.0 mg, 94% yield).

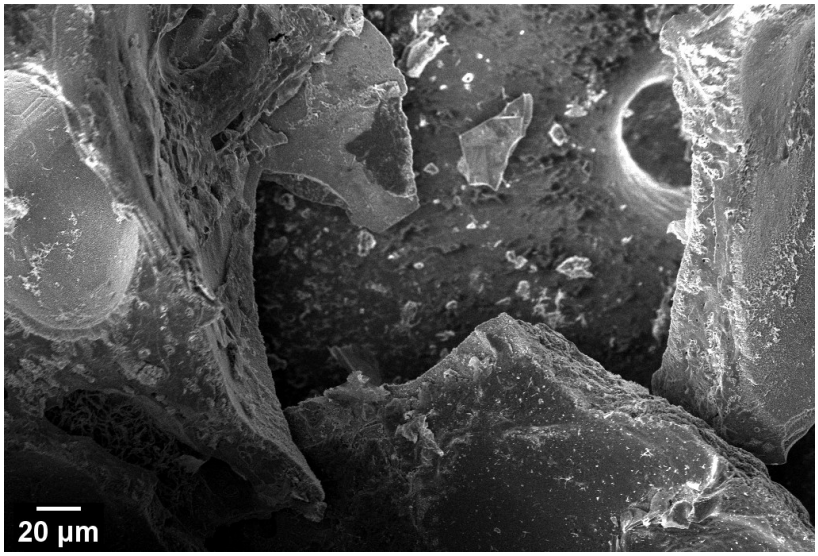

Figure S41. SEM image of **DABP-CMP** synthesized with 5.00 equivalents of $ZnBr_2$ for 72 h.

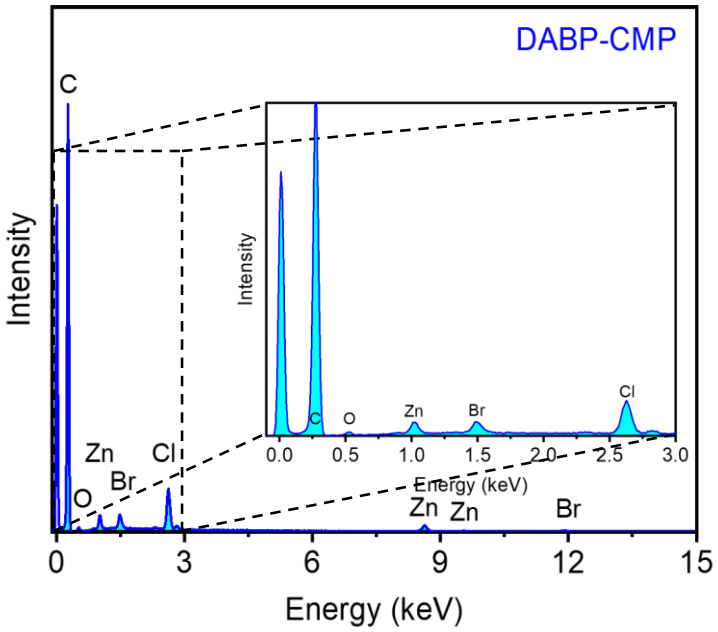

Figure S42. EDS spectrum for **DABP-CMP** synthesized with 5.00 equivalents of $ZnBr_2$ for 72 h. The residual Cl likely arises from the HCl wash used to remove zinc salts.

Table S5. Tabulated EDS data for **DABP-CMP** synthesized with 5.00 equivalents of $ZnBr_2$ for 72 h.

Element	Line Type	Wt %	Atomic %	Theoretical Atomic %[1]
C	K series	91.82	96.48	100.00
O	K series	2.54	2.03	0.00
Cl	K series	2.59	0.93	0.00
Zn	K series	2.16	0.42	0.00
Br	K series	0.89	0.14	0.00
Total:		100.00	100.00	100.00

[1]Excludes hydrogen.

Table S6. Tabulated elemental analysis data through combustion and ion chromatography for **DABP-CMP** synthesized with 5.00 equivalents of $ZnBr_2$ for 72 h.

Element	Wt %	Theoretical Wt %
C	82.96	95.02
H	3.38	4.98
Cl	2.26	0.00
N	0.10	0.00
Br	1.80	0.00
O and Zn	9.50[1]	0.00
Total:	10.00	100.00

[1]The remaining mass not attributed to C, H, Cl, and Br was assumed to come from Zn and O, as they were not directly analyzed during combustion analysis.

Table S7. Tabulated XPS data for **DABP-CMP** synthesized with 5.00 equivalents of $ZnBr_2$ for 72 h.

Element	Peak label	Position	Atomic %
C	C 1s	532.80	95.41
O	O 1s	285.20	3.63
Cl	Cl 2p	198.80	0.76
Zn	Zn 2p	1022.80	0.14
Br	Br 3d	69.60	0.06
Total:			100.00

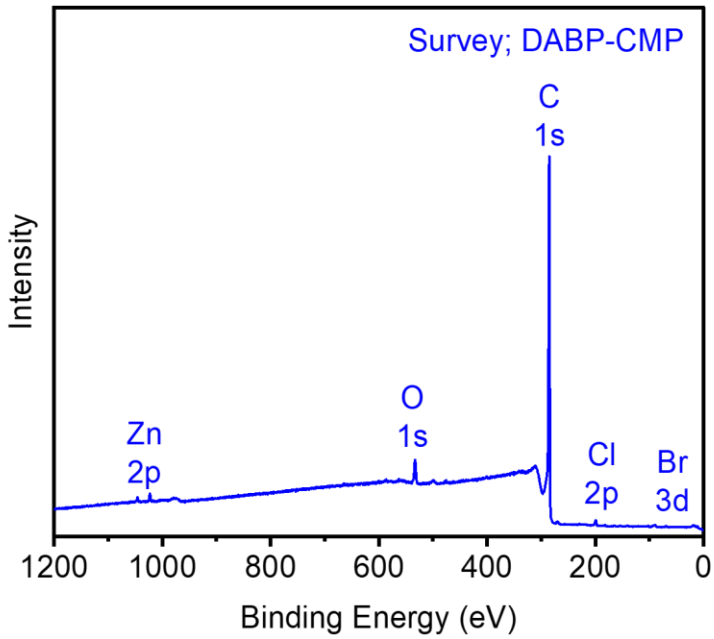

Figure S43. XPS spectrum for **DABP-CMP** synthesized with 5.00 equivalents of $ZnBr_2$ for 72 h. The relevant energies and transitions are labeled at the expected energies.

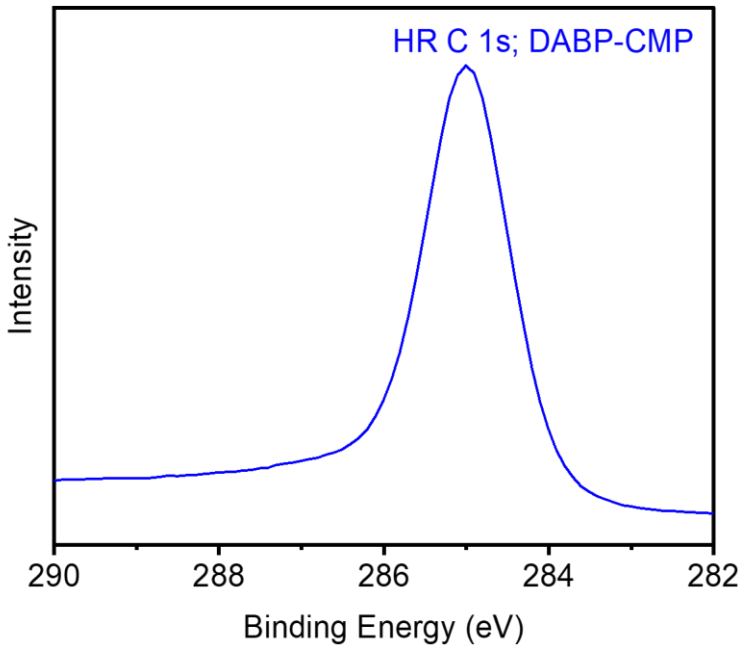

Figure S44. HR C 1s XPS spectrum of **DABP-CMP** synthesized with 5.00 equivalents of $ZnBr_2$ for 72 h.

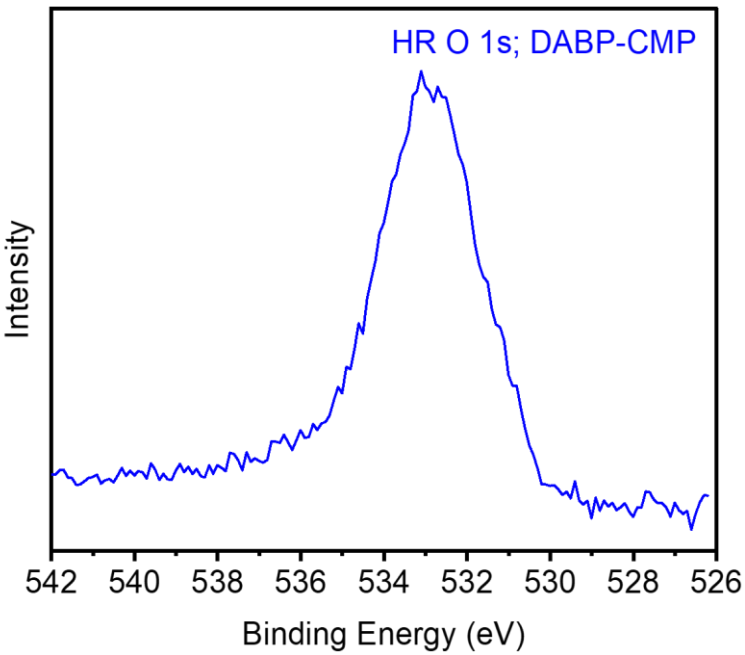

Figure S45. HR O 1s XPS spectrum of **DABP-CMP** synthesized with 5.00 equivalents of $ZnBr_2$ for 72 h.

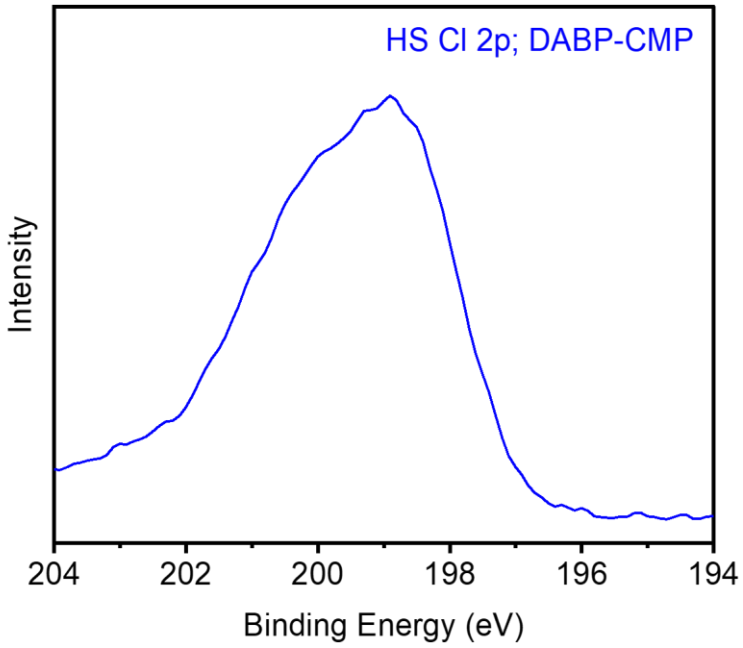

Figure S46. HS Cl 2p XPS spectrum of **DABP-CMP** synthesized with 5.00 equivalents of $ZnBr_2$ for 72 h.

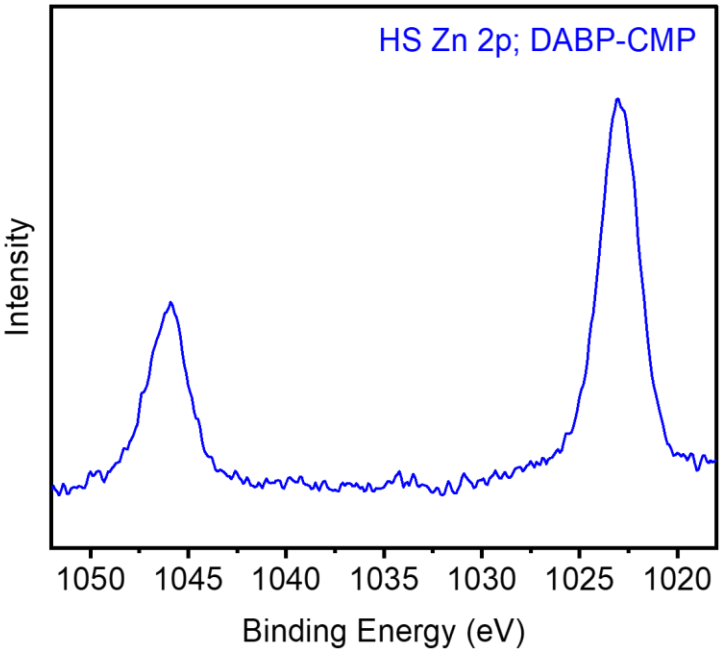

Figure S47. HS Zn 2p XPS spectrum of **DABP-CMP** synthesized with 5.00 equivalents of $ZnBr_2$ for 72 h.

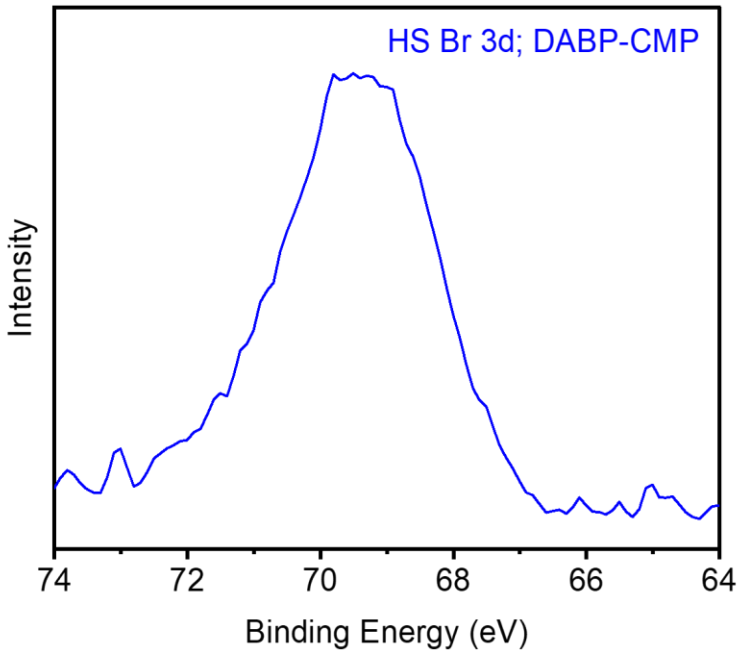

Figure S48. HS Br 3d XPS spectrum of **DABP-CMP** synthesized with 5.00 equivalents of $ZnBr_2$ for 72 h.

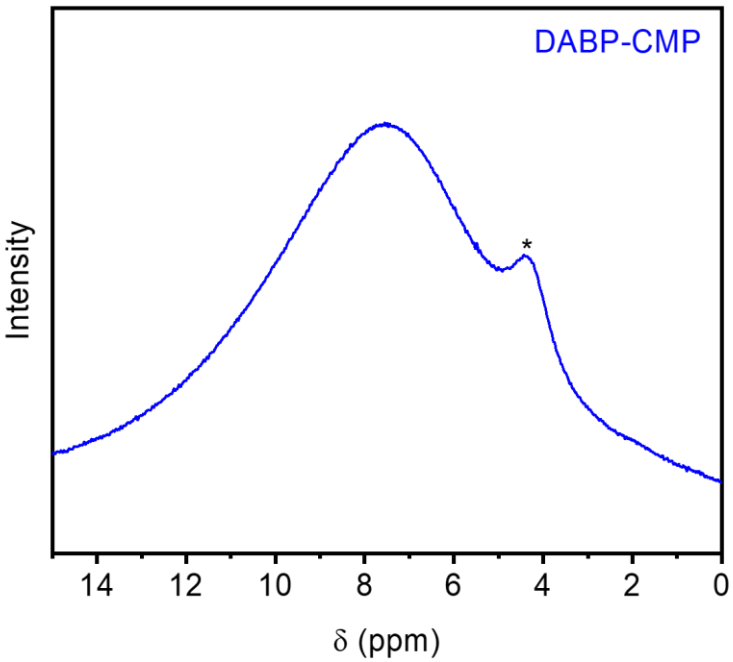

Figure S49. MAS ^{1}H SSNMR (500 MHz) spectrum of **DABP-CMP** synthesized with 5.00 equivalents of $ZnBr_2$ for 72 h, collected at a spinning speed of 20 kHz. The asterisk corresponds to adsorbed water.

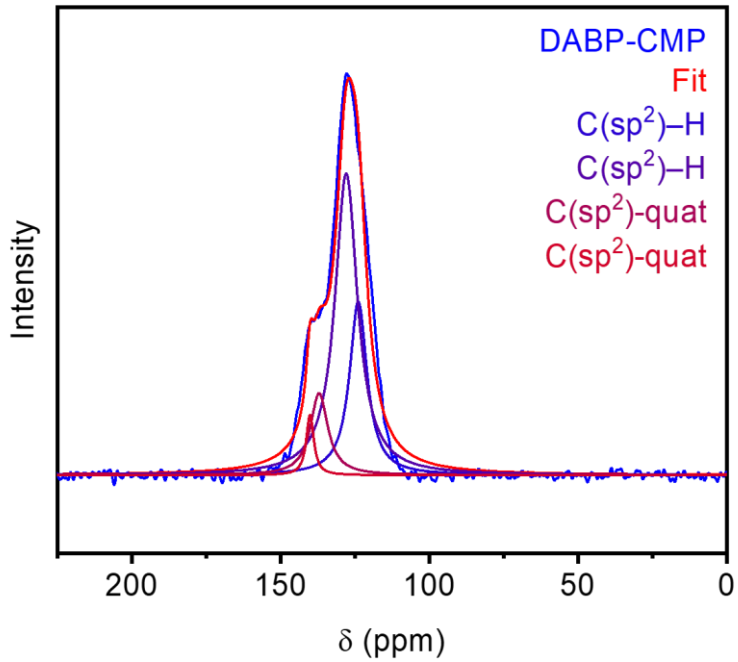

Figure S50. CP MAS ^{13}C SSNMR (125 MHz) spectrum of **DABP-CMP** synthesized with 5.00 equivalents of $ZnBr_2$ for 72 h with a ^{1}H–^{13}C contact time of 2 ms, collected at a spinning speed of 20 kHz. Deconvolution fits to the spectrum are shown.

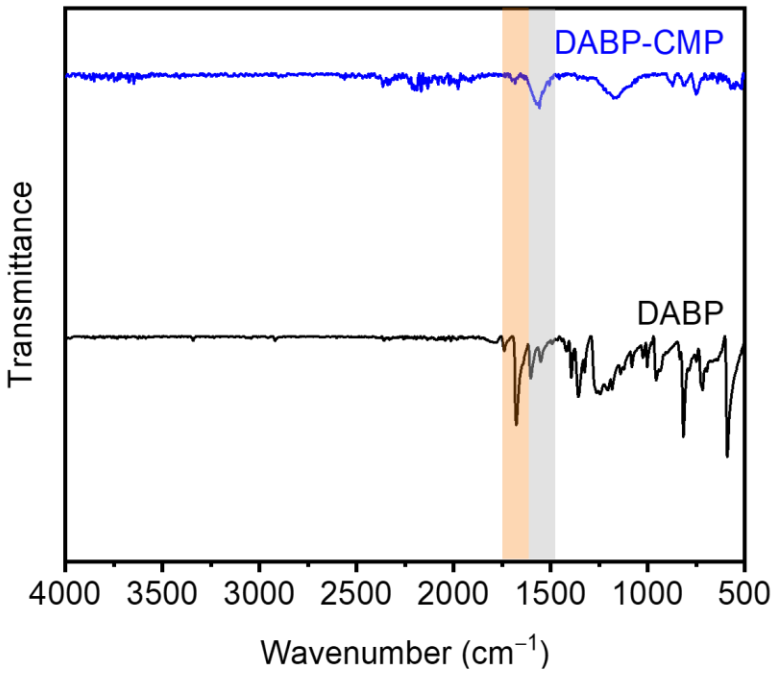

Figure S51. ATR-IR spectra of **DABP** and **DABP-CMP** synthesized with 5.00 equivalents of $ZnBr_2$ for 72 h. The indicated peaks correspond to carbonyl C=O (orange) and aromatic C=C (gray) stretches.

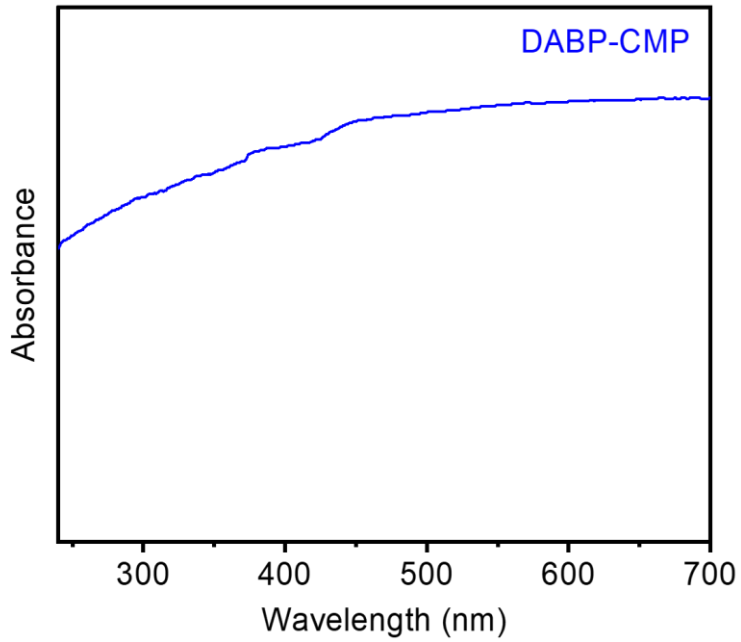

Figure S52. Diffuse reflectance UV-Vis absorbance spectrum of **DABP-CMP** synthesized with 5.00 equivalents of $ZnBr_2$ for 72 h.

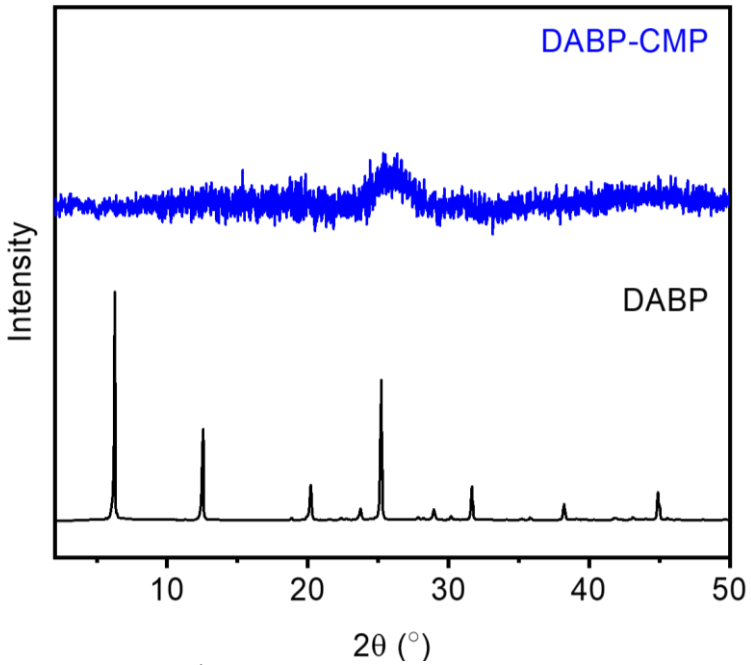

Figure S53. PXRD (λ = 1.5406 Å) patterns of **DABP** and **DABP-CMP** synthesized with 5.00 equivalents of $ZnBr_2$ for 72 h, indicating that **DABP-CMP** is an amorphous polymer.

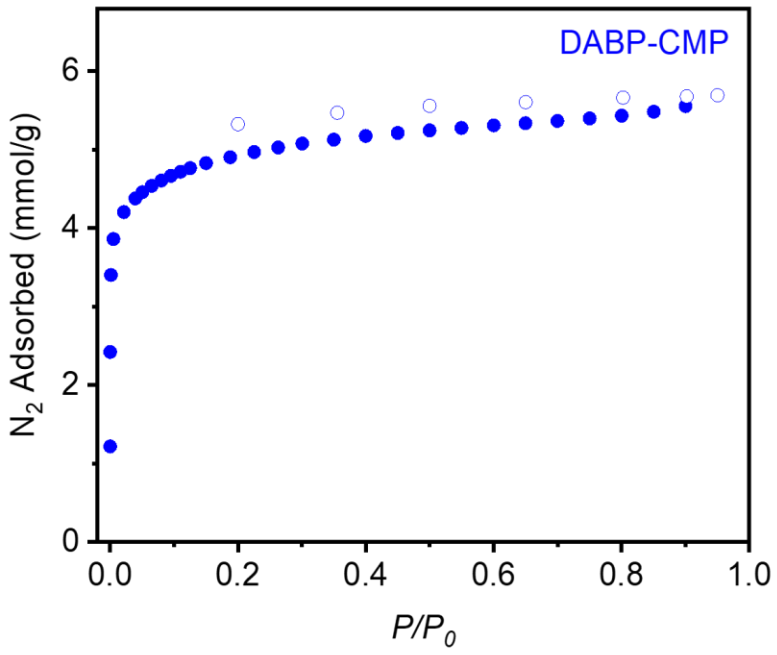

Figure S54. 77 K N_2 adsorption (filled circles) and desorption (open circles) isotherm for **DABP-CMP** synthesized with 5.00 equivalents of $ZnBr_2$ for 72 h. The Brunauer-Emmett-Teller (BET) and Langmuir surface areas were determined to be 415 ± 2 m^2/g and 541 ± 4 m^2/g, respectively.

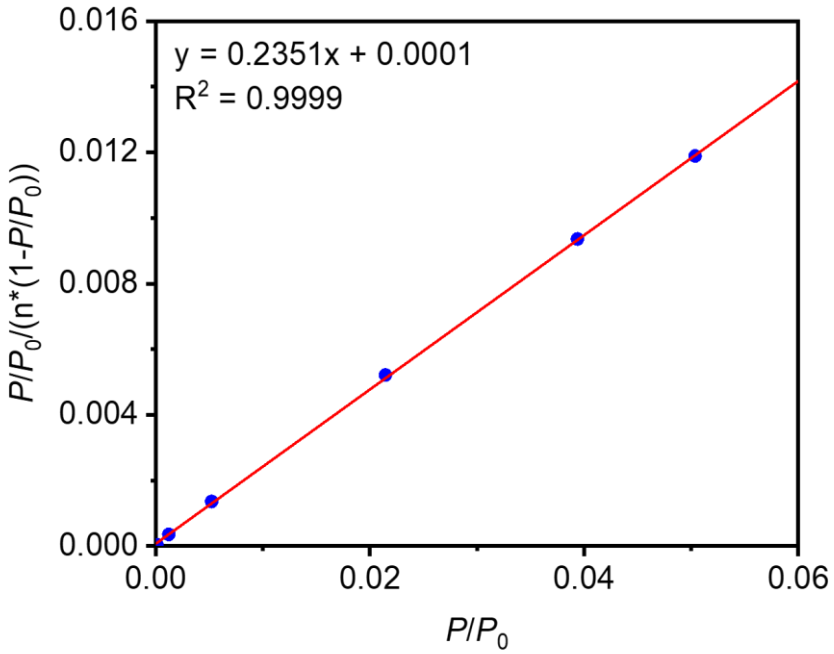

Figure S55. Linearized BET plot of **DABP-CMP** synthesized with 5.00 equivalents of $ZnBr_2$ for 72 h.

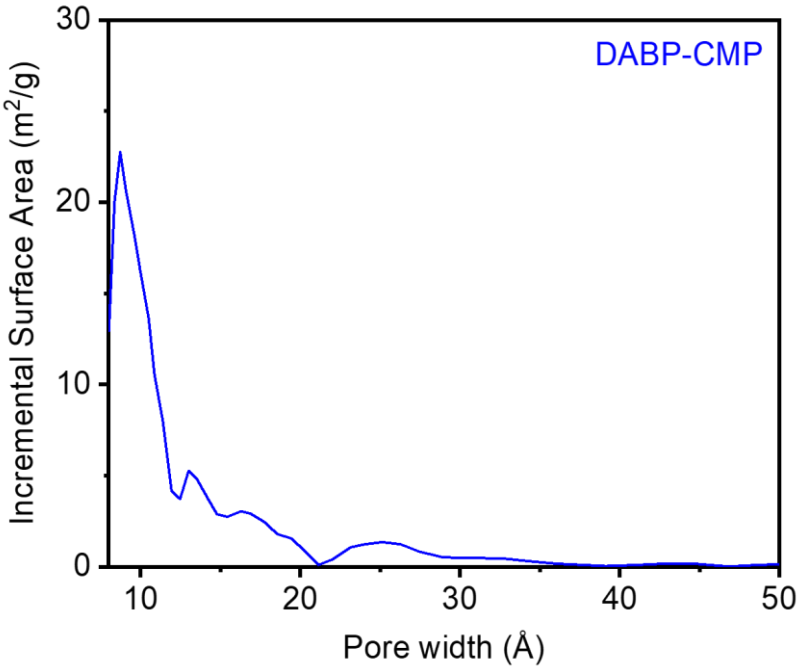

Figure S56. DFT-calculated pore size distribution of **DABP-CMP** synthesized with 5.00 equivalents of $ZnBr_2$ for 72 h, assuming a carbon slit pore geometry.

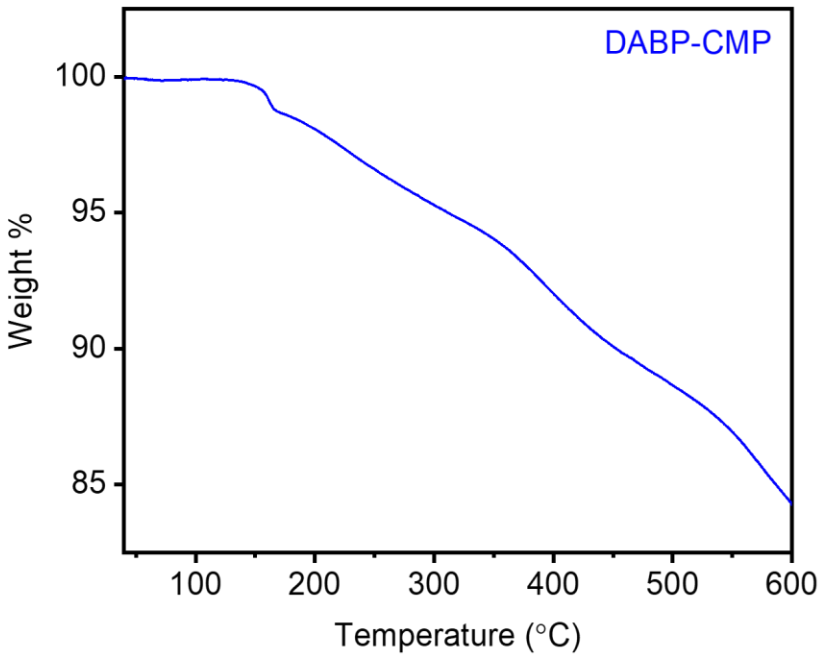

Figure S57. Thermogravimetric decomposition profile of **DABP-CMP** synthesized with 5.00 equivalents of $ZnBr_2$ for 72 h.

c. 2,7-diacetylfluorene trimerization.

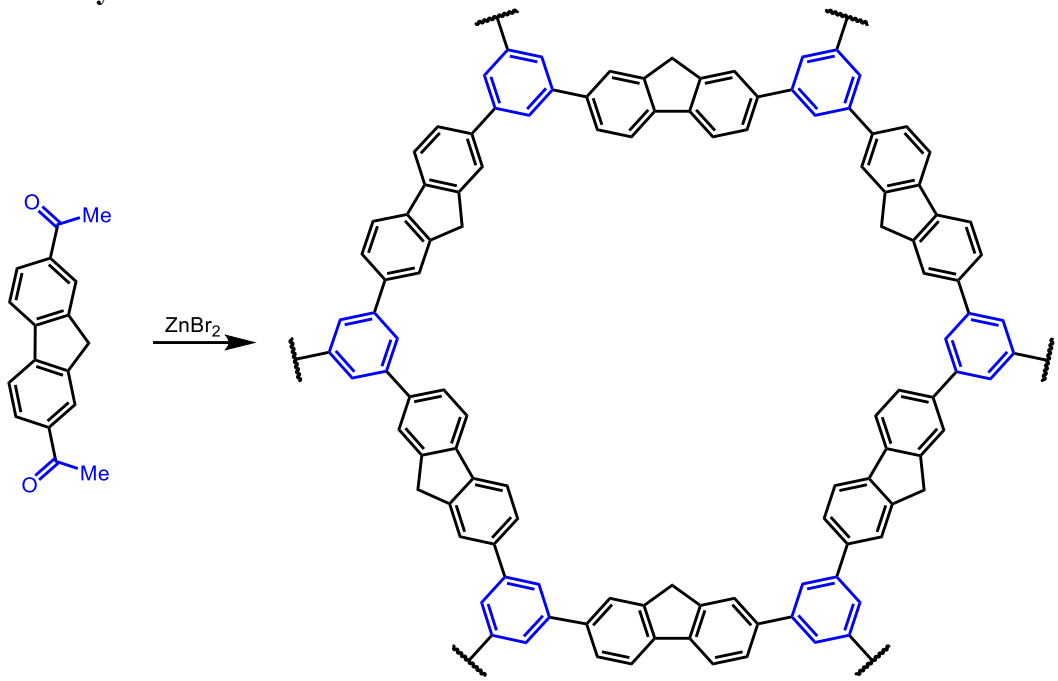

Figure S58. Synthesis of DAF-CMP from 2,7-diacetylfluorene (DAF).

Following the general procedure, three tubes were charged with 2,7-diacetylfluorene (**DAF**) (40.0 mg, 0.160 mmol, 1.00 equiv) and $ZnBr_2$ (180 mg, 0.799 mmol, 5.00 equiv), and the products were combined to yield **DAF-CMP** as a shiny black solid (93.9 mg, 91% yield).

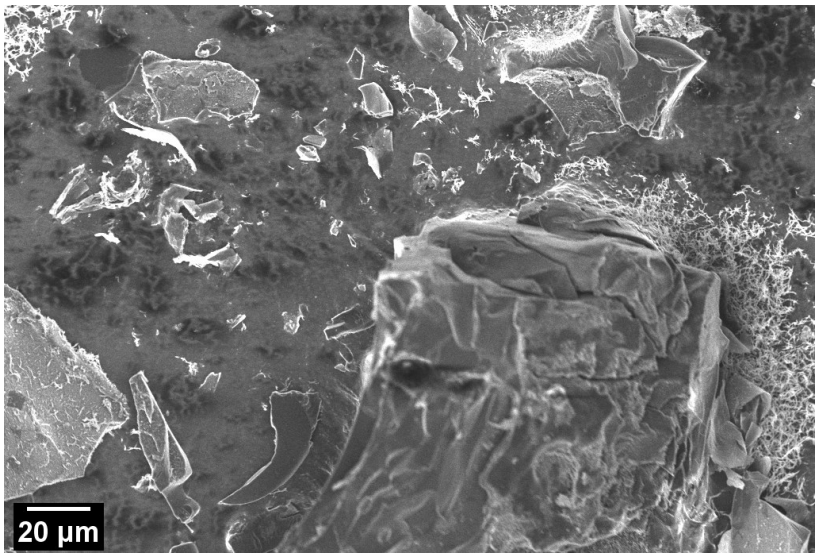

Figure S59. SEM image of **DAF-CMP** synthesized with 5.00 equivalents of $ZnBr_2$ for 72 h.

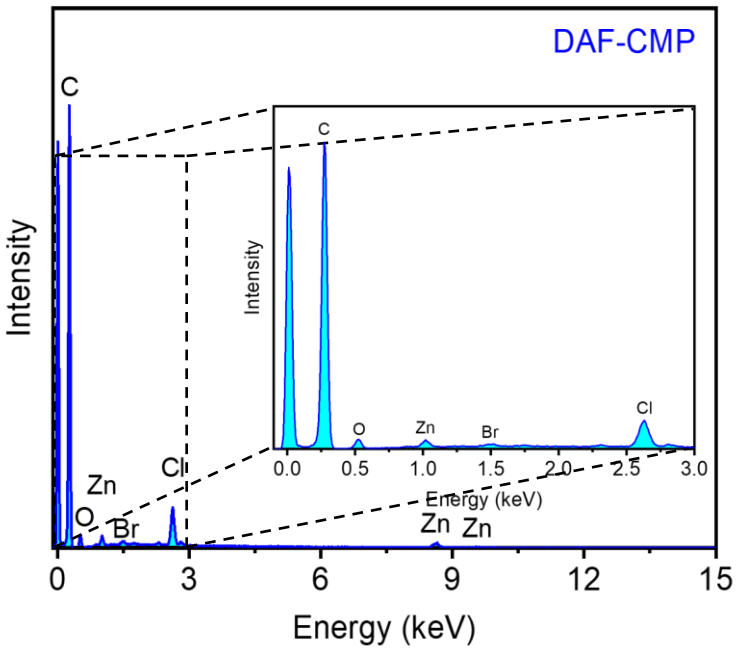

Figure S60. EDS spectrum for **DAF-CMP** synthesized with 5.00 equivalents of $ZnBr_2$ for 72 h. The residual Cl likely arises from the HCl wash used to remove zinc salts.

Table S8. Tabulated EDS data for **DAF-CMP** synthesized with 5.00 equivalents of $ZnBr_2$ for 72 h

Element	Line Type	Wt %	Atomic %	Theoretical Atomic %[1]
C	K series	95.33	98.53	100.00
O	K series	1.07	0.37	0.00
Cl	K series	2.18	0.82	0.00
Zn	K series	1.36	0.27	0.00
Br	K series	0.06	0.01	0.00
Total:		100.00	100.00	100.00

[1]Excludes hydrogen.

Table S9. Tabulated elemental analysis data through combustion and ion chromatography for **DAF-CMP** synthesized with 5.00 equivalents of $ZnBr_2$ for 72 h.

Element	Wt %	Theoretical Wt %
C	77.84	95.30
H	2.96	4.70
Cl	2.61	0.00
N	0.20	0.00
Br	1.71	0.00
O and Zn	14.68[1]	0.00
Total:	100.00	100.00

[1]The remaining mass not attributed to C, H, Cl, and Br was assumed to come from Zn and O, as they were not directly analyzed during combustion analysis.

Table S10. Tabulated XPS data for **DAF-CMP** synthesized with 5.00 equivalents of $ZnBr_2$ for 72 h.

Element	Peak label	Position	Atomic %
C	C 1s	532.80	92.07
O	O 1s	285.20	6.29
Cl	Cl 2p	198.80	0.89
Zn	Zn 2p	1022.80	0.39
Br	Br 3d	69.60	0.36
Total:			100.00

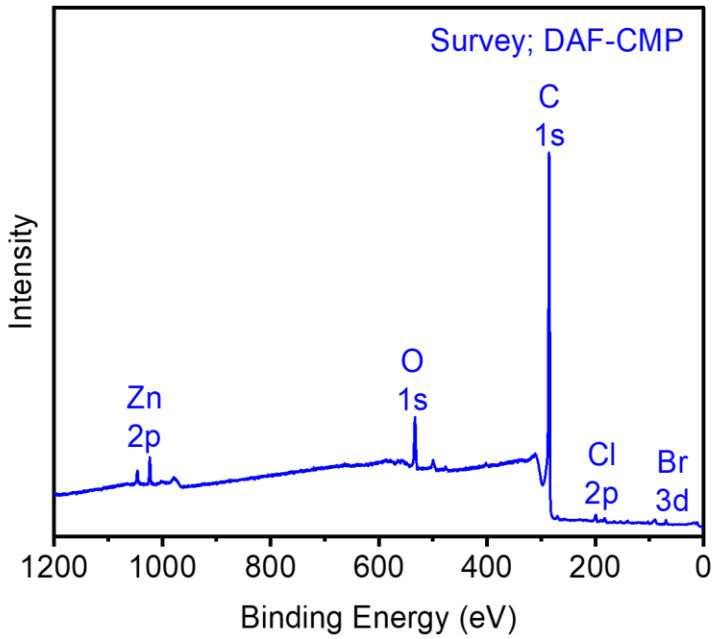

Figure S61. XPS spectrum for **DAF-CMP** synthesized with 5.00 equivalents of $ZnBr_2$ for 72 h. The relevant energies and transitions are labeled at the expected energies.

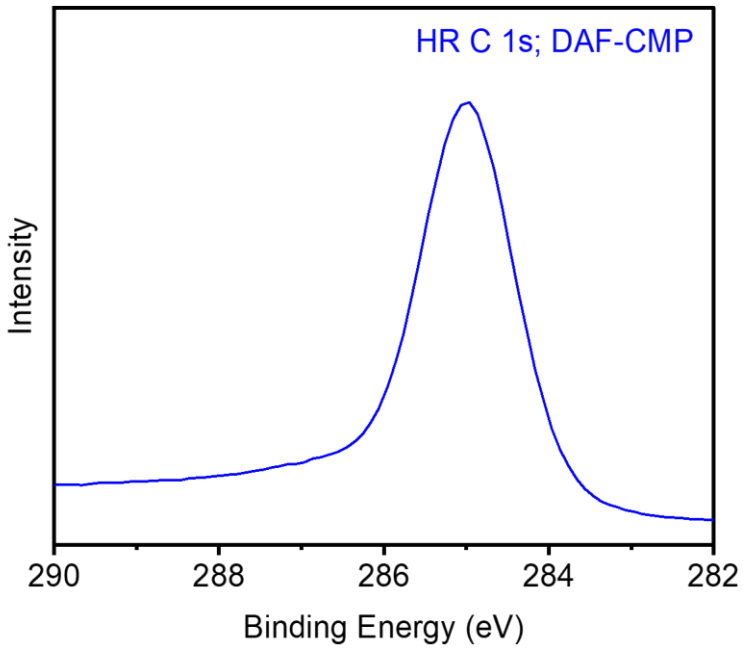

Figure S62. HR C 1s XPS spectrum of **DAF-CMP** synthesized with 5.00 equivalents of $ZnBr_2$ for 72 h.

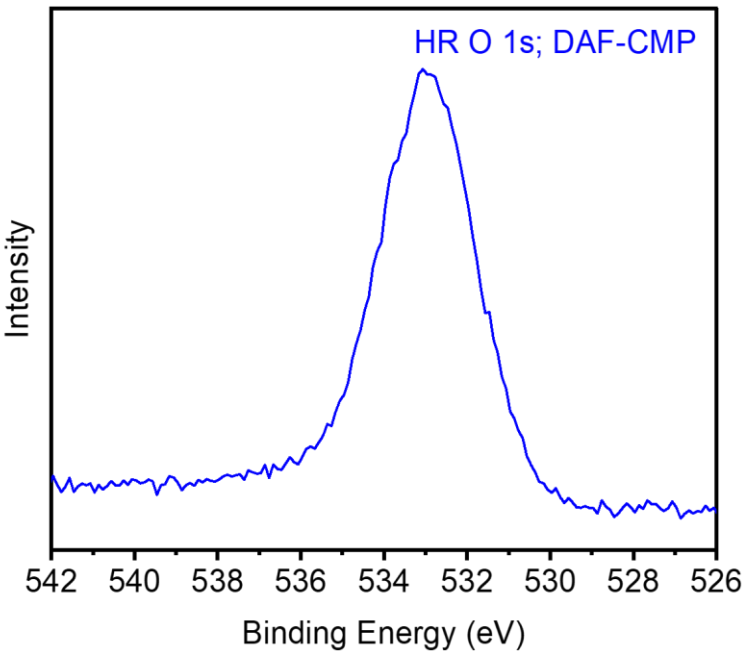

Figure S63. HR O 1s XPS spectrum of **DAF-CMP** synthesized with 5.00 equivalents of $ZnBr_2$ for 72 h.

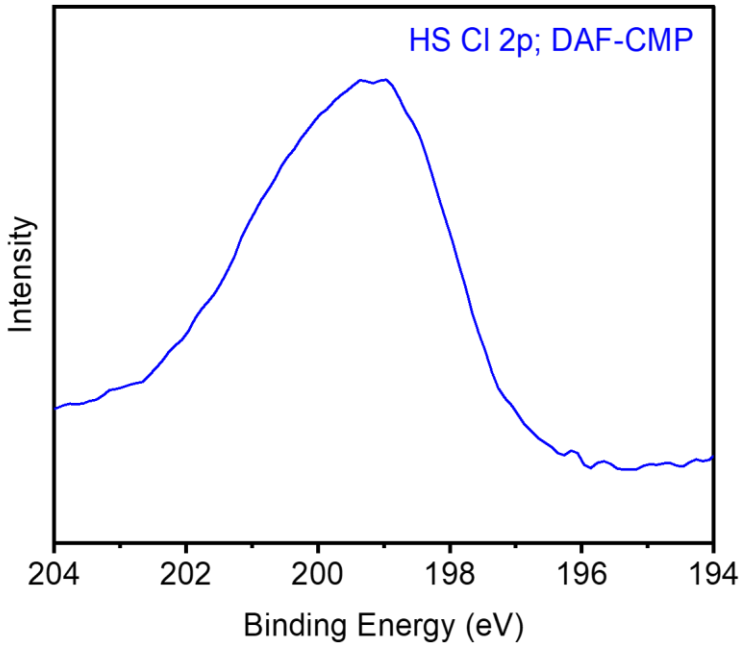

Figure S64. HS Cl 2p XPS spectrum of **DAF-CMP** synthesized with 5.00 equivalents of $ZnBr_2$ for 72 h.

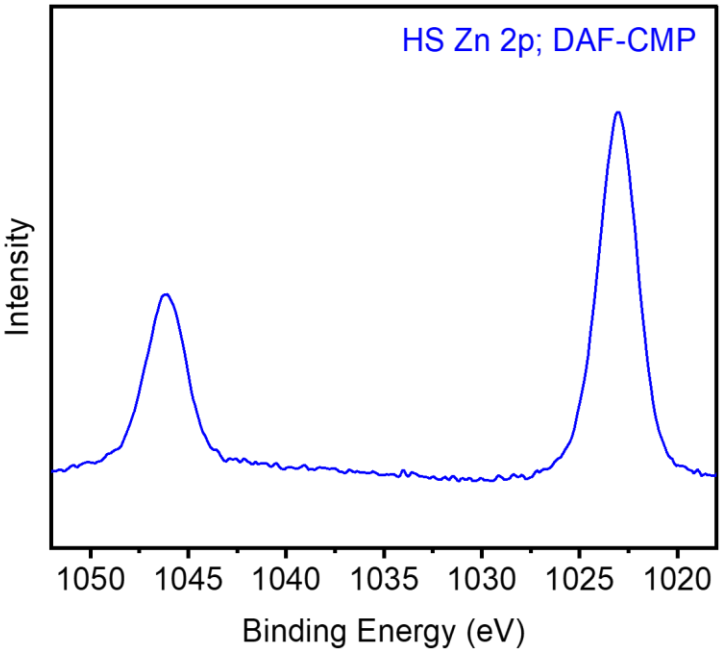

Figure S65. HS Zn 2p XPS spectrum of **DAF-CMP** synthesized with 5.00 equivalents of $ZnBr_2$ for 72 h.

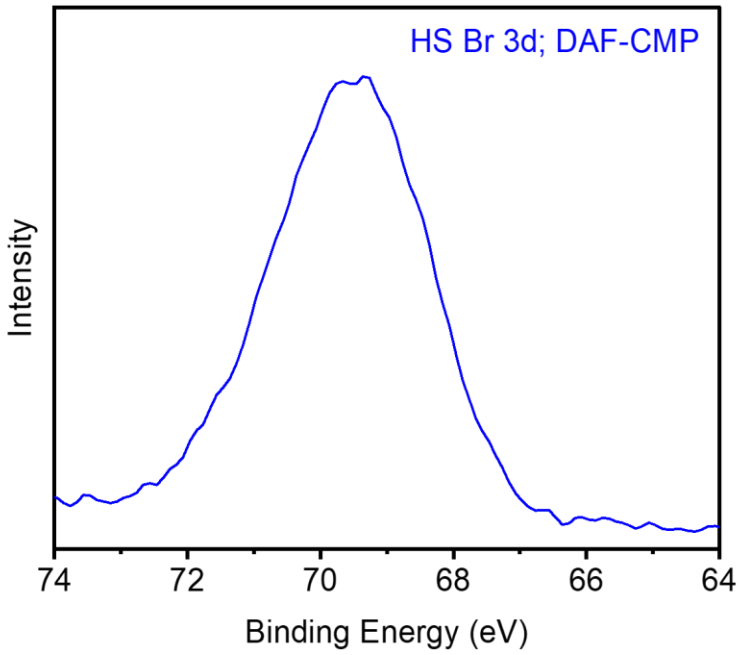

Figure S66. HS Br 3d XPS spectrum of **DAF-CMP** synthesized with 5.00 equivalents of $ZnBr_2$ for 72 h.

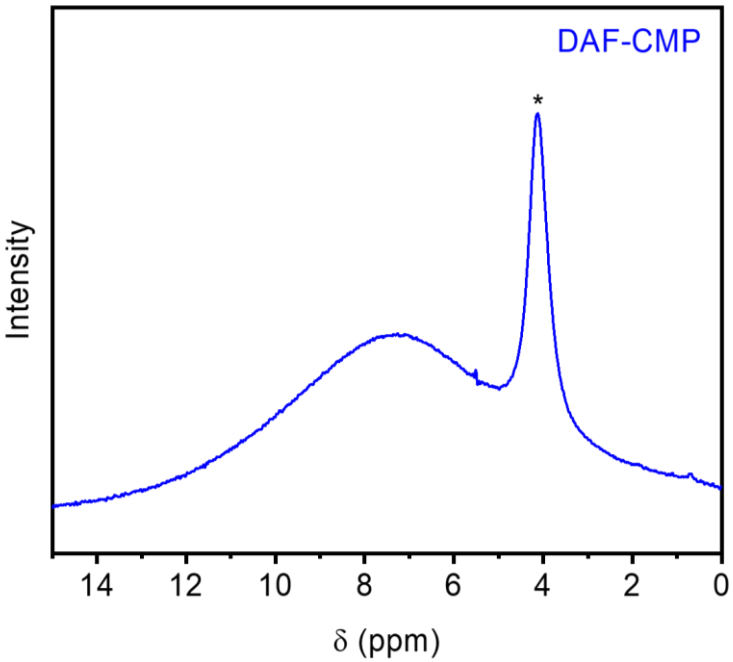

Figure S67. MAS ^1H SSNMR (500 MHz) spectrum of **DAF-CMP** synthesized with 5.00 equivalents of $ZnBr_2$ for 72 h, collected at a spinning speed of 20 kHz. The asterisk corresponds to adsorbed water.

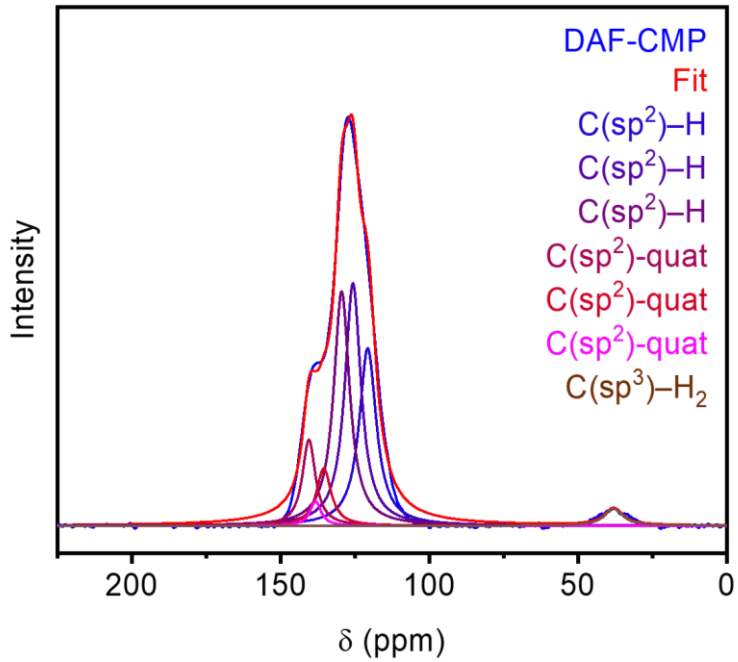

Figure S68. CP MAS ^{13}C SSNMR (125 MHz) spectrum of **DAF-CMP** synthesized with 5.00 equivalents of $ZnBr_2$ for 72 h with a ^{1}H–^{13}C contact time of 0.5 ms, collected at a spinning speed of 20 kHz. Deconvolution fits to the spectrum are shown. Notably, **DAF-CMP** retains the methylene carbon signal centered at 40 ppm.

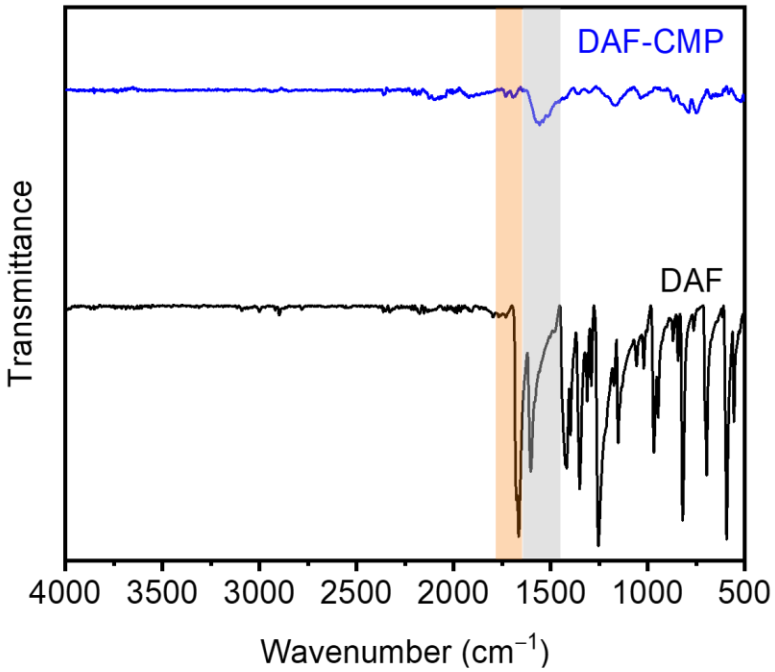

Figure S69. ATR-IR spectra of **DAF** and **DAF-CMP** synthesized with 5.00 equivalents of $ZnBr_2$ for 72 h. The indicated peaks correspond to carbonyl C=O (orange) and aromatic C=C (gray) stretches.

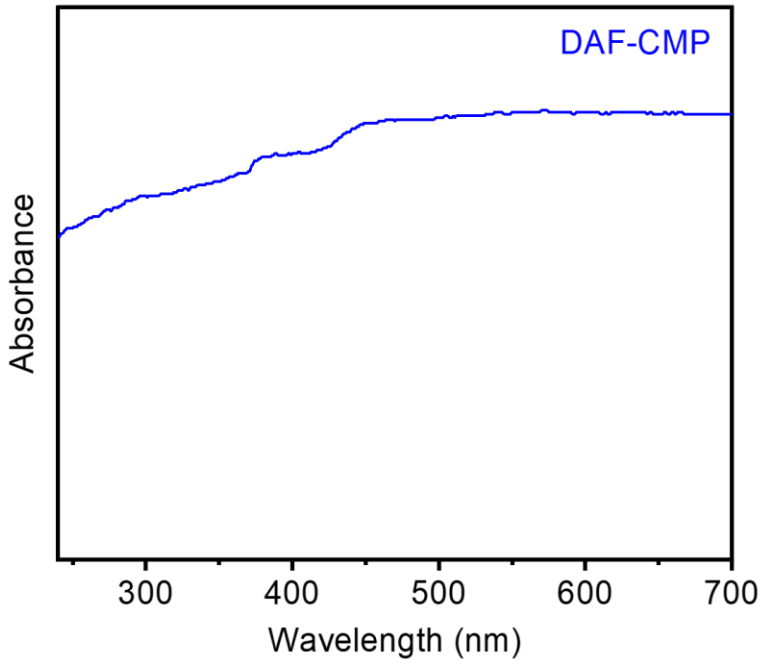

Figure S70. Diffuse reflectance UV-Vis absorbance spectrum of **DAF-CMP** synthesized with 5.00 equivalents of $ZnBr_2$ for 72 h.

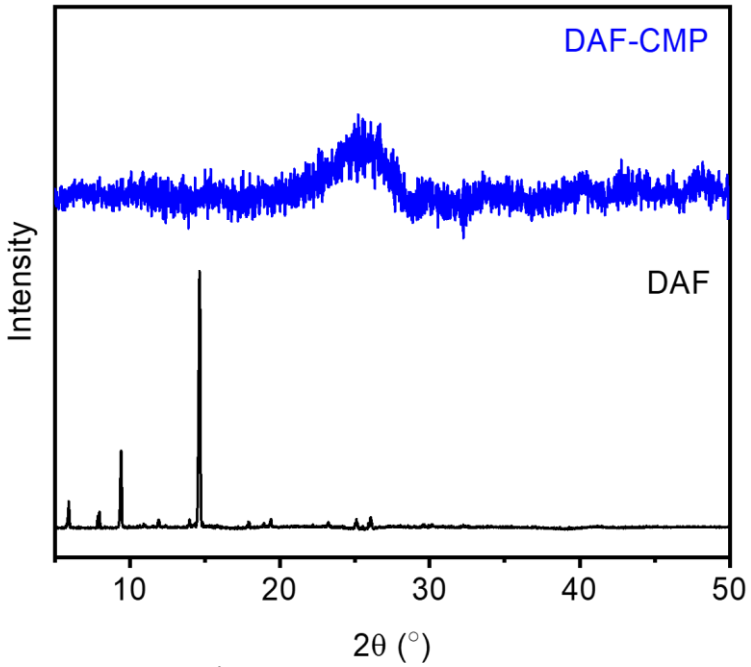

Figure S71. PXRD (λ = 1.5406 Å) patterns of **DAF** and **DAF-CMP** synthesized with 5.00 equivalents of $ZnBr_2$ for 72 h, indicating that **DAF-CMP** is an amorphous polymer.

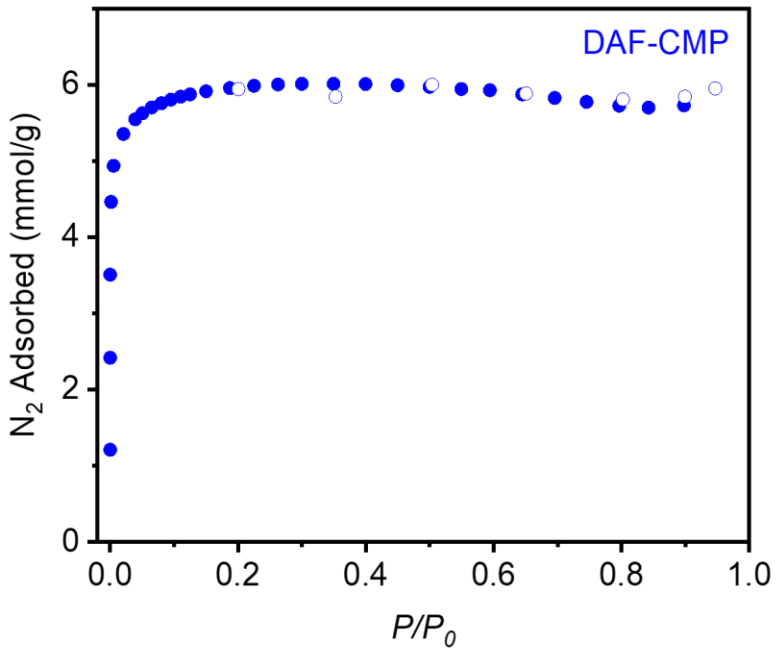

Figure S72. 77 K N_2 adsorption (filled circles) and desorption (open circles) isotherm for **DAF-CMP** synthesized with 5.00 equivalents of $ZnBr_2$ for 72 h. The Brunauer-Emmett-Teller (BET) and Langmuir surface areas were determined to be 522 ± 2 m^2/g and 567 ± 3 m^2/g, respectively.

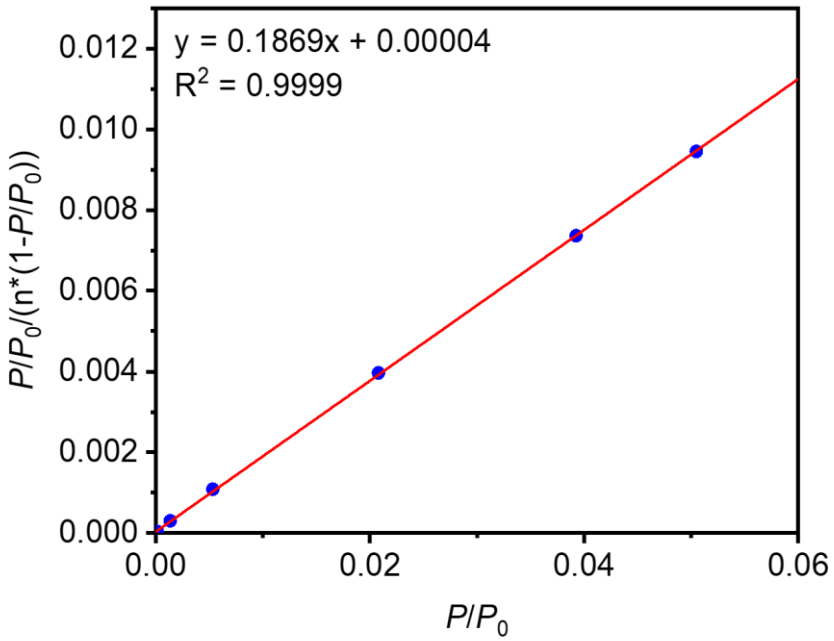

Figure S73. Linearized BET plot of **DAF-CMP** synthesized with 5.00 equivalents of $ZnBr_2$ for 72 h.

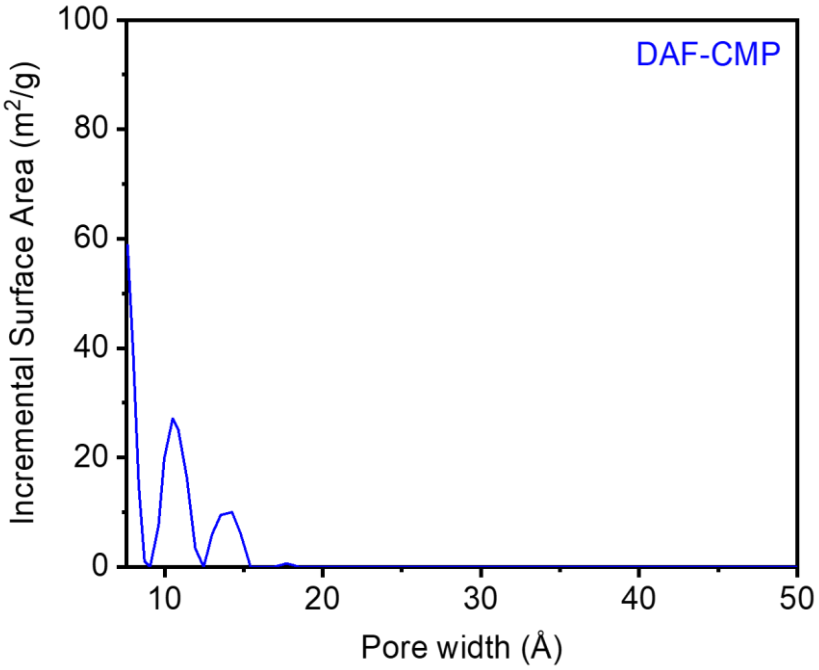

Figure S74. DFT-calculated pore size distribution of **DAF-CMP** synthesized with 5.00 equivalents of $ZnBr_2$ for 72 h, assuming a carbon slit pore geometry.

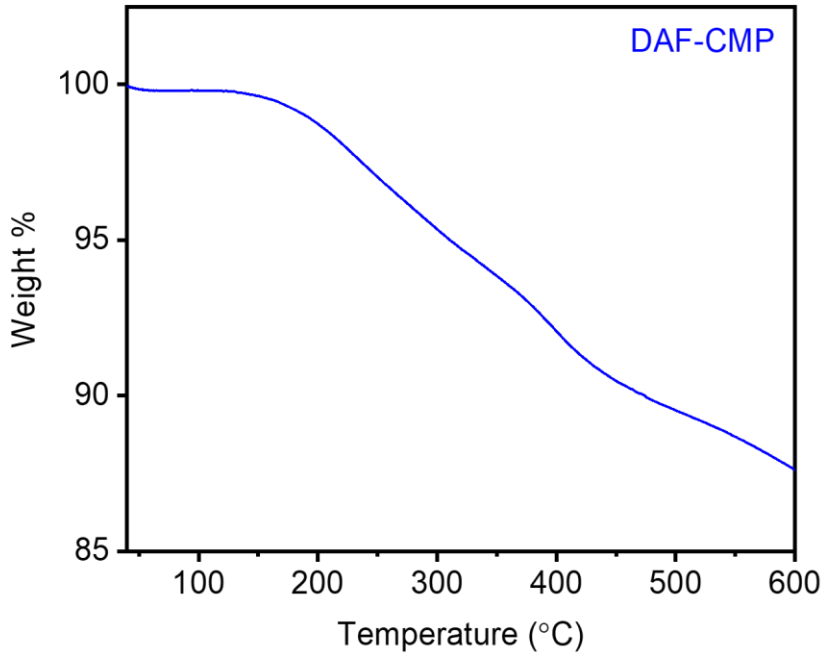

Figure S75. Thermogravimetric decomposition profile of **DAF-CMP** synthesized with 5.00 equivalents of $ZnBr_2$ for 72 h.

d. 1,3,5-triacetylbenzene trimerization.

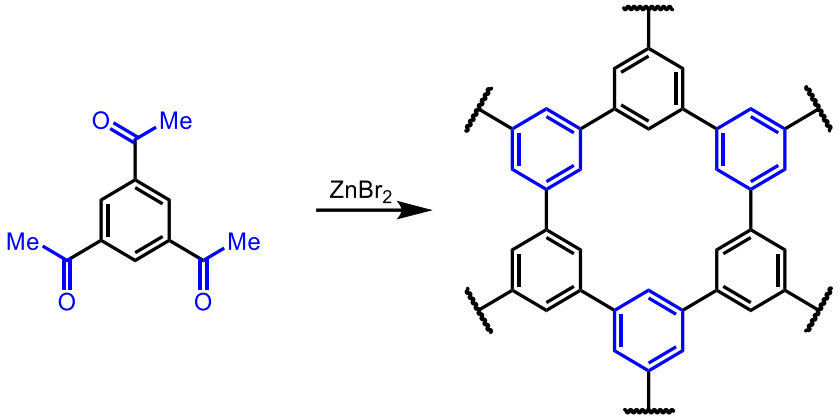

Figure S76. Synthesis of **TAB-CMP** from 1,3,5-triacetylbenzene (**TAB**).

Following the general procedure, three tubes were charged with 1,3,5-triacetylbenzene (**TAB**) (40.0 mg, 0.160 mmol, 1.00 equiv) and $ZnBr_2$ (221 mg, 0.979 mmol, 5.00 equiv), and the products were combined to yield **TAB-CMP** as a shiny black solid (93.9 mg, 106%). The >100% yield is likely due to residual untrimerized groups in the resulting polymer, which should increase its weight.

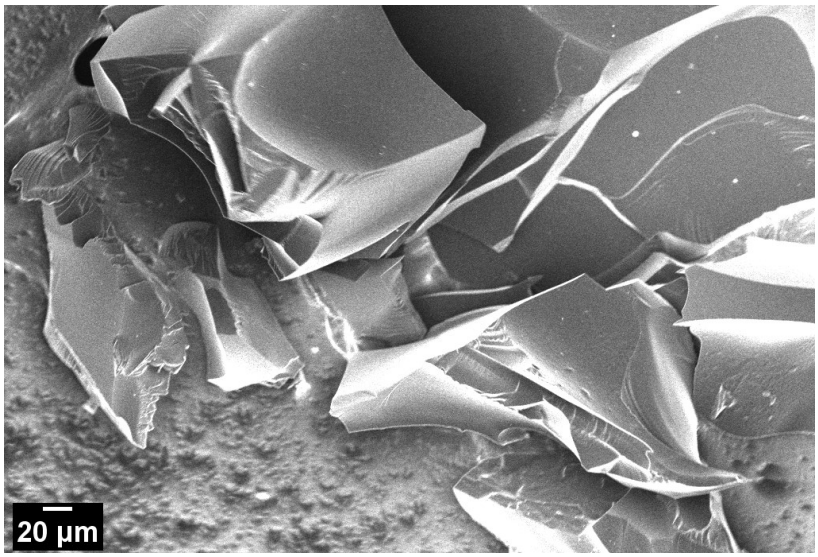

Figure S77. SEM image of **TAB-CMP** synthesized with 5.00 equivalents of $ZnBr_2$ for 72 h.

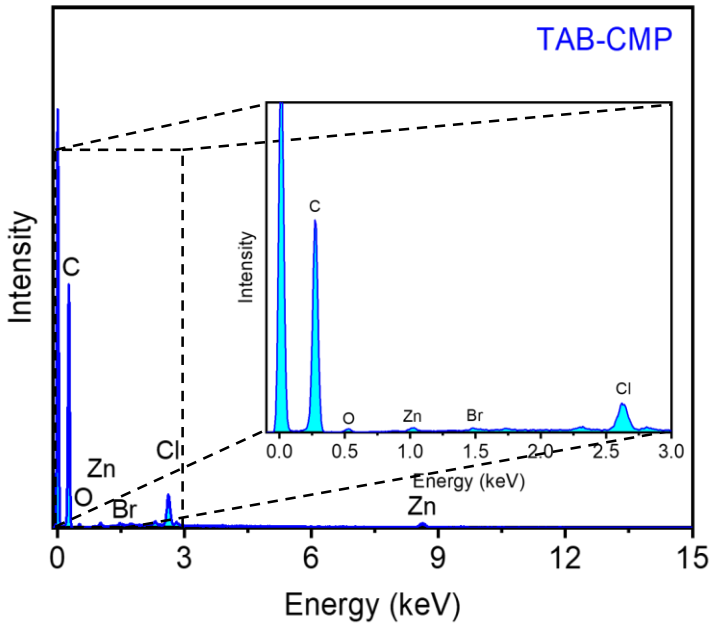

Figure S78. EDS spectrum of **TAB-CMP** synthesized with 5.00 equivalents of $ZnBr_2$ for 72 h. The residual Cl likely arises from the HCl wash used to remove zinc salts.

Table S11. Tabulated EDS data for **TAB-CMP** synthesized with 5.00 equivalents of $ZnBr_2$ for 72 h.

Element	Line Type	Wt %	Atomic %	Theoretical Atomic %[1]
C	K series	92.90	97.19	100.00
O	K series	1.76	1.39	0.00
Cl	K series	2.42	0.85	0.00
Zn	K series	2.85	0.56	0.00
Br	K series	0.07	0.01	0.00
Total:		100.00	100.00	100.00

[1]Excludes hydrogen.

Table S12. Tabulated combustion analysis data through combustion and ion chromatography for **TAB-CMP** synthesized with 5.00 equivalents of $ZnBr_2$ for 72 h.

Element	Wt %	Theoretical Wt %
C	87.05	95.97
H	4.03	4.03
Cl	1.88	0.00
N	0.25	0.00
Br	0.00	0.00
O and Zn	6.79[1]	0.00
Total:	100.00	100.00

[1]The remaining mass not attributed to C, H, Cl, and Br was assumed to come from Zn and O, as they were not directly analyzed during combustion analysis.

Table S13. Tabulated XPS data through for **TAB-CMP** synthesized with 5.00 equivalents of $ZnBr_2$ for 72 h.

Element	Peak label	Position	Atomic %
C	C 1s	532.00	89.74
O	O 1s	285.00	9.34
Cl	Cl 2p	198.00	0.65
Zn	Zn 2p	1022.00	0.16
Br	Br 3d	69.20	0.11
Total:			100.00

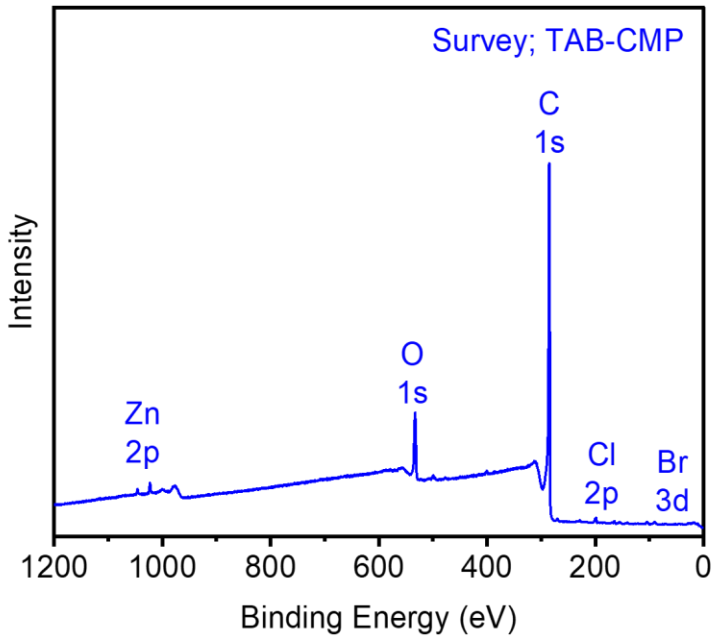

Figure S79. XPS spectrum for **TAB-CMP** synthesized with 5.00 equivalents of $ZnBr_2$ for 72 h. The relevant energies and transitions are labeled at the expected energies.

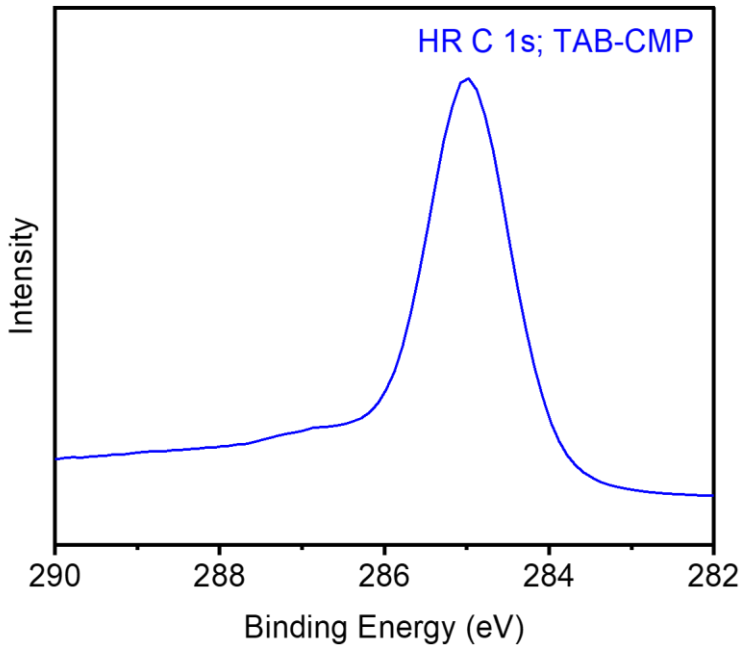

Figure S80. HR C 1s XPS spectrum of **TAB-CMP** synthesized with 5.00 equivalents of $ZnBr_2$ for 72 h.

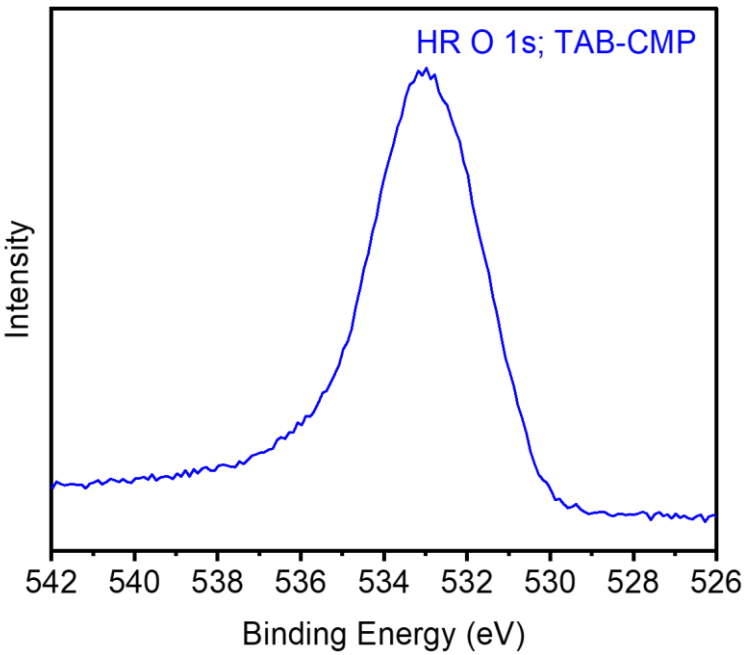

Figure S81. HR O 1s XPS spectrum of **TAB-CMP** synthesized with 5.00 equivalents of $ZnBr_2$ for 72 h.

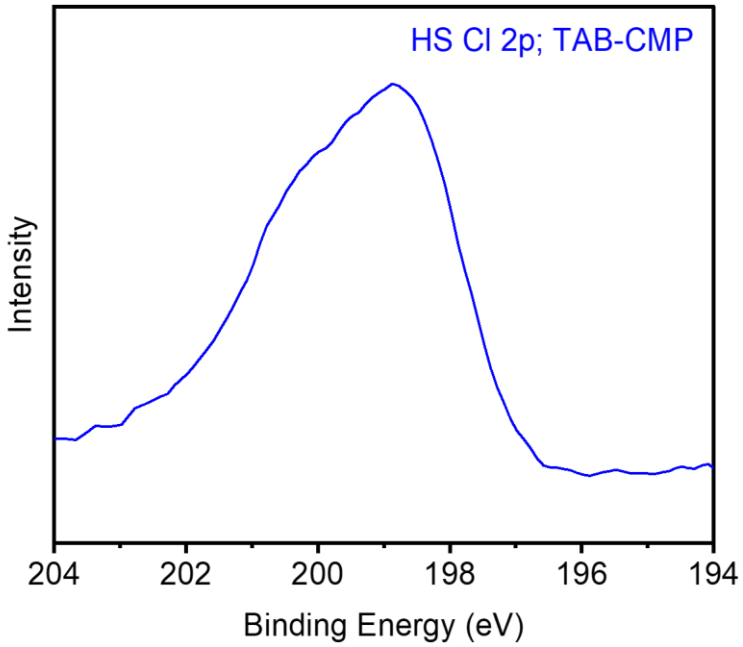

Figure S82. HS Cl 2p XPS spectrum of **TAB-CMP** synthesized with 5.00 equivalents of $ZnBr_2$ for 72 h.

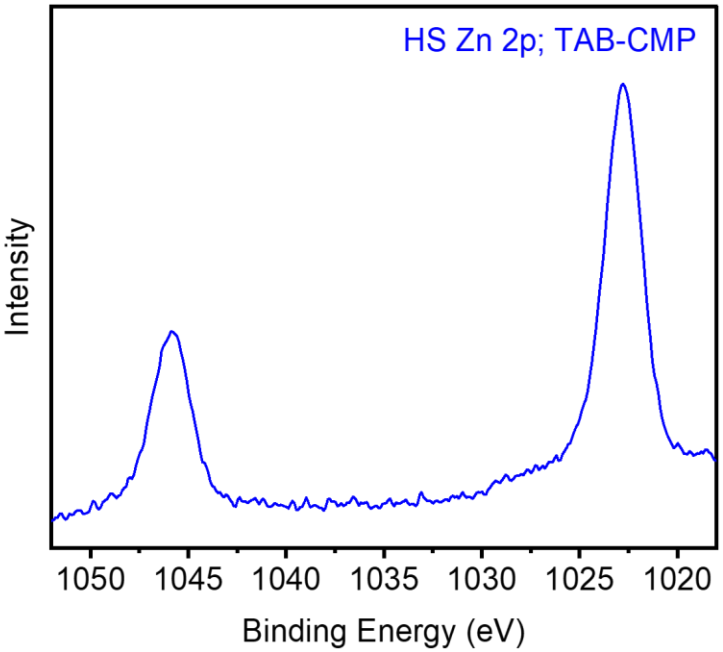

Figure S83. HS Zn 2p XPS spectrum of **TAB-CMP** synthesized with 5.00 equivalents of $ZnBr_2$ for 72 h.

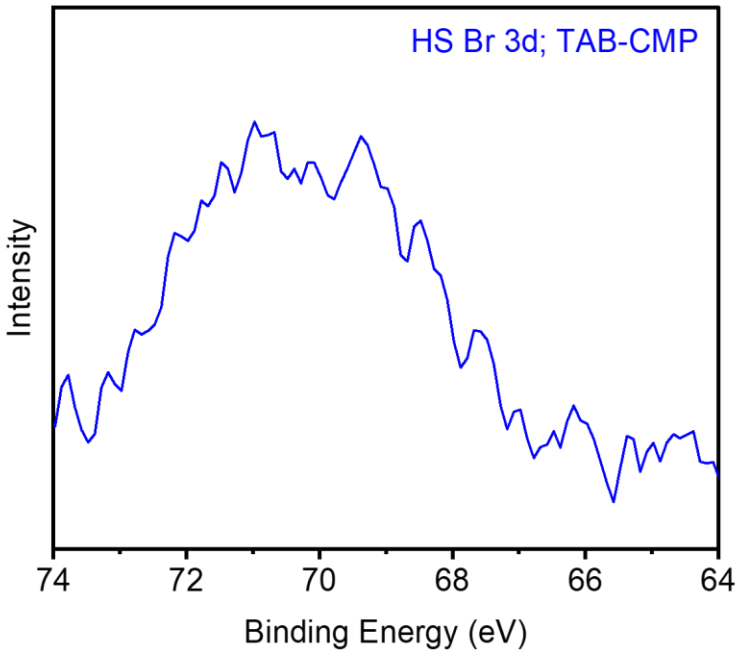

Figure S84. HS Br 3d XPS spectrum of **TAB-CMP** synthesized with 5.00 equivalents of $ZnBr_2$ for 72 h.

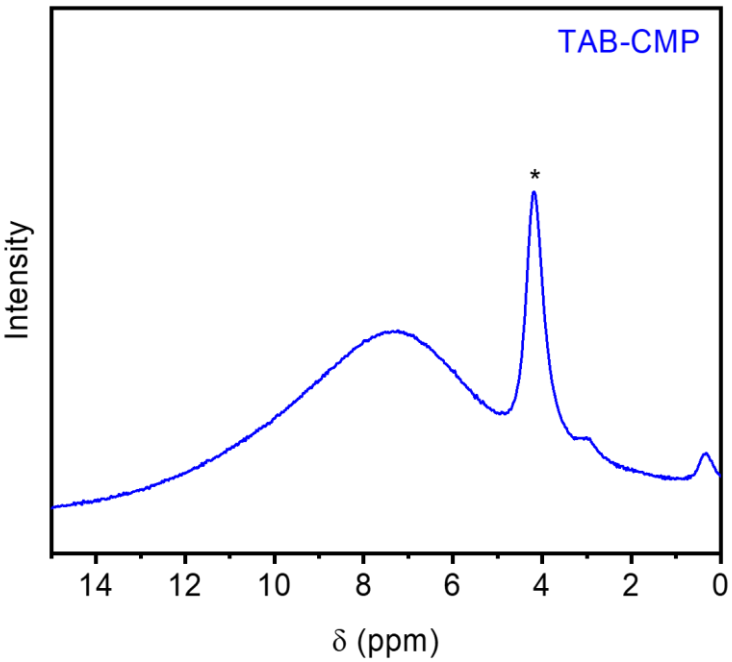

Figure S85. MAS ^1H SSNMR (500 MHz) spectrum of **TAB-CMP** synthesized with 5.00 equivalents of $ZnBr_2$ for 72 h, collected at a spinning speed of 20 kHz. The asterisk corresponds to adsorbed water.

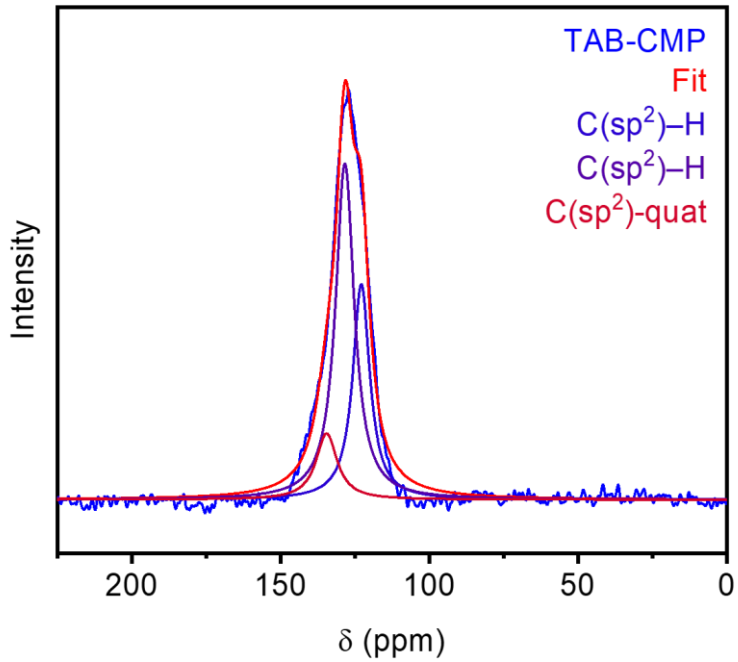

Figure S86. CP MAS ^{13}C SSNMR (125 MHz) spectrum of **TAB-CMP** synthesized with 5.00 equivalents of $ZnBr_2$ for 72 h with a ^{1}H–^{13}C contact time of 2 ms, collected at a spinning speed of 20 kHz. Deconvolution fits to the spectrum are shown.

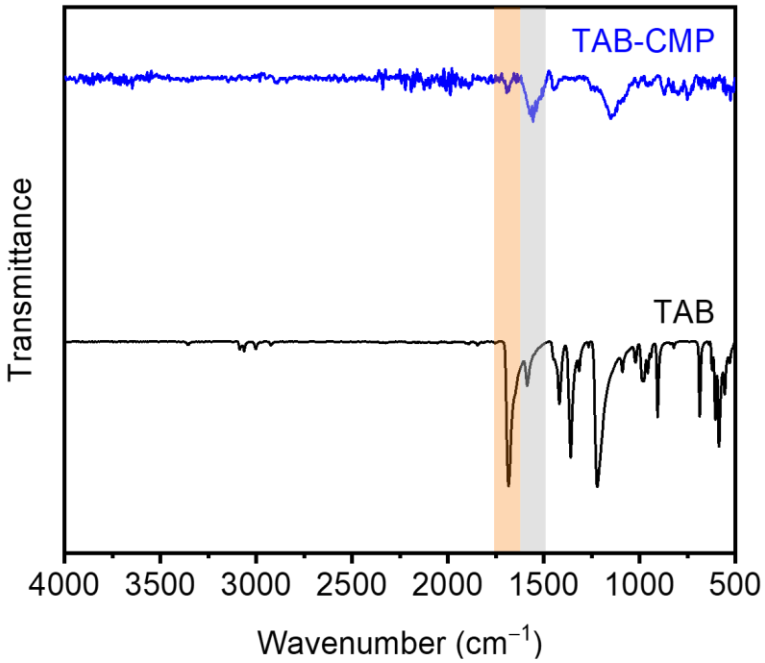

Figure S87. ATR-IR spectra of **TAB** and **TAB-CMP** synthesized with 5.00 equivalents of $ZnBr_2$ for 72 h. The indicated peaks correspond to carbonyl C=O (orange) and aromatic C=C (gray) stretches.

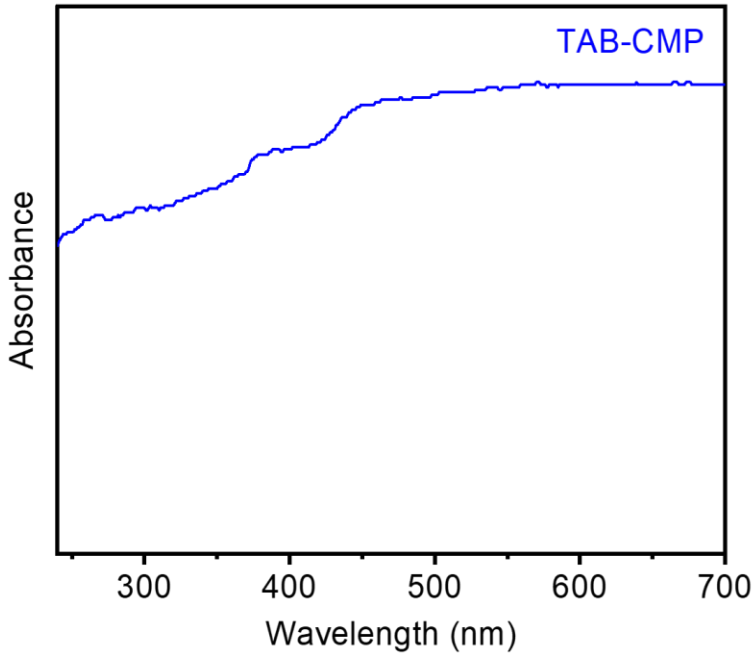

Figure S88. Diffuse reflectance UV-Vis absorbance spectrum of **TAB-CMP** synthesized with 5.00 equivalents of $ZnBr_2$ for 72 h.

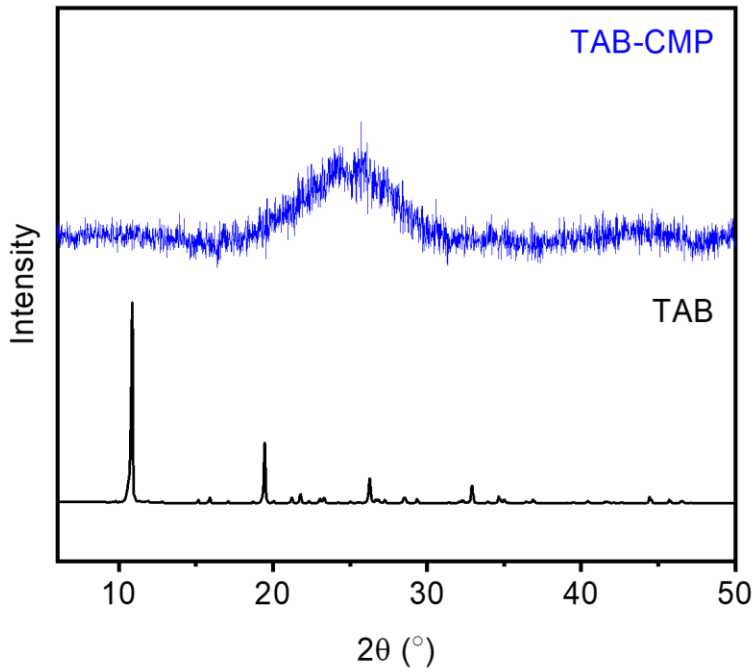

Figure S89. PXRD (λ = 1.5406 Å) patterns of **TAB** and **TAB-CMP** synthesized with 5.00 equivalents of $ZnBr_2$ for 72 h, indicating that **TAB-CMP** is an amorphous polymer.

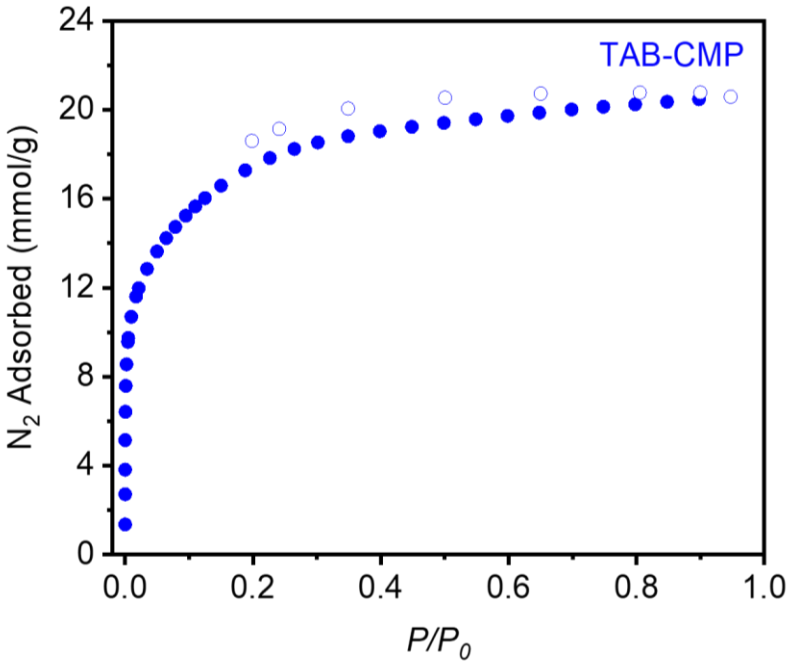

Figure S90. 77 K N_2 adsorption (filled circles) and desorption (open circles) isotherm for **TAB-CMP** synthesized with 5.00 equivalents of $ZnBr_2$ for 72 h. The Brunauer-Emmett-Teller (BET) and Langmuir surface areas were determined to be 1373 ± 11 m^2/g and 2001 ± 15 m^2/g, respectively.

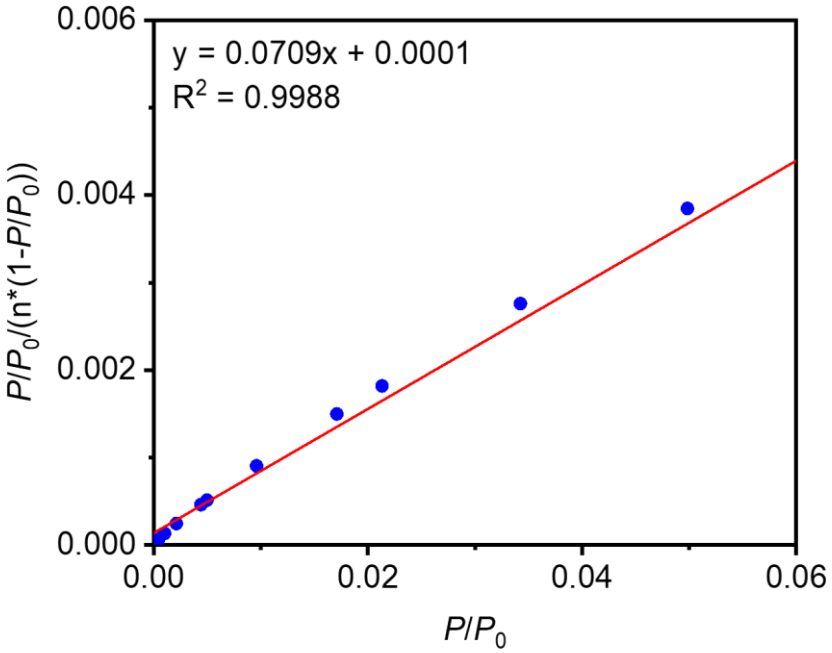

Figure S91. Linearized BET plot of **TAB-CMP** synthesized with 5.00 equivalents of $ZnBr_2$ for 72 h.

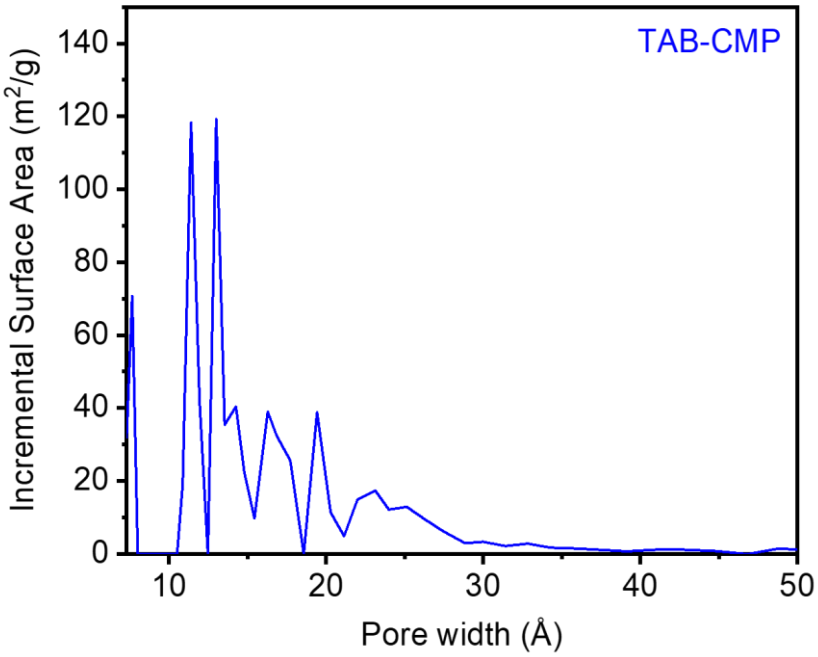

Figure S92. DFT-calculated pore size distribution of **TAB-CMP** synthesized with 5.00 equivalents of $ZnBr_2$ for 72 h, assuming a carbon slit pore geometry.

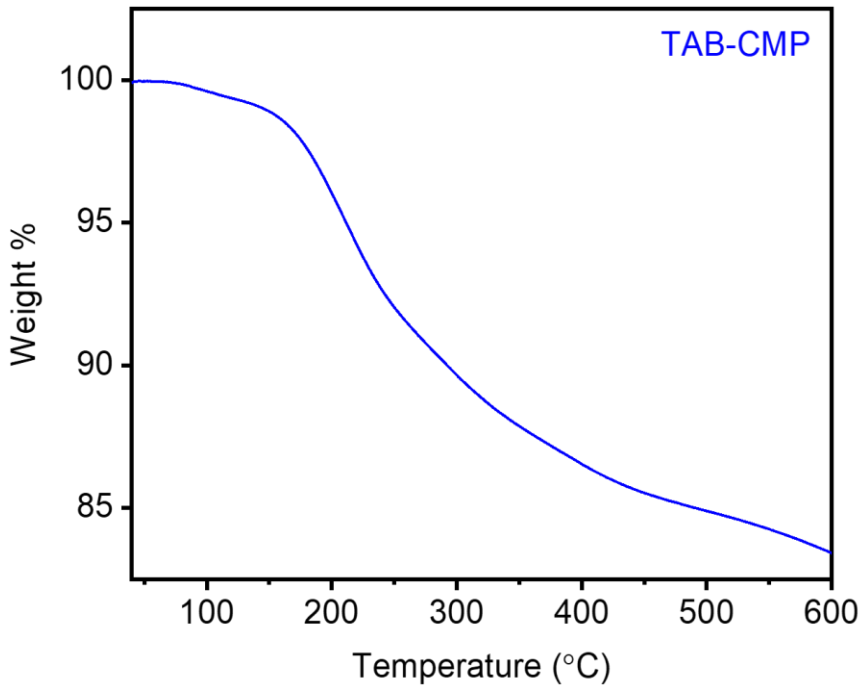

Figure S93. Thermogravimetric decomposition profile of **TAB-CMP** synthesized with 5.00 equivalents of $ZnBr_2$ for 72 h.

e. Tetrakis(4-acetylphenyl)methane trimerization.

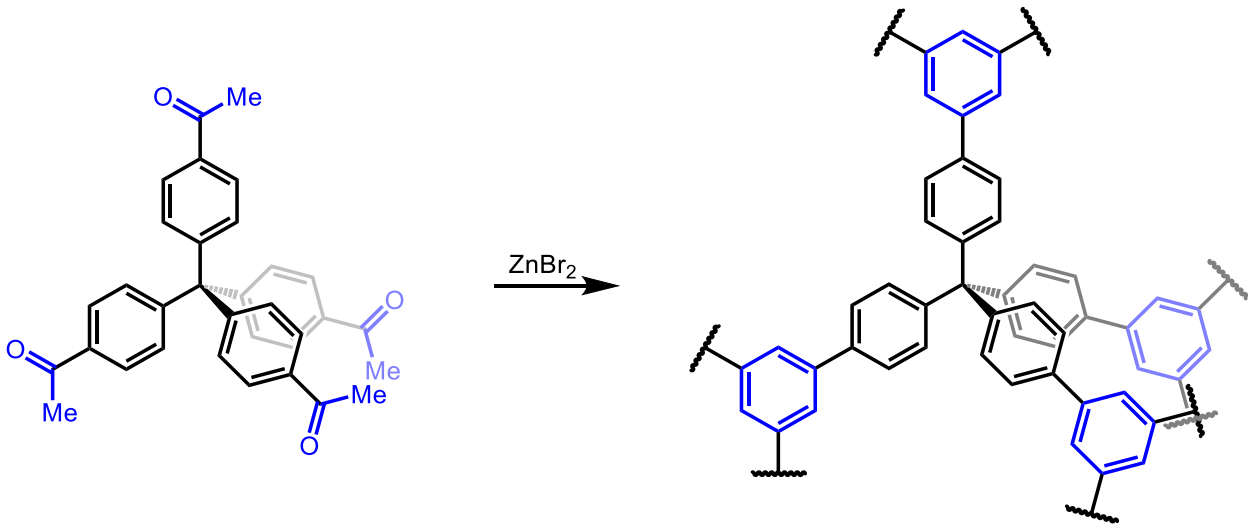

Figure S94. Synthesis of **TAPM-PAF** series from tetrakis(4-acetylphenyl)methane (**TAPM**) synthesized with 5.00 equivalents of $ZnBr_2$ for 72 h.

Following the general procedure, three tubes were charged with tetrakis(4-acetylphenyl)methane (**TAPM**) (40.0 mg, 0.0819 mmol, 1.00 equiv) and $ZnBr_2$ (92.2 mg, 0.409 mmol, 5.00 equiv), and the products were combined to yield **TAPM-PAF** as a shiny black solid (100 mg, 98%).

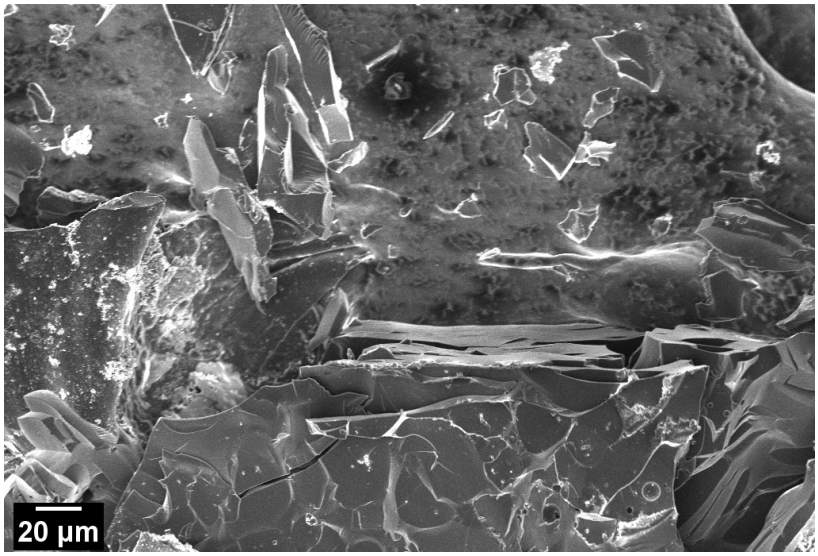

Figure S95. SEM image of **TAPM-PAF** synthesized with 5.00 equivalents of $ZnBr_2$ for 72 h.

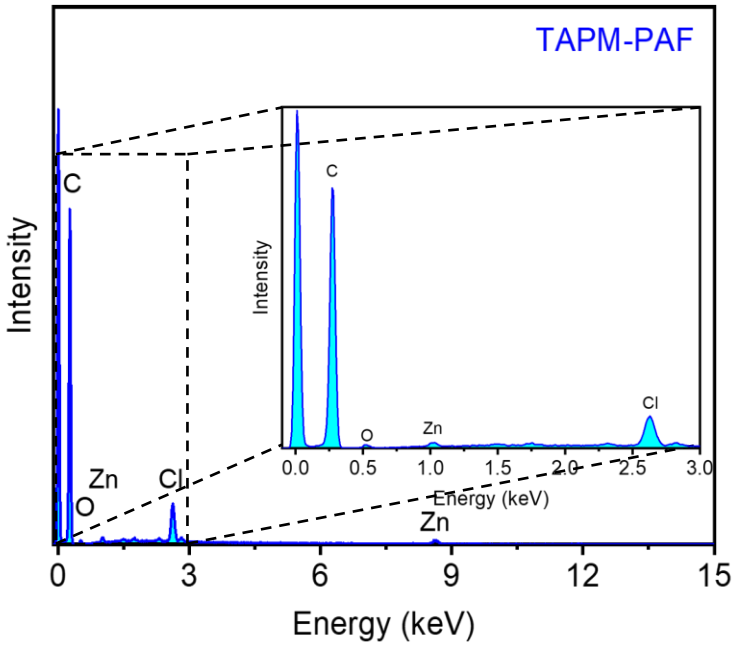

Figure S96. EDS spectrum of **TAPM-PAF** synthesized with 5.00 equivalents of $ZnBr_2$ for 72 h. The residual Cl likely arises from the HCl wash used to remove zinc salts.

Table S14. Tabulated EDS data for **TAPM-PAF** synthesized with 5.00 equivalents of $ZnBr_2$ for 72 h.

Element	Line Type	Wt %	Atomic %	Theoretical Atomic %[1]
C	K series	95.08	97.46	100.00
O	K series	2.25	1.75	0.00
Cl	K series	1.80	0.63	0.00
Zn	K series	0.87	0.16	0.00
Br	K series	0.00	0.00	0.00
Total:		100.00	100.00	100.00

[1]Excludes hydrogen.

Table S15. Tabulated combustion analysis data for **TAPM-PAF** synthesized with 5.00 equivalents of $ZnBr_2$ for 72 h.

Element	Wt %	Theoretical Wt %
C	85.85	95.16
H	4.14	4.84
Cl	1.65	0.00
N	0.67	0.00
Br	0.00	0.00
O and Zn	7.69[1]	0.00
Total:	100.00	100.00

[1]The remaining mass not attributed to C, H, Cl, and Br was assumed to come from Zn and O, as they were not directly analyzed during combustion analysis.

Table S16. Tabulated XPS data through for **TAPM-PAF** synthesized with 5.00 equivalents of $ZnBr_2$ for 72 h.

Element	Peak label	Position	Atomic %
C	C 1s	533.60	89.11
O	O 1s	285.00	10.30
Cl	Cl 2p	197.60	0.50
Zn	Zn 2p	1021.60	0.06
Br	Br 3d	70.80	0.02
Total:			100.00

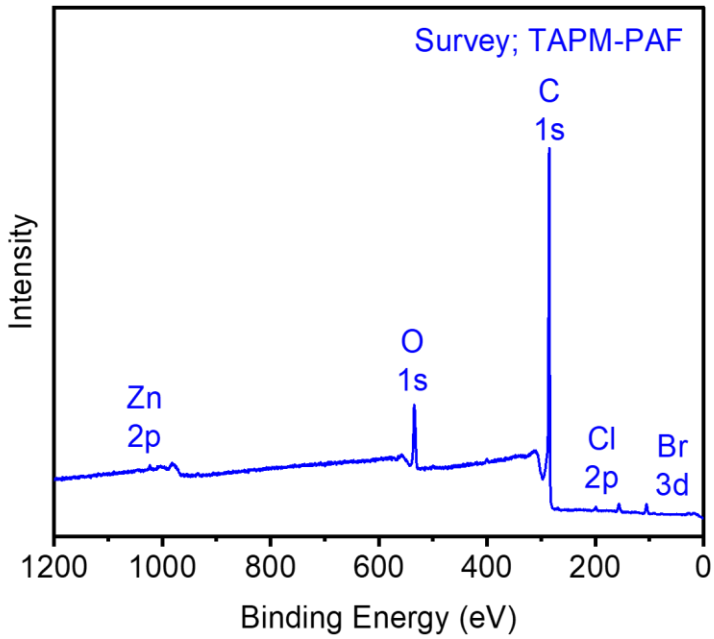

Figure S97. XPS spectrum for **TAPM-PAF** synthesized with 5.00 equivalents of $ZnBr_2$ for 72 h. The relevant energies and transitions are labeled at the expected energies.

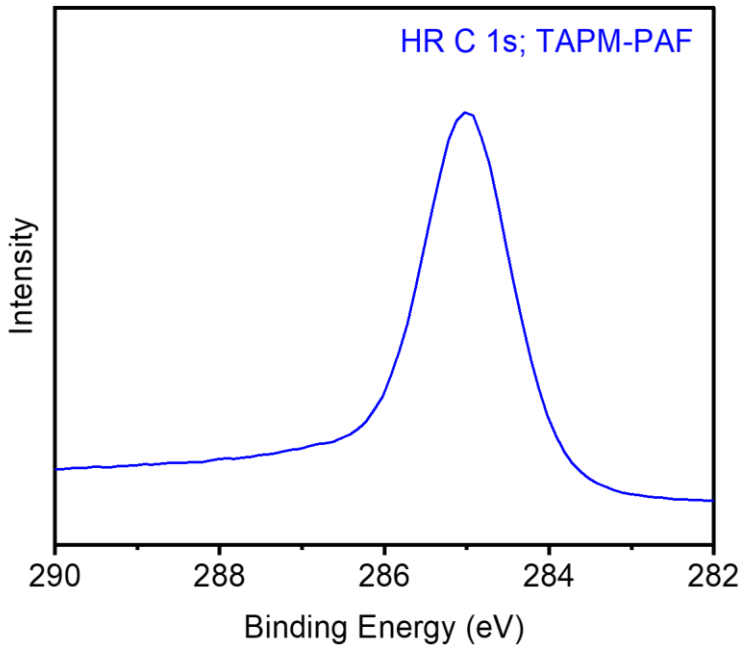

Figure S98. HR C 1s XPS spectrum of **TAPM-PAF** synthesized with 5.00 equivalents of $ZnBr_2$ for 72 h.

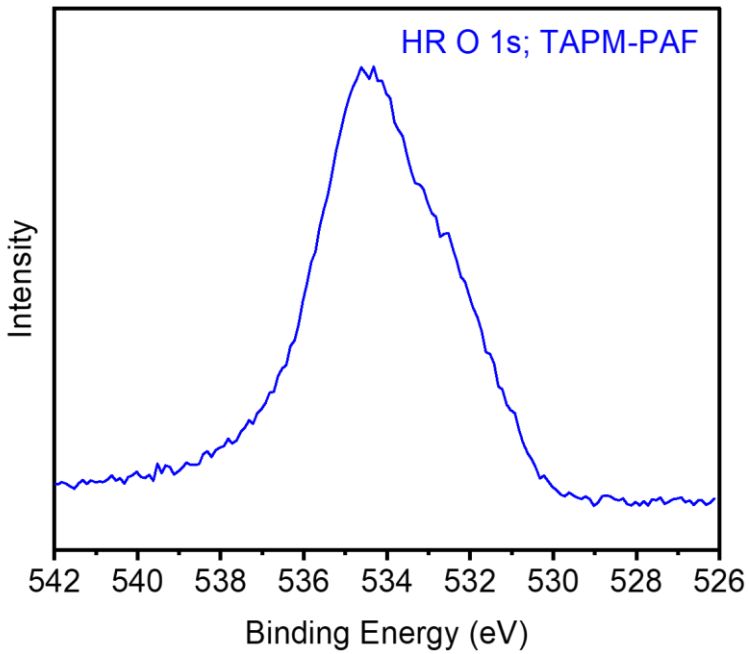

Figure S99. HR O 1s XPS spectrum of **TAPM-PAF** synthesized with 5.00 equivalents of $ZnBr_2$ for 72 h.

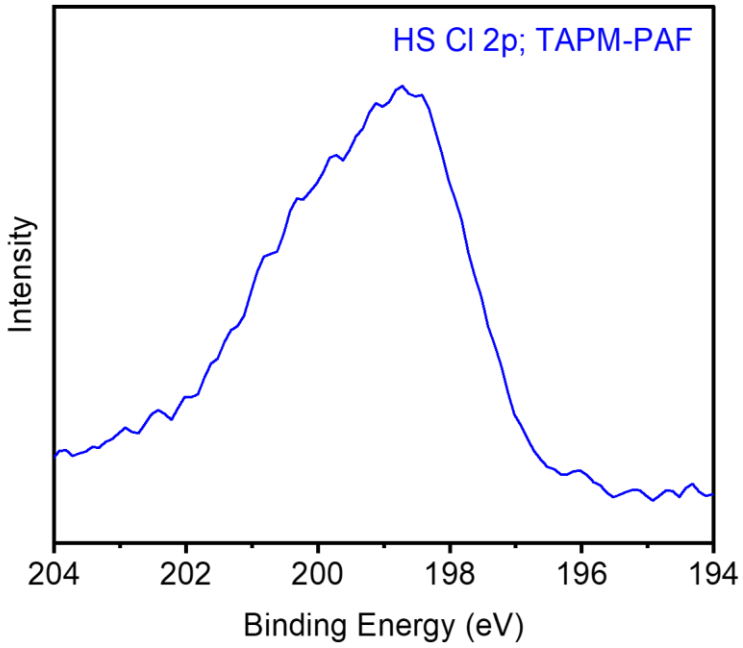

Figure S100. HS Cl 2p XPS spectrum of **TAPM-PAF** synthesized with 5.00 equivalents of $ZnBr_2$ for 72 h.

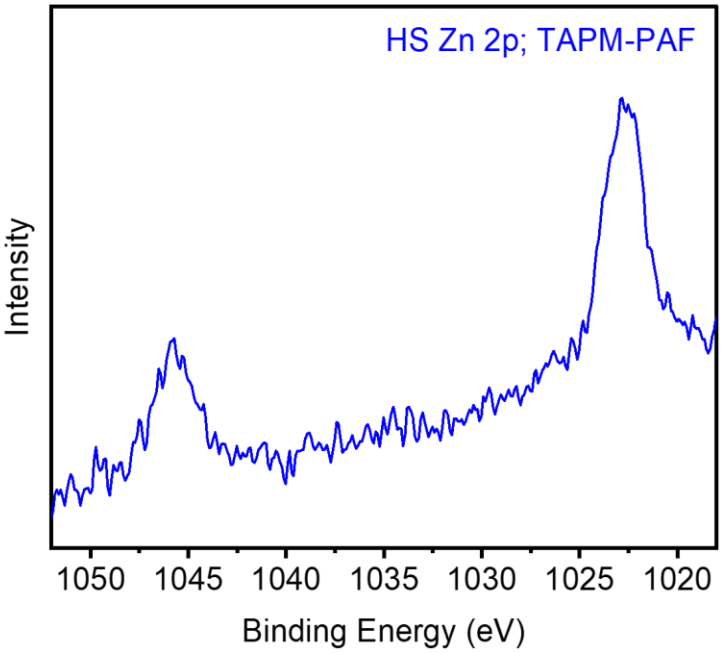

Figure S101. HS Zn 2p XPS spectrum of **TAPM-PAF** synthesized with 5.00 equivalents of $ZnBr_2$ for 72 h.

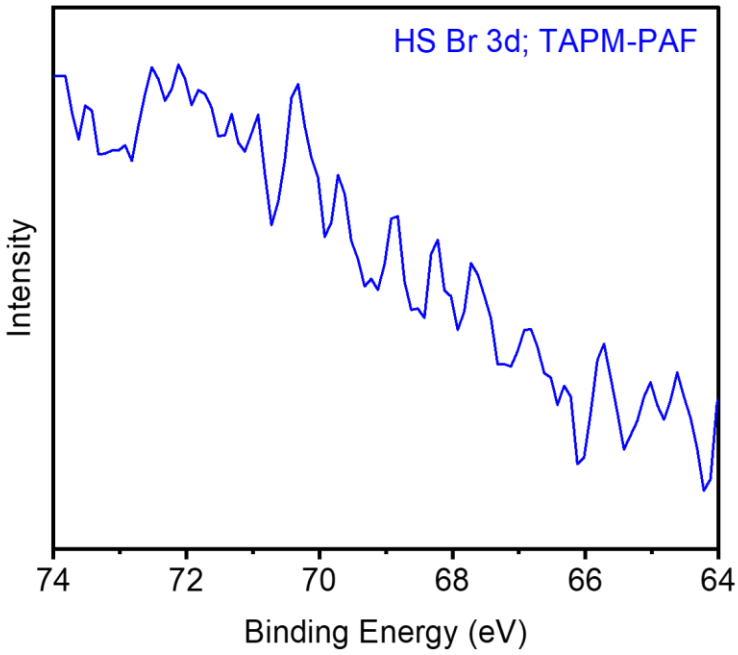

Figure S102. HS Br 3d XPS spectrum of **TAPM-PAF** synthesized with 5.00 equivalents of $ZnBr_2$ for 72 h.

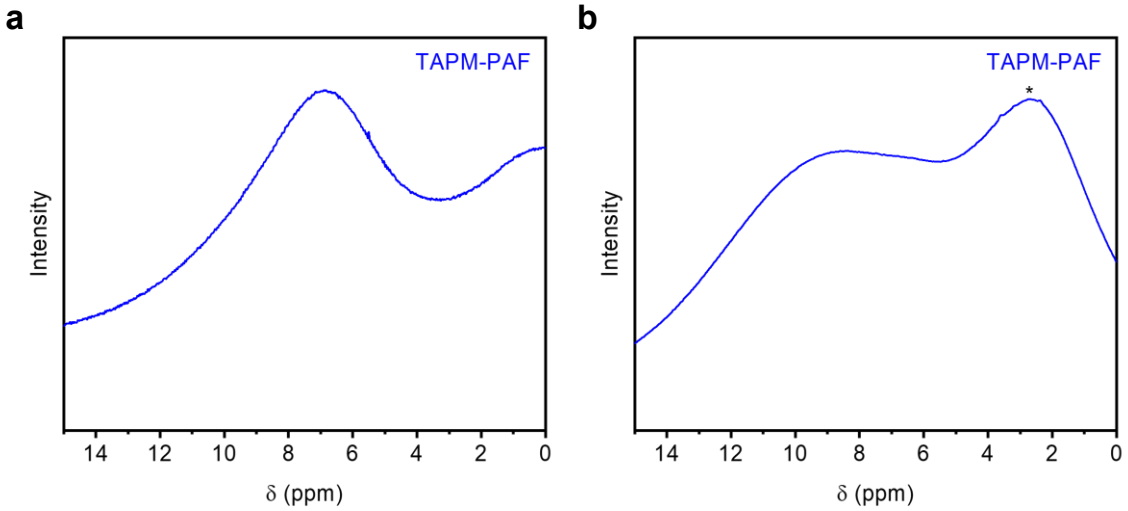

Figure S103. MAS ^{1}H SSNMR spectra at (a) 500 MHz and (b) 400 MHz spectra of **TAPM-PAF** synthesized with 5.00 equivalents of $ZnBr_2$ for 72 h, collected at a spinning speed of 20 kHz. The asterisk (b) corresponds to residual solvent.

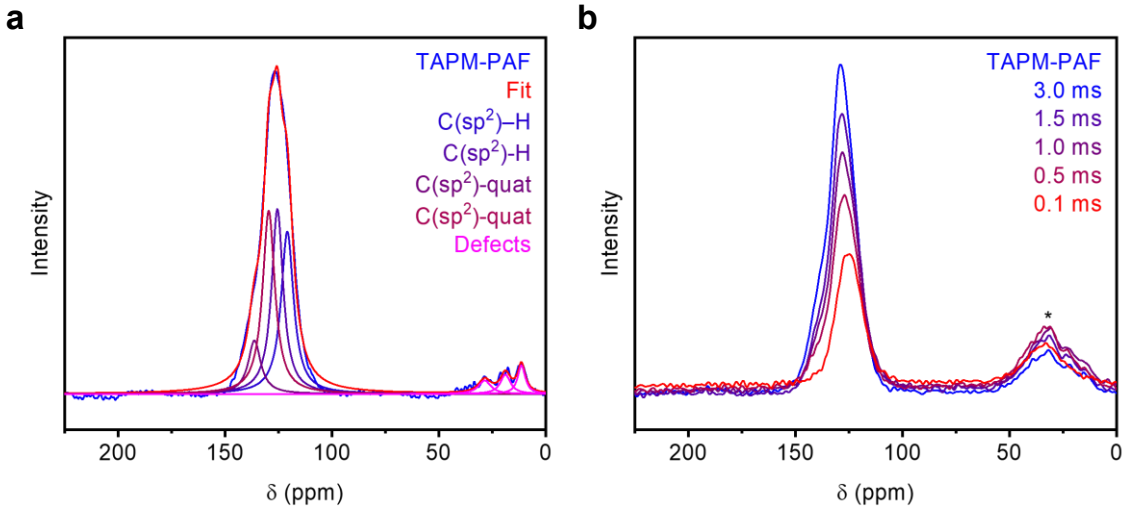

Figure S104. CP MAS ^{13}C SSNMR spectra at (a) 125 MHz and (b) 100 MHz of **TAPM-PAF** synthesized with 5.00 equivalents of $ZnBr_2$ for 72 h with a ^{1}H–^{13}C contact time of 5 ms for (a), or at the listed contact times in (b), collected at a spinning speed of 20 kHz. Deconvolution fits to the 125 MHz spectrum (a) are shown. The sp^3 quaternary carbon was not observed, likely due to the combination of the expectedly weak signal and partial carbonization.[7] The asterisk (b) corresponds to residual solvent.

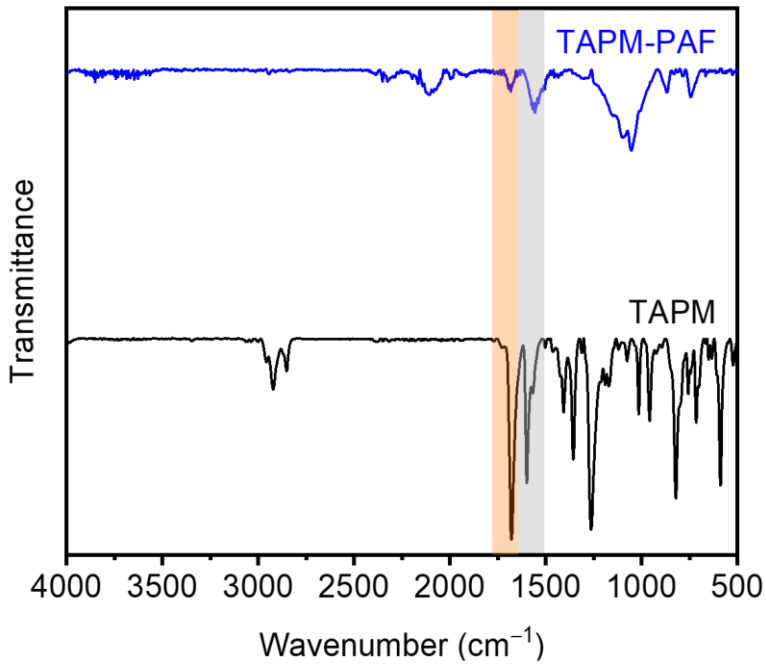

Figure S105. ATR-IR spectra of **TAPM** and **TAPM-PAF** synthesized with 5.00 equivalents of $ZnBr_2$ for 72 h. The indicated peaks correspond to carbonyl C=O (orange) and aromatic C=C (gray) stretches.

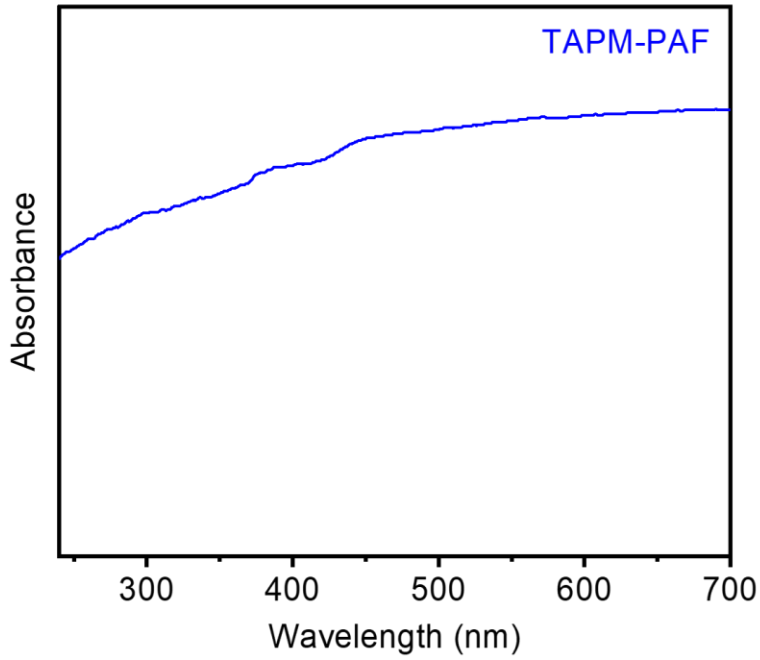

Figure S106. Diffuse reflectance UV-Vis absorbance spectrum of **TAPM-PAF** synthesized with 5.00 equivalents of $ZnBr_2$ for 72 h.

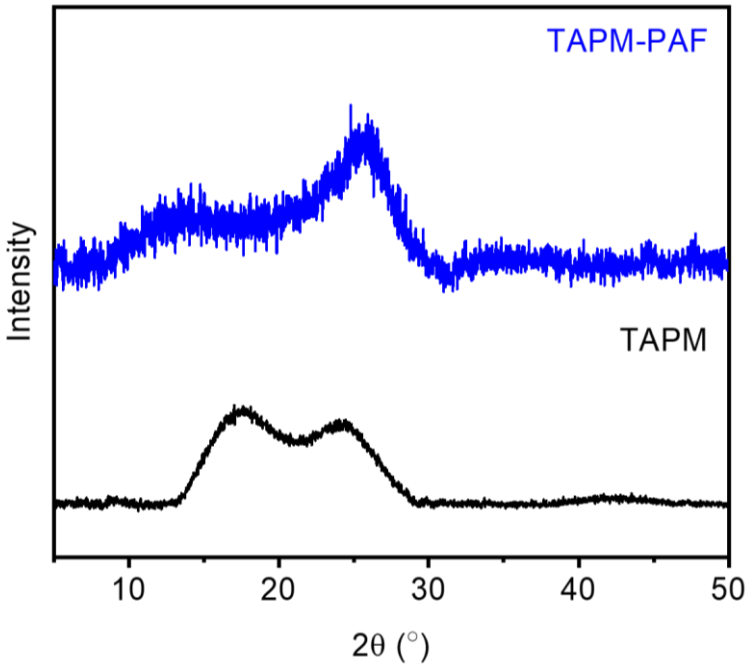

Figure S107. PXRD (λ = 1.5406 Å) patterns of **TAPM** and **TAPM-PAF** synthesized with 5.00 equivalents of $ZnBr_2$ for 72 h, indicating that **TAPM-PAF** is an amorphous polymer.

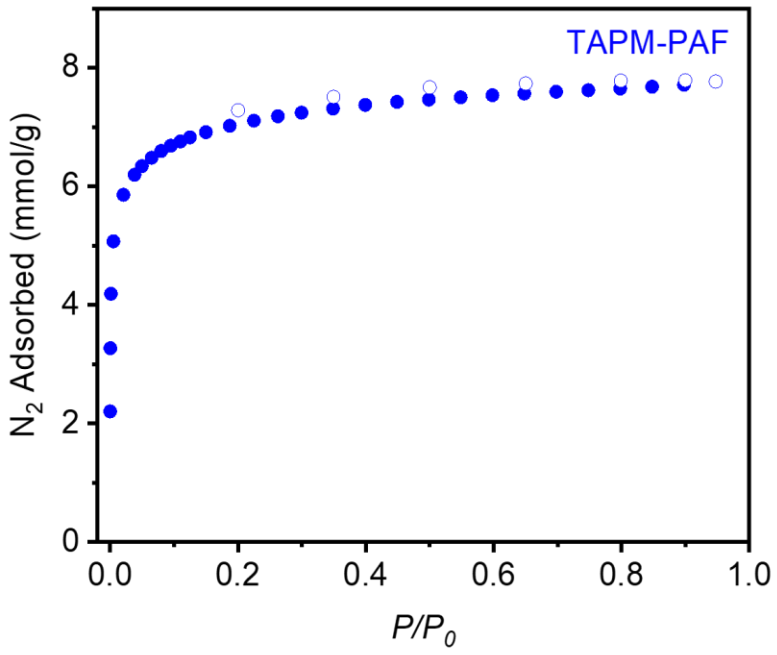

Figure S108. 77 K N_2 adsorption (filled circles) and desorption (open circles) isotherm for **TAPM-PAF** synthesized with 5.00 equivalents of $ZnBr_2$ for 72 h. The Brunauer-Emmett-Teller (BET) and Langmuir surface areas were determined to be 594 ± 3 m^2/g and 755 ± 3 m^2/g, respectively.

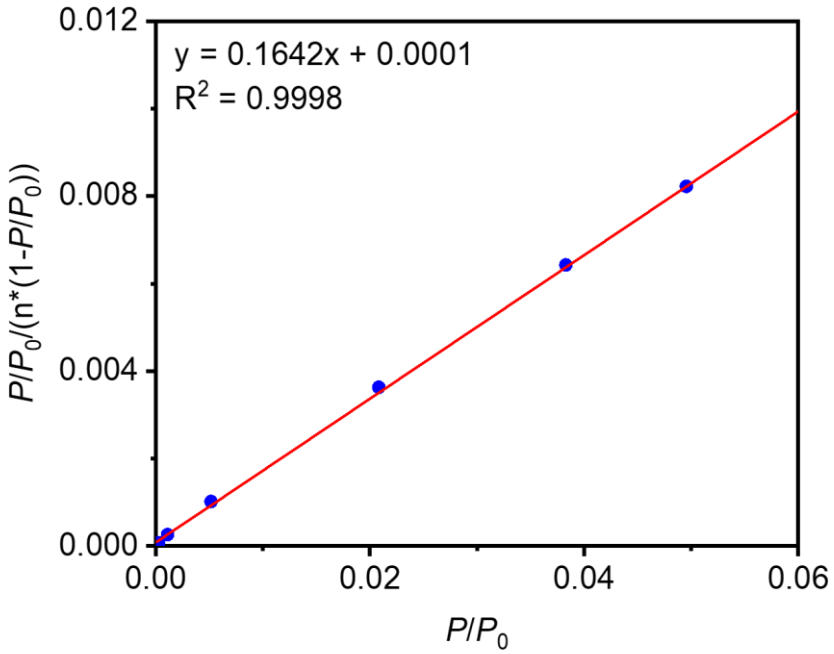

Figure S109. Linearized BET plot of **TAPM-PAF** synthesized with 5.00 equivalents of $ZnBr_2$ for 72 h.

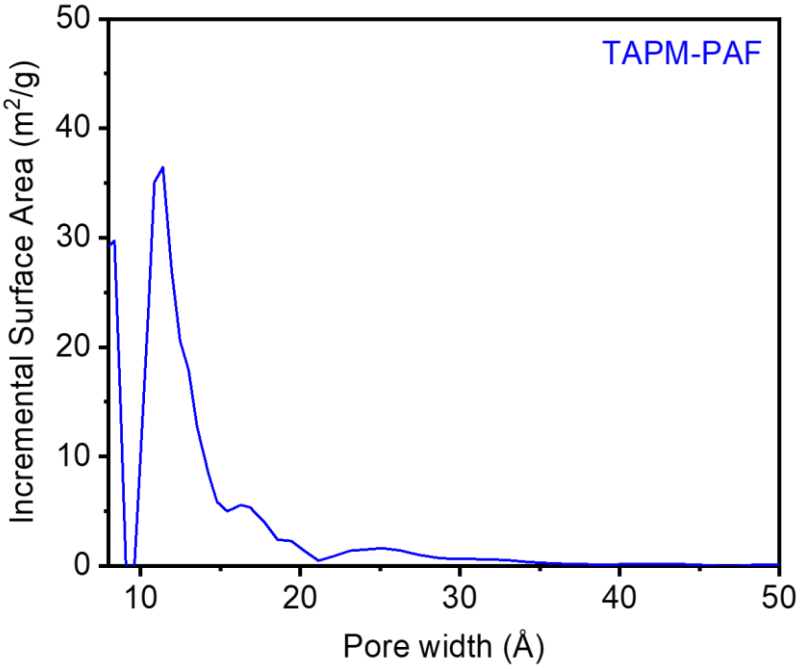

Figure S110. DFT-calculated pore size distribution of **TAPM-PAF** synthesized with 5.00 equivalents of $ZnBr_2$ for 72 h, assuming a carbon slit pore geometry.

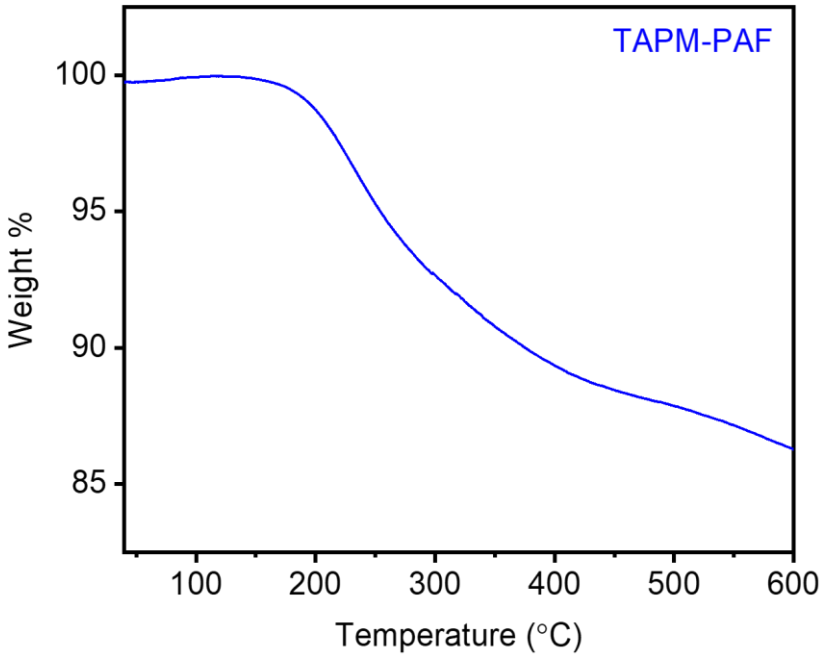

Figure S111. Thermogravimetric decomposition profile of **TAPM-PAF** synthesized with 5.00 equivalents of $ZnBr_2$ for 72 h.

f. 1,4-dicyanobenzene trimerization.

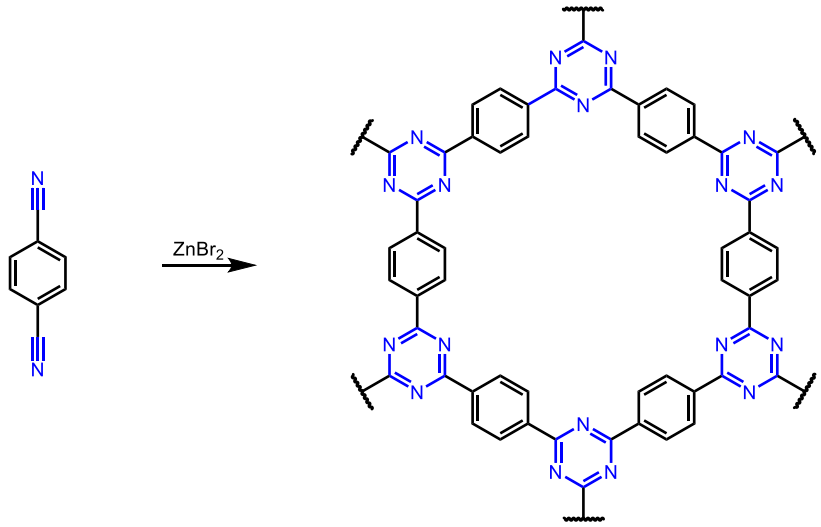

Figure S112. Synthesis of DCNB-CTF-A from 1,4-dicyanobenzene (DCNB).

Adapted from the literature procedure using $ZnCl_2$.[8] Three 10 mm diameter borosilicate glass tubes were charged with 1,4-dicyanobenzene (**DCNB**) (40.0 mg, 0.312 mmol, 1.00 equiv) and $ZnBr_2$ (351.5 mg, 1.560 mmol, 5.00 equiv) in a N_2-filled glovebox. The tubes were evacuated (<100 mTorr) and then flame-sealed under high vacuum using a natural gas torch and a custom-built apparatus (**Figure S7**). The tubes were placed in a furnace and heated at 400 °C for 40 h (temperature sequence: ramp up to 400 °C over 6 h from room temperature, hold at 400 °C for 40 h, cool down to 25 °C over 6 h). The time and temperature were taken directly from the literature for consistency.[8] The tubes were cooled to room temperature and snapped using a glass tube cutter. The black reaction mixture was scraped out of the tubes with a spatula, using water (10 mL) to help slide the mixture off the tube walls. The reaction mixtures from all three tubes were first grounded carefully by pressing the spatula on the solid, and the resulting solid was then rinsed with distilled water (10 mL). The mixture was transferred to a 24 mL scintillation vial and suspended in 3 M HCl (20 mL). The suspension was allowed to stir for 15 h. The heterogeneous mixture was filtered, and the resulting shiny black solid was rinsed with distilled water (20 mL) and then THF (20 mL). The solid was oven-dried under vacuum at 150 °C overnight and then allowed to cool to room temperature. Next, 1 M HCl (20 mL) was added, and the mixture was allowed to stir for 24 h at room temperature. The heterogenous mixture was filtered, and the black solid was transferred back to the same 24 mL scintillation vial filled with fresh 1 M HCl (20 mL) and allowed to stir for 24 h at room temperature. This soaking process was repeated one more time for a total of three HCl soaks. After the third HCl soak, the heterogenous mixture was filtered, and the shiny black solid was transferred back to the same 24 mL scintillation vial filled with distilled water (20 mL). The vial was allowed to stir for 24 h at room temperature, at which time the heterogenous mixture was filtered. The shiny black solid was then transferred back to the initial scintillation vial with the help of acetone (5 mL). The acetone was decanted, and the solid was oven-dried under vacuum at 150 °C overnight and allowed to cool to room temperature prior to

characterization. The products were combined to yield **DCNB-CTF-A** as a shiny black solid (108 mg, 90%).

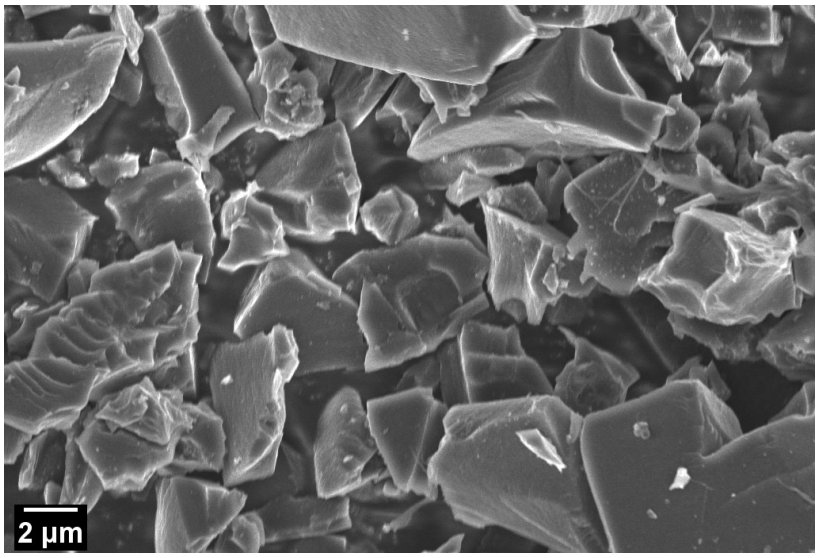

Figure S113. SEM image of **DCNB-CTF-A** synthesized with 5.00 equivalents of $ZnBr_2$ for 72 h.

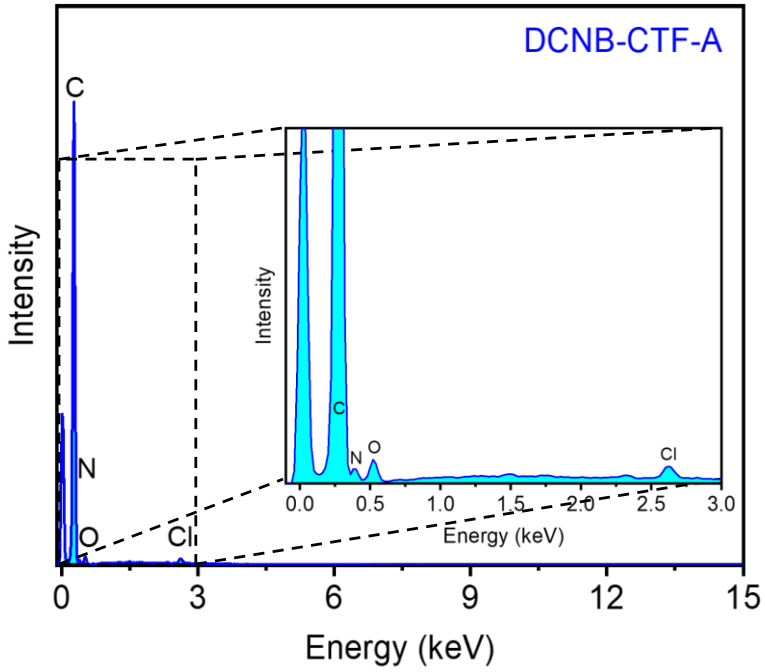

Figure S114. EDS spectrum for **DCNB-CTF-A** synthesized with 5.00 equivalents of $ZnBr_2$ for 72 h. The residual Cl likely arises from the HCl wash used to remove zinc salts.

EDS of light elements ($Z < 30$) is challenging, which likely accounts in part for the low amounts of detected N in this experiment.[9]

Table S17. Tabulated EDS data for **DCNB-CTF-A** synthesized with 5.00 equivalents of $ZnBr_2$ for 72 h.

Element	Line Type	Wt %	Atomic %	Theoretical Atomic %[1]
C	K series	92.83	94.10	80.00
N	K series	4.90	4.26	20.00
O	K series	1.99	1.54	0.00
Cl	K series	0.28	0.10	0.00
Zn	K series	0	0.00	0.00
Br	K series	0	0.00	0.00
Total:		100.00	100.00	100.00

[1]Excludes hydrogen.

Table S18. Tabulated combustion analysis data for **DCNB-CTF-A** synthesized with 5.00 equivalents of $ZnBr_2$ for 72 h.

Element	Wt %	Theoretical Wt %
C	64.79	73.82
N	11.22	21.53
H	2.60	4.65
Cl	1.20	0.00
Br	0.00	0.00
O and Zn	20.19[1]	0.00
Total:	100.00	100.00

[1]The remaining mass not attributed to C, H, Cl, and Br was assumed to come from Zn and O, as they were not directly analyzed during combustion analysis.

Notably, the observed C:N ratio from combustion analysis (5.7:1) is comparable to that reported in the literature for a sample prepared with $ZnCl_2$ (5.1:1).[8] Both values are higher than the theoretical value (3.4:1), indicating that some graphitization occurs under both conditions.[10]

Table S19. Tabulated XPS data for **DCNB-CTF-A** synthesized with 5.00 equivalents of $ZnBr_2$ for 72 h.

Element	Peak label	Position	Atomic %
C	C 1s	284.40	74.93
N	N 1s	399.20	7.75
O	O 1s	532.40	16.75
Cl	Cl 2p	200.40	0.55
Zn	Zn 2p	-	0.00
Br	Br 3d	-	0.00
Total:			100.00

The O signal detected by XPS is significantly higher in this sample than in the other samples, despite negligible Zn content and the fact that neither the starting material nor product contain O atoms. This is likely due to strongly adsorbed water, as supported by the ^{1}H SSNMR spectrum under ambient conditions (**Figure S122**). Furthermore, XPS is a highly surface sensitive technique that can change in composition of light elements depending on ambient conditions.[11]

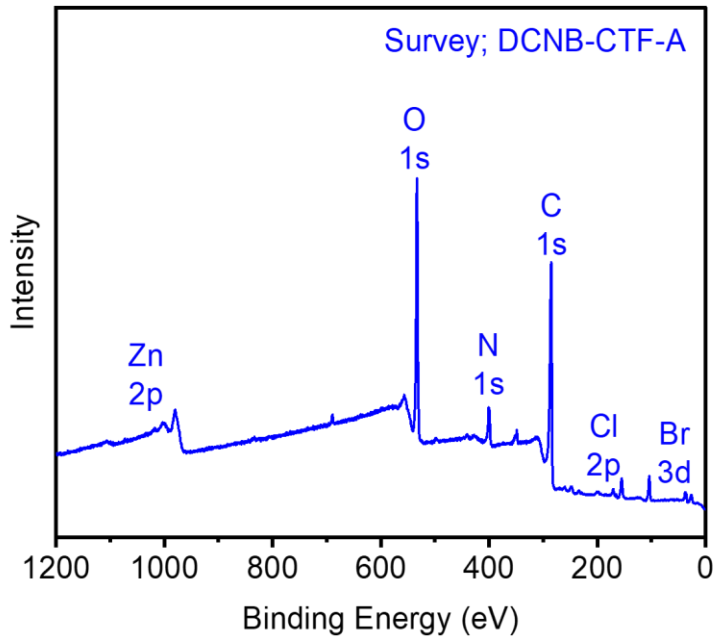

Figure S115. XPS spectrum for **DCNB-CTF-A** synthesized with 5.00 equivalents of $ZnBr_2$ for 40 h. The relevant energies and transitions are labeled at the expected energies.

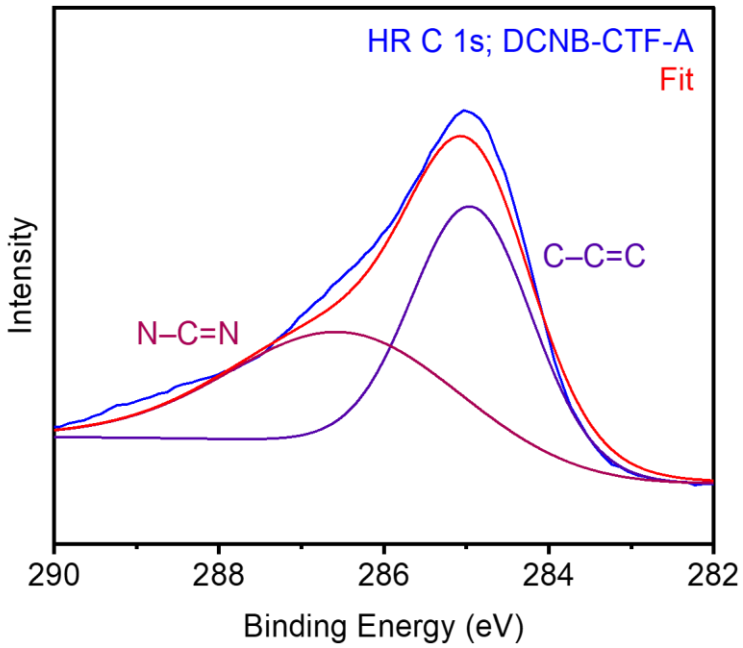

Figure S116. HR C 1s XPS spectrum of **DCNB-CTF-A** synthesized with 5.00 equivalents of $ZnBr_2$ for 40 h. The carbon peak is noticeably broader than that in the other CMPs and **TAPM-PAF**, and it can be fitted and deconvoluted with two distinguishable carbon environments centered at 285.0 eV (C–C=C) and 286.6 eV (N–C=N), respectively.

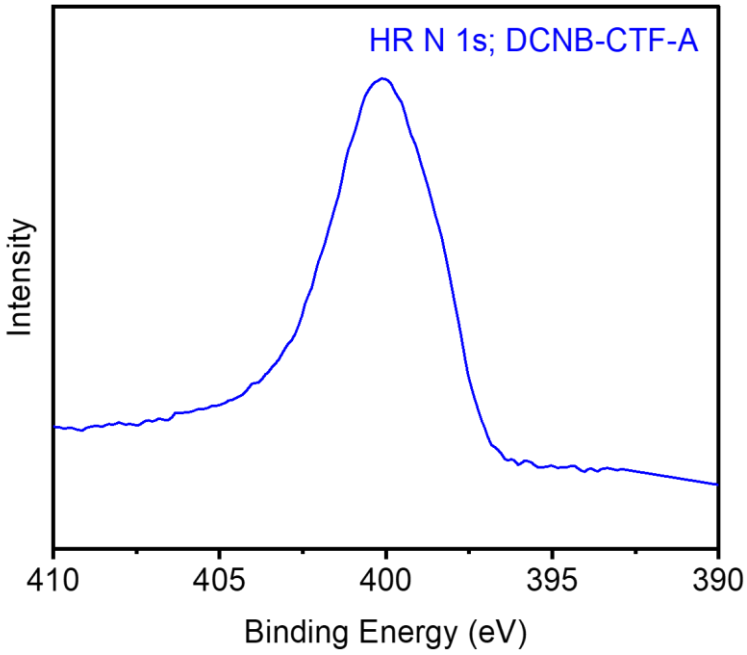

Figure S117. HR N 1s XPS spectrum of **DCNB-CTF-A** synthesized with 5.00 equivalents of $ZnBr_2$ for 40 h.

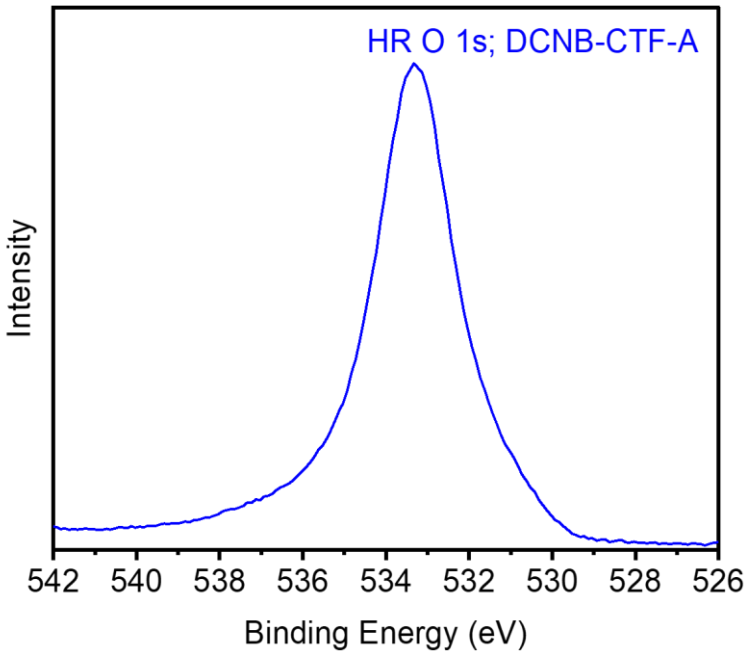

Figure S118. HR O 1s XPS spectrum of **DCNB-CTF-A** synthesized with 5.00 equivalents of $ZnBr_2$ for 40 h.

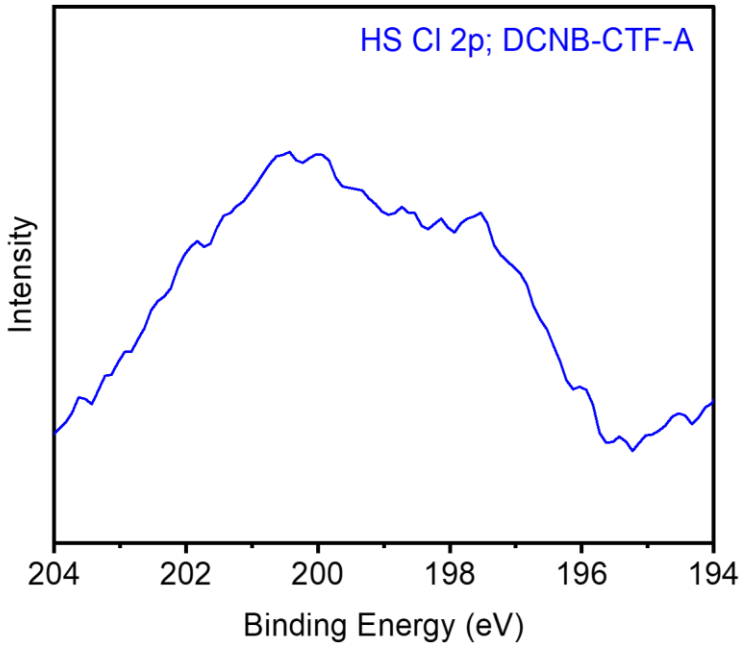

Figure S119. HS Cl 2p XPS spectrum of **DCNB-CTF-A** synthesized with 5.00 equivalents of $ZnBr_2$ for 40 h

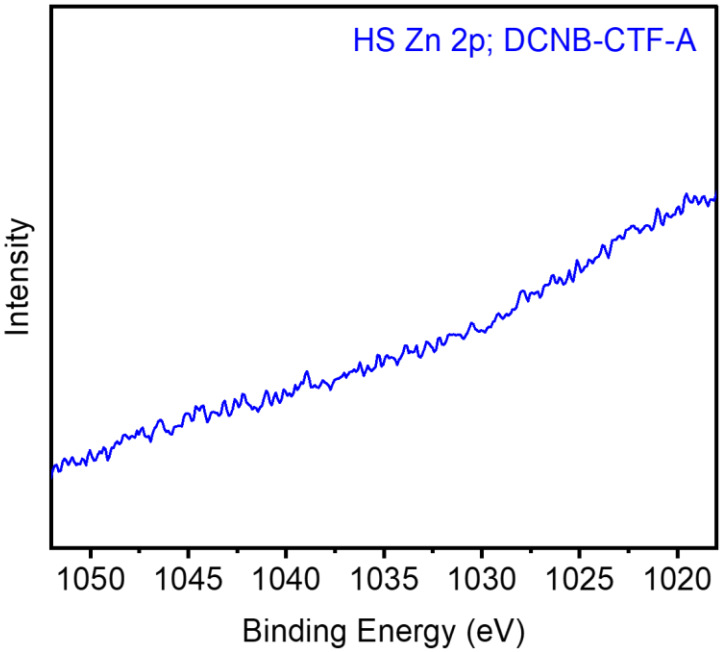

Figure S120. HS Zn 2p XPS spectrum of **DCNB-CTF-A** synthesized with 5.00 equivalents of $ZnBr_2$ for 40 h.

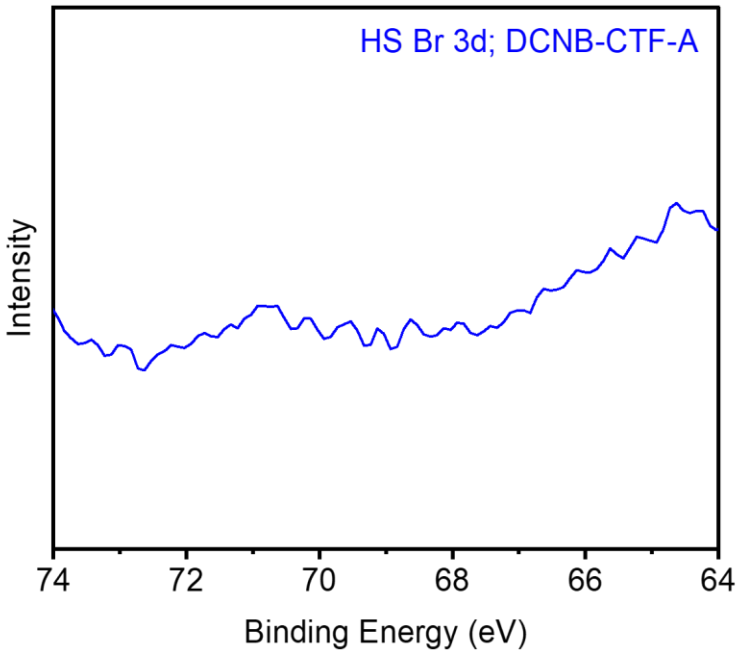

Figure S121. HS Br 3d XPS spectrum of **DCNB-CTF-A** synthesized with 5.00 equivalents of $ZnBr_2$ for 40 h.

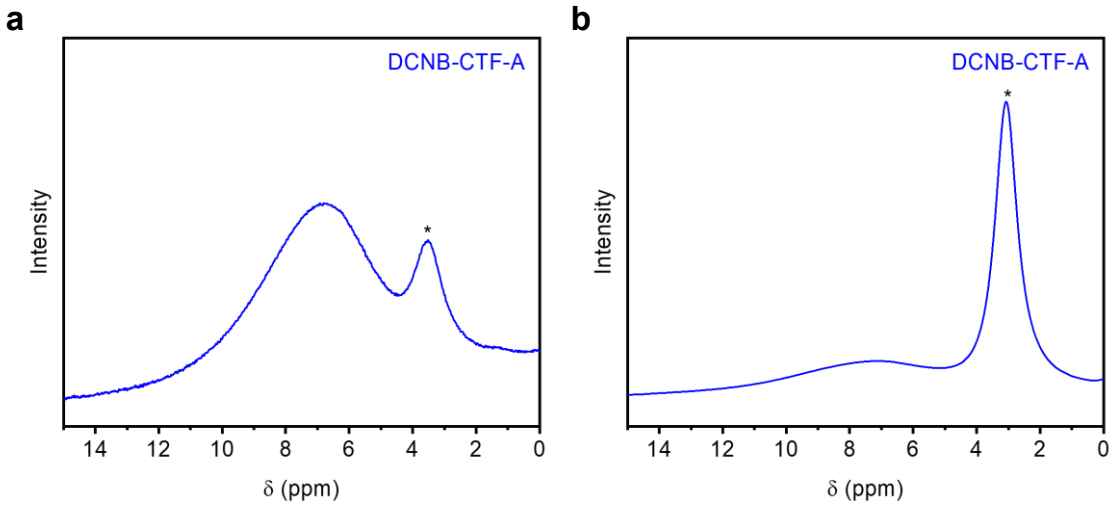

Figure S122. MAS ^{1}H SSNMR spectra at (a) 500 MHz and (b) 400 MHz of **DCNB-CTF-A** synthesized with 5.00 equivalents of $ZnBr_2$ for 72 h, collected at a spinning speed of 20 kHz. The asterisk corresponds to adsorbed water.

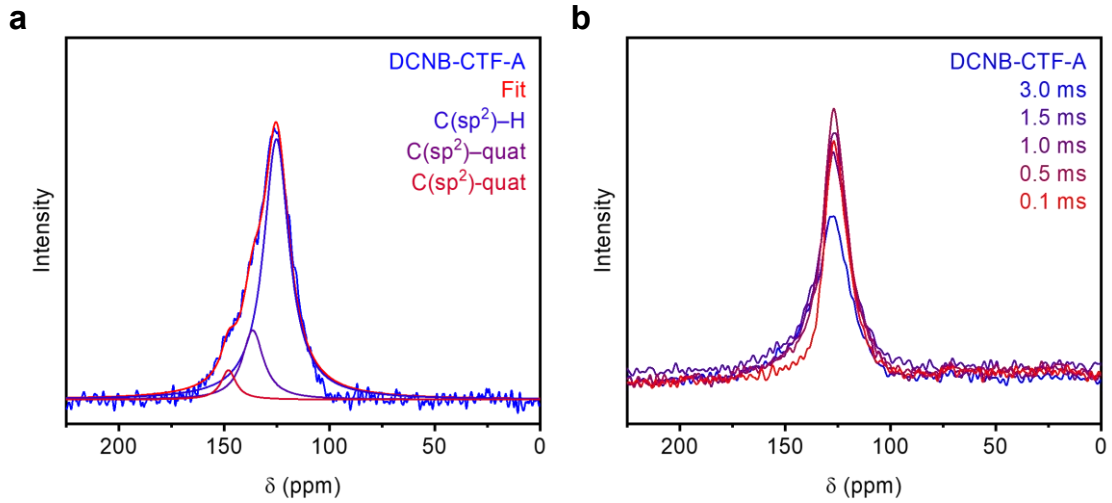

Figure S123. CP MAS ^{13}C SSNMR spectra at (a) 125 MHz and (b) 100 MHz of **DCNB-CTF-A** synthesized with 5.00 equivalents of $ZnBr_2$ for 72 h, with a $^{1}H–^{13}C$ contact time of 5 ms (a) or at the listed contact times (b), collected at a spinning speed of 20 kHz. Deconvolution fits to the 125 MHz spectrum (a) are shown. The spectrum is consistent with those reported for ionothermal CTFs.[12,13]

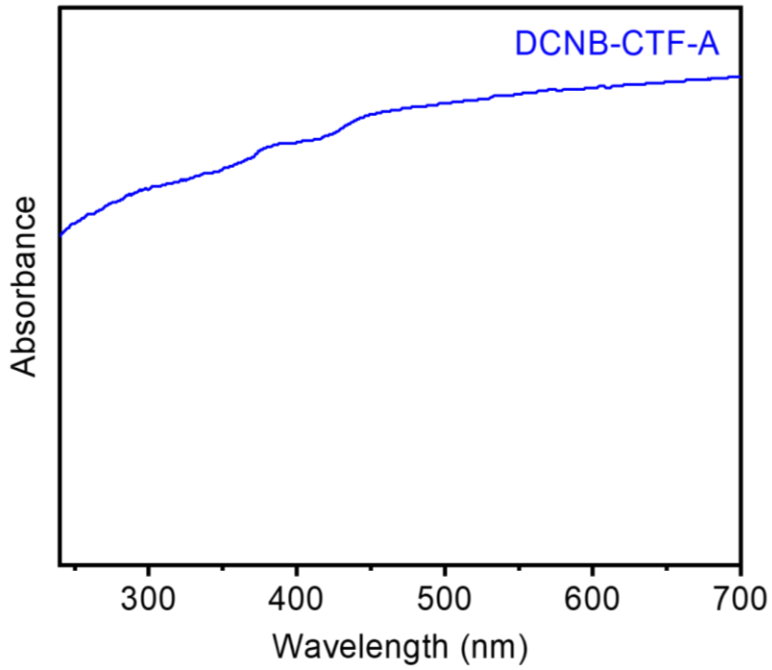

Figure S124. Diffuse reflectance UV-Vis absorbance spectrum of **DCNB-CTF-A** synthesized with 5.00 equivalents of $ZnBr_2$ for 72 h.

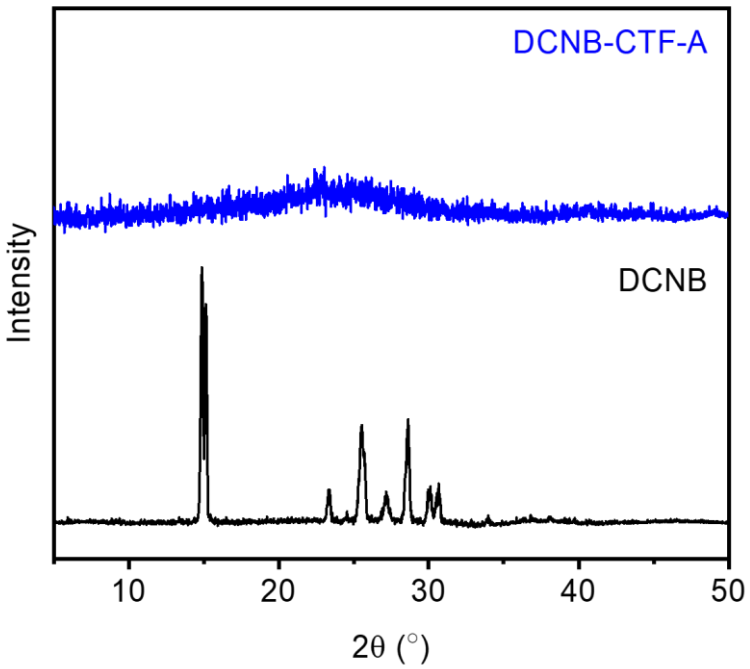

Figure S125. PXRD (λ = 1.5406 Å) patterns of **DCNB** and **DCNB-CTF-A** synthesized with 5.00 equivalents of $ZnBr_2$ for 72 h, indicating that **DCNB-CTF-A** is an amorphous polymer.

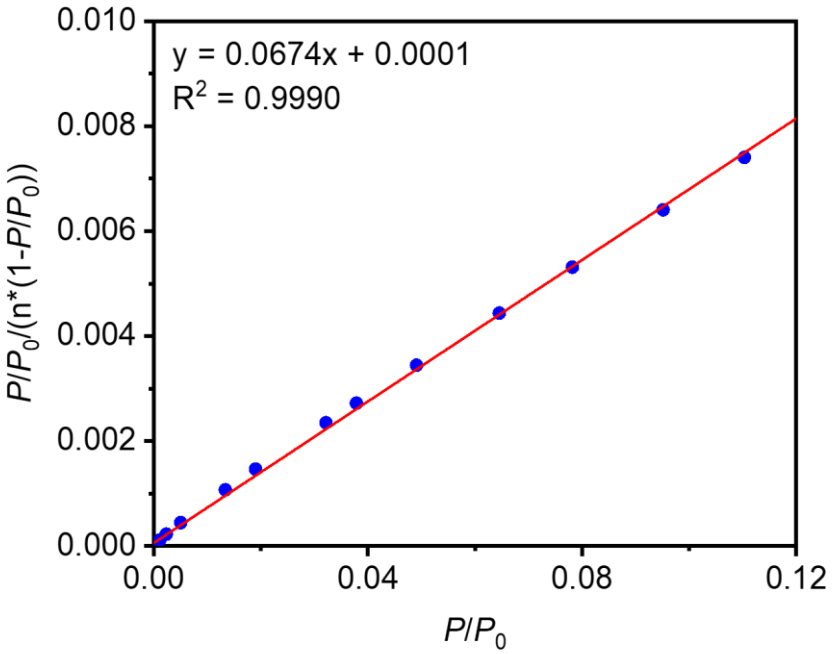

Figure S126. Linearized BET plot of **DCNB-CTF-A** synthesized with 5.00 equivalents of $ZnBr_2$ for 72 h.

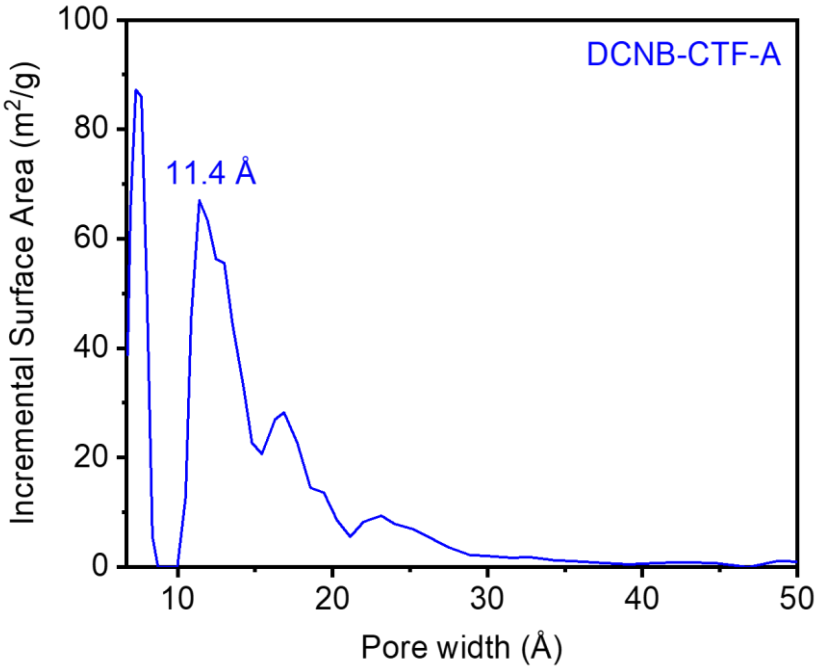

Figure S127. DFT-calculated pore size distribution of **DCNB-CTF-A** synthesized with 5.00 equivalents of $ZnBr_2$ for 72 h, assuming a carbon slit pore geometry.

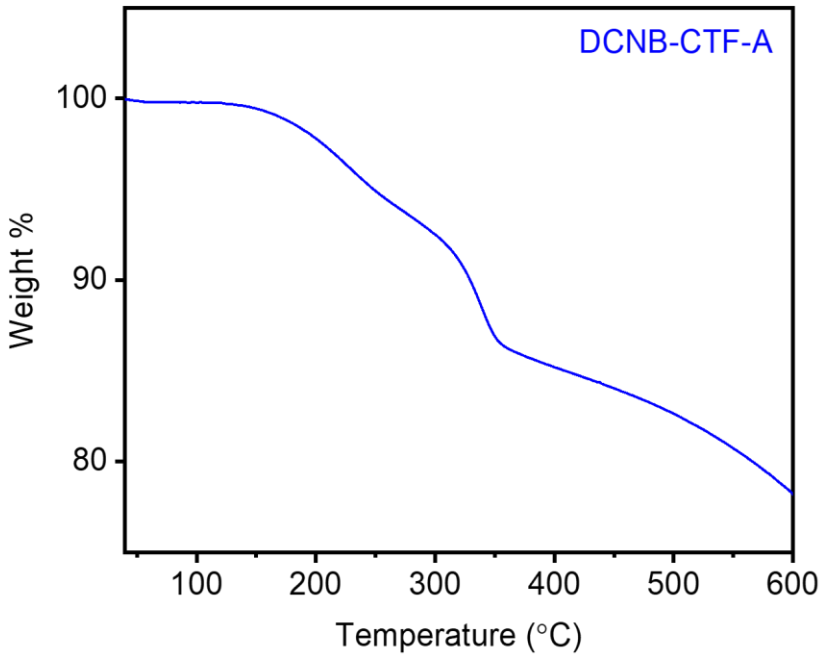

Figure S128. Thermogravimetric decomposition profile of **DCNB-CTF-A** synthesized with 5.00 equivalents of $ZnBr_2$ for 72 h.

5. Molecular studies of cyclotrimerization.

a. Synthesis of tris(4-methylphenyl)benzene (TMPB).

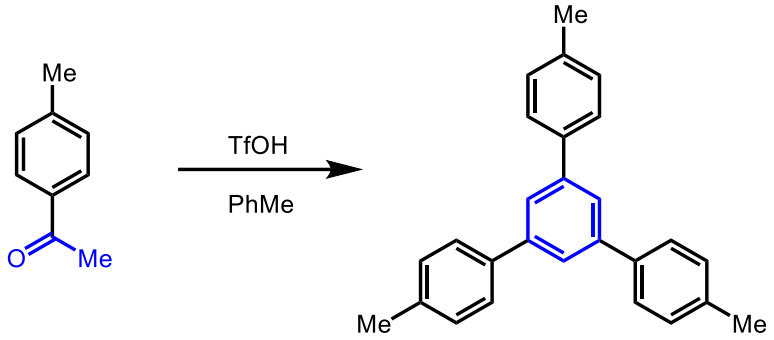

Figure S129. Synthesis of an authentic sample of tris(4-methylphenyl)benzene (**TMPB**).

In a 50 mL round-bottom flask, 4-methylacetophenone (1.00 mL, 12.4 mmol) was dissolved in toluene (15 mL). Triflic acid (0.13 mL, 0.50 mmol, 0.040 equiv) was added dropwise to the stirring mixture, and the reaction mixture was allowed to reflux in a Dean-Stark apparatus for 48 h. The reaction mixture turned black within 1 h of heating, and the progress of the reaction was monitored by thin layer chromatography (TLC). The reaction mixture was allowed to cool to room temperature and neutralized with saturated aqueous $NaHCO_3$ (5 mL). The layers were separated, and the aqueous layer was further extracted with CH_2Cl_2 (3 × 10 mL). The combined organic extracts were dried over Na_2SO_4 and filtered. The solvent was removed under reduced pressure, and the resulting dark brown oily residue was purified by column chromatography (SiO_2, gradient of 0% → 1% → 3% → 10% CH_2Cl_2/hexanes) to afford **TMPB** (0.479 g, 33% yield) as an off-white solid. ^{1}H NMR (500 MHz, $CDCl_3$): δ 7.74 (s, 3H), 7.60 (d, J = 8.0 Hz, 6H), 7.29 (d, J = 8.0 Hz, 6H), 2.43 (s, 9H) ppm. ^{13}C NMR (125 MHz, $CDCl_3$) δ 142.2, 138.4, 137.3, 129.6, 127.2, 124.2, 21.2 ppm. These spectra are consistent with those reported in the literature.[14]

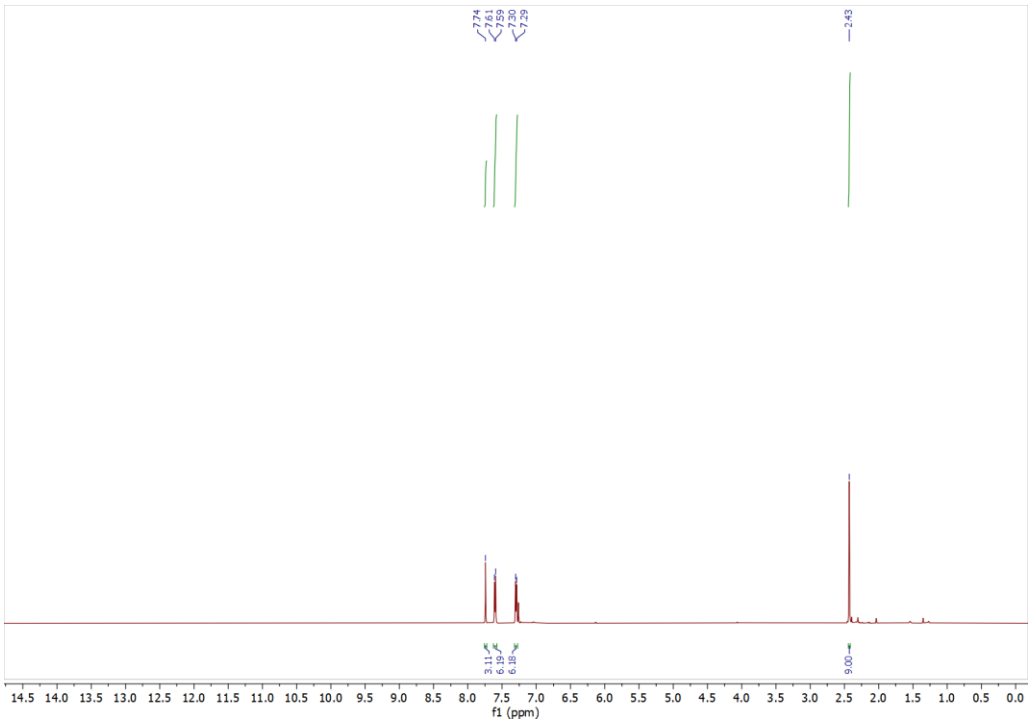

Figure S130. ^{1}H NMR (500 MHz, $CDCl_3$) spectrum of **TMPB** used in this work.

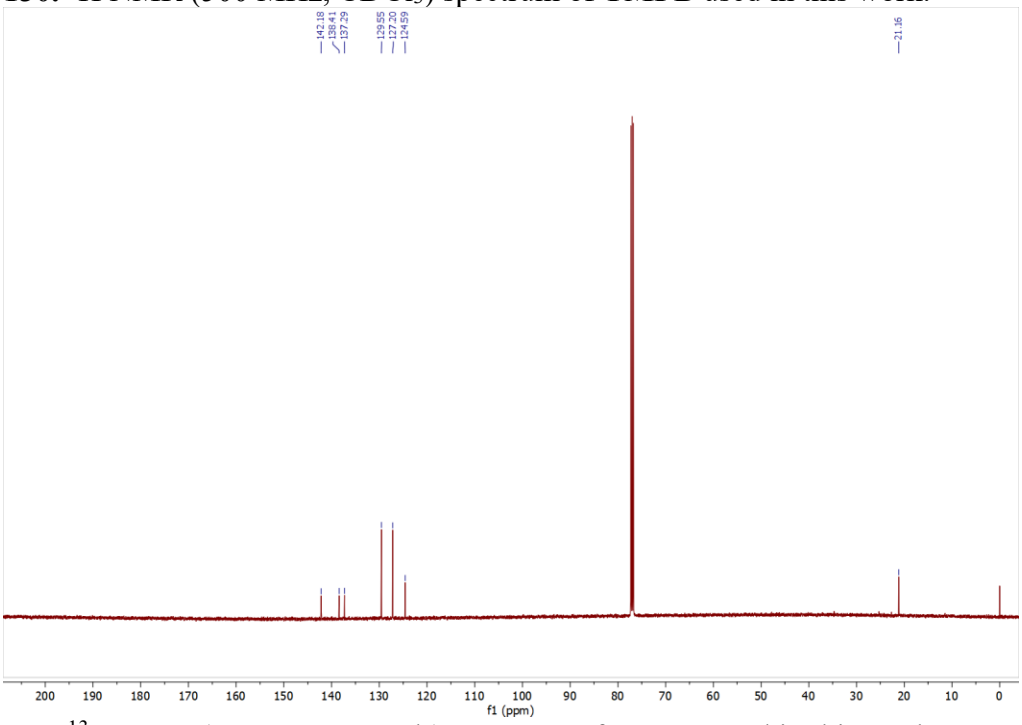

Figure S131. ^{13}C NMR (125 MHz, $CDCl_3$) spectrum of **TMPB** used in this work.

b. Molecular investigation of $ZnCl_2$ and $ZnBr_2$ catalysis.

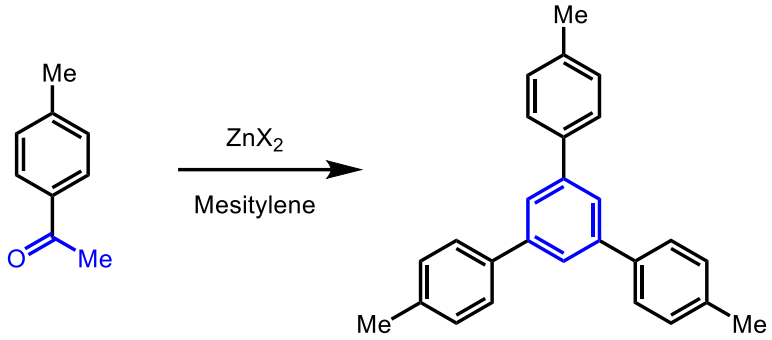

Figure S132. Molecular trimerization of 4-methylacetophenone (**SM**) with ZnX_2 (X = Br or Cl) to yield **TMPB**.

The following procedure was adapted from literature.[15] $ZnBr_2$ (33.8 mg, 0.150 mmol, 0.0500 equiv) and $ZnCl_2$ (20.4 mg, 0.150 mmol, 0.0500 equiv) were each freshly charged into two separate 15 mL screw-cap tubes (four total tubes) equipped with stir bars in a N_2-filled glovebox. The tubes were removed from the glovebox, and mesitylene (3.00 mL) was added to each. To one of each tubes containing $ZnBr_2$ and $ZnCl_2$, 4-methylacetophenone (**SM**, 0.400 mL, 3.00 mmol, 1.00 equiv) was added, and the other two tubes were left as blank reactions for reference. The reaction mixtures were then allowed to stir at 160 °C for 120 h in an oil bath. After 120 h, each of the four crude reaction mixtures (0.060 mL) was allowed to cool to room temperature and diluted with freshly prepared 0.111 M pivalic acid in $CDCl_3$ (0.540 mL) as an internal standard for ^1H NMR analyses. Yields are not reported due to the formation of insoluble brown solids (not **TMPB,** which is fully soluble under the reaction conditions) in both trimerization reactions.

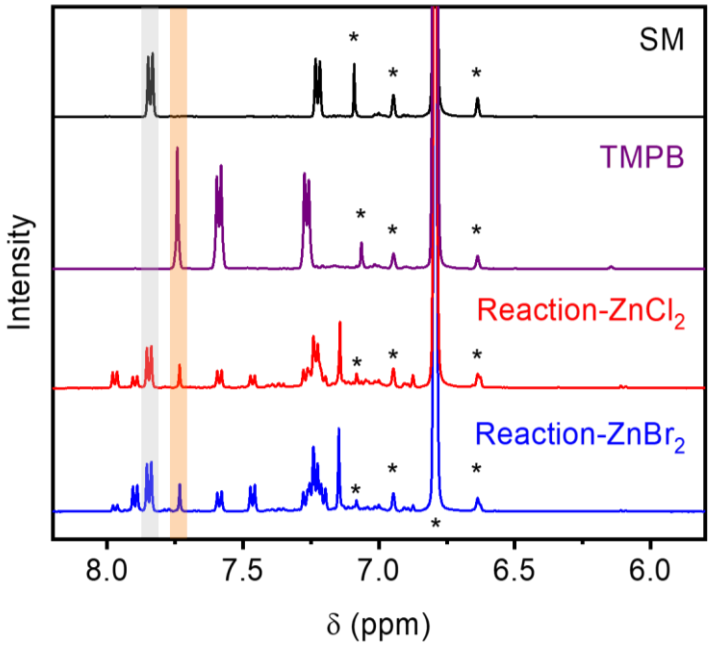

Figure S133. ^{1}H NMR (500 MHz, $CDCl_3$) spectra of 4-methylacetylphenone (**SM**, gray) trimerization into **TMPB** (orange) catalyzed by both $ZnBr_2$ and $ZnCl_2$, indicating that the two zinc halide salts catalyze the reaction similarly. The asterisks correspond to mesitylene and chloroform.

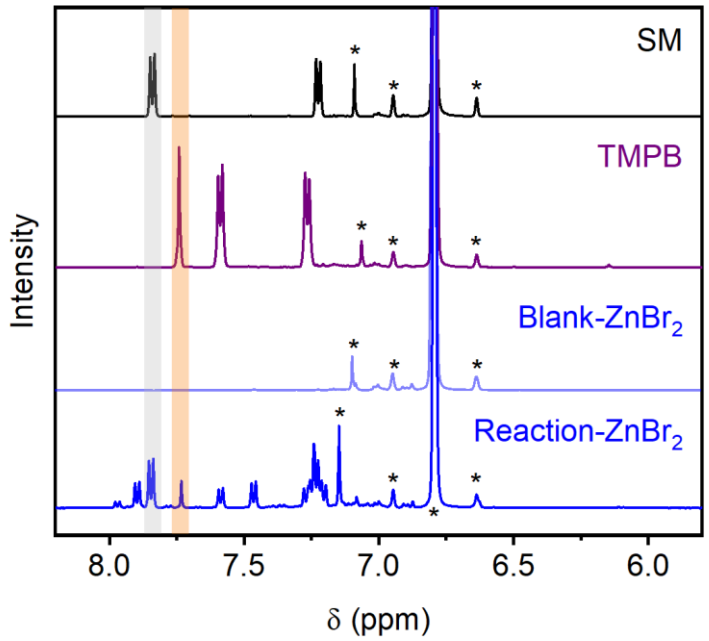

Figure S134. ^{1}H NMR (500 MHz, $CDCl_3$) spectrum of 4-methylacetylphenone (**SM**) trimerization into **TMPB** catalyzed by $ZnBr_2$ in comparison to a reaction in which $ZnBr_2$ and mesitylene were combined together without 4-methylacetylphenone. The asterisks correspond to mesitylene and chloroform.

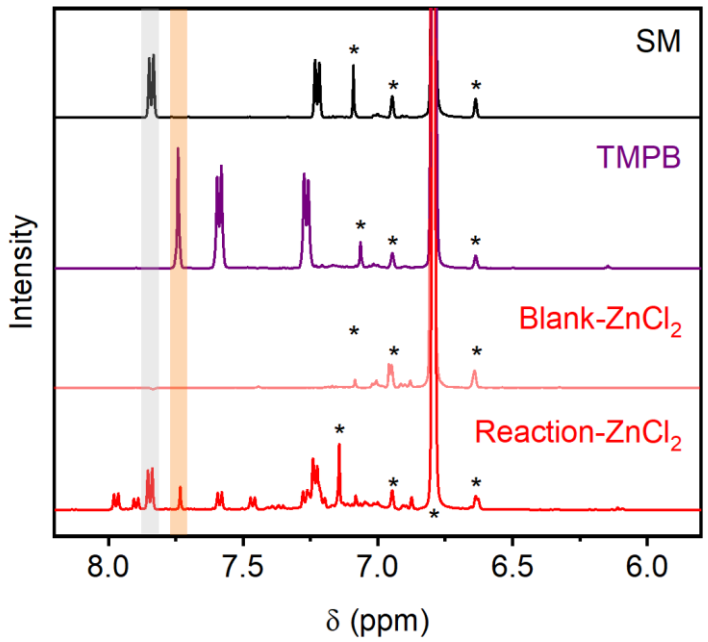

Figure S135. ^{1}H NMR (500 MHz, $CDCl_3$) spectrum of 4-methylacetylphenone (**SM**) trimerization into **TMPB** catalyzed by $ZnCl_2$ in comparison to a reaction in which $ZnCl_2$ and mesitylene were combined together without 4-methylacetylphenone. The asterisks correspond to mesitylene and chloroform.

6. Evaluation of other mediators using 1,4-diacetylbenzene (DAB).

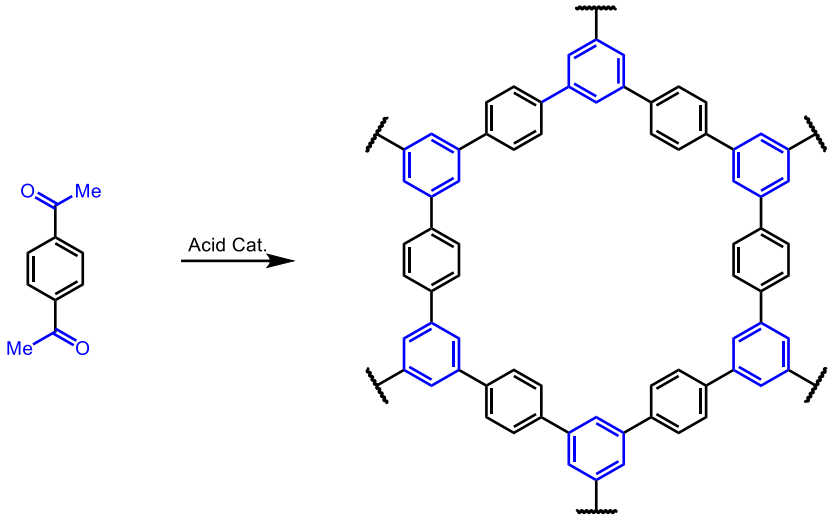

Figure S136. Synthesis of **poly(DAB)** from **DAB** using different acidic catalysts.

General Procedure: The following procedure was adapted from the procedure employed for the $ZnBr_2$-mediated trimerization of **DAB**. Three 10 mm diameter borosilicate glass tubes were each charged with **DAB** (40.0 mg, 0.247 mmol, 1.00 equiv) and the Bronsted or Lewis acid mediator (10.0 equiv) in air or in a N_2-filled glovebox when necessary. The tubes were evacuated (<100 mTorr) and then flame-sealed under high vacuum using a natural gas torch and a custom-built apparatus (**Figure S7**). Liquid mediators underwent three freeze-pump-thaw cycles before being sealed. The tubes were placed in an oven and heated at 10 °C above their melting points for solid mediators or 10 °C below their atmospheric boiling points for liquid mediators, unless specified otherwise. The tubes were cooled to room temperature and were snapped using a glass tube cutter. The reaction mixture was scraped out of the tubes with a spatula, using water (10 mL) or ice-cold EtOH (10 mL for $SiCl_4$, $TiCl_4$, $TiBr_4$, and $SbCl_5$) to help slide the mixture off the tube walls. The same soaking and drying procedure employed for the $ZnBr_2$-mediated trimerization of **DAB** was then used to yield the activated material, **poly(DAB)**, which was characterized by ATR-IR, PXRD, and surface area analysis.

a. Lewis acid mediators.

Table S20. List of conditions for the trimerization of **poly(DAB)** using different Lewis acids.

Mediator	Total Mass of Mediator (mg)	Temperature (°C)	Carbonyl Present by IR?	Yield (mg (%))[a]	BET Surface Area (m^2/g)
$AlBr_3$	1973 (658 × 3)	100	Yes	56.8 (61)	nonporous
$TiCl_4$	1406 (469 × 3)	125	Yes	69.4 (74)	nonporous
$AlCl_3$	986 (329 × 3)	200	Yes	43.4 (46)	345 ± 2
$FeBr_3$	2189 (729 × 3)	200	Yes	102.8 (109)	280 ± 2
$TiBr_4$[b]	2723 (908 × 3)	230	Weak	93.7 (82)	489 ± 7
$BiCl_3$[b]	2333 (778 × 3)	250	Yes	119.8 (128)	50 ± 1
$SnCl_2$	1403 (468 × 3)	250	No	72.7 (78)	nonporous
3:1:1 $ZnCl_2$:KCl:NaCl	1347 (446 ×3)	260	Yes	23.3 (85)	nonporous
$FeCl_3$	1200 (400 × 3)	310	Yes	98.2 (105)	302 ± 1
$Zn(SO_3CF_3)_2$	2690 (896 × 3)	310	Weak	74.0 (69)	101 ± 1
$ZnCl_2$	1008 (336 × 3)	300	No	42.3 (46)	nonporous
		400 [c]	No	56.4 (61)	nonporous
$Al(NO_3)_3•9H_2O$[d]	925 (308 × 3)	110	0 (0)	0 (0)	not measured
$SbCl_5$[d]	737 (246 × 3)	130	0 (0)	0 (0)	not measured
$SiCl_4$[d]	419 (140 × 3)	48	0 (0)	0 (0)	not measured
$Zn(NO_3)_2•6H_2O$[d]	734 (245 × 3)	110	0 (0)	0 (0)	not measured
$Zn(OAc)_2•2H_2O$[d]	541 (180 × 3)	250	0 (0)	0 (0)	not measured

[a]Yields over 100% are indicative of contamination by residual metal salts, even after stirring in aqueous HCl solution, and/or due to incomplete water elimination from the aldol condensation.
[b]Residual salt detected by PXRD, even with additional acid washes.
[c]Reported previously.[7]
[d]No insoluble solids were isolated.

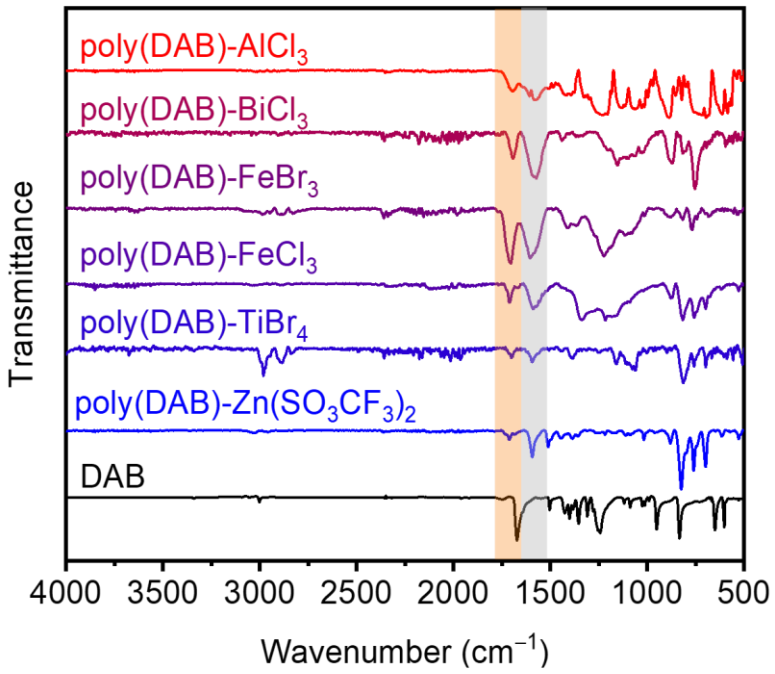

Figure S137. ATR-IR spectra of **DAB** and the porous **poly(DAB)** synthesized with the Lewis acids $AlCl_3$, $BiCl_3$, $FeBr_3$, $FeCl_3$, $TiBr_4$, and $Zn(SO_3CF_3)_2$. The indicated peaks correspond to carbonyl C=O (orange) and aromatic C=C (gray) stretches.

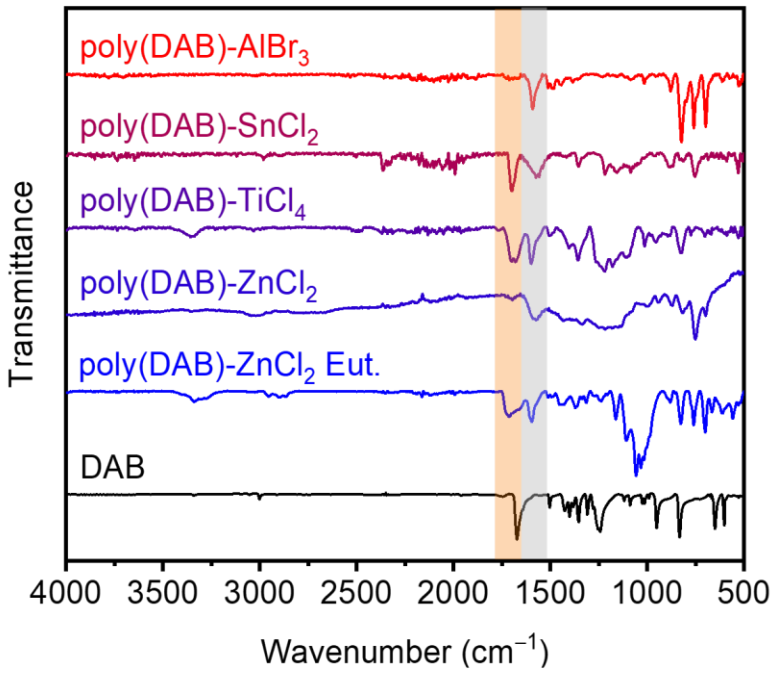

Figure S138. ATR-IR spectra of **DAB** and the non-porous **poly(DAB)** synthesized with the Lewis acids $AlBr_3$, $SnCl_2$, $TiCl_4$, $ZnCl_2$ (at 300 °C), and 3:1:1 $ZnCl_2$:KCl:NaCl eutectic mixture. The indicated peaks correspond to carbonyl C=O (orange) and aromatic C=C (gray) stretches.

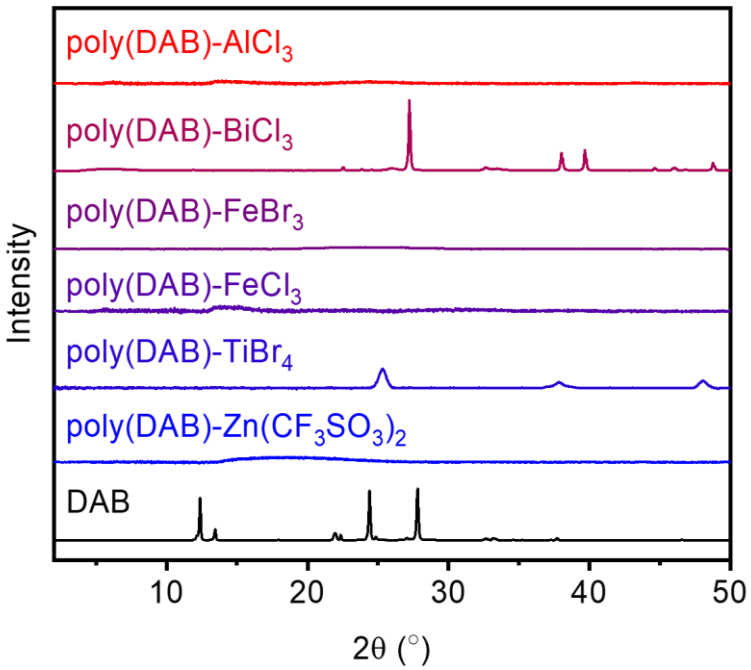

Figure S139. PXRD (λ = 1.5406 Å) patterns of **DAB** and the porous **poly(DAB)** synthesized with the Lewis acids $AlCl_3$, $BiCl_3$, $FeBr_3$, $FeCl_3$, $TiBr_4$, and $Zn(SO_3CF_3)_2$. The sample synthesized with $TiBr_4$ shows diffraction peaks that align with TiO_2 nanoparticles.[16,17]

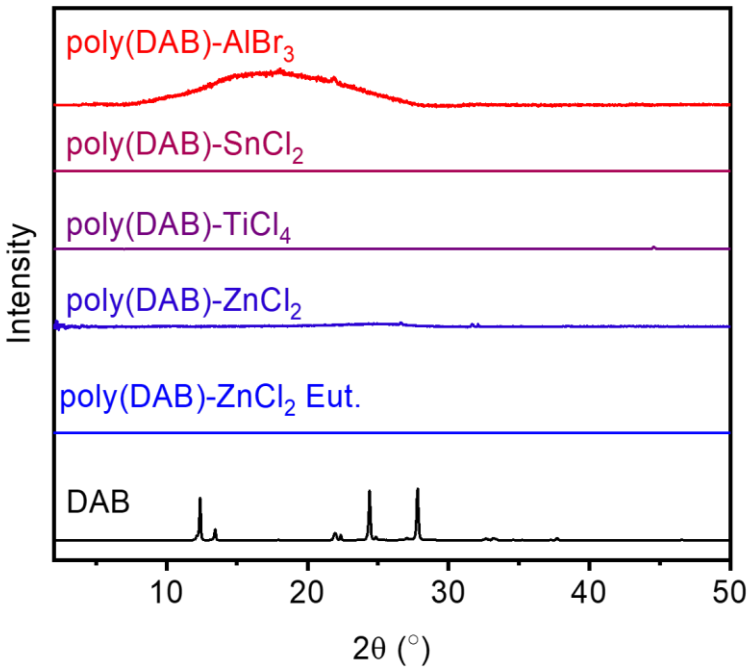

Figure S140. PXRD (λ = 1.5406 Å) patterns of **DAB** and the non-porous **poly(DAB)** synthesized with the Lewis acids $AlBr_3$, $SnCl_2$, $TiCl_4$, $ZnCl_2$ (at 300 °C), and 3:1:1 $ZnCl_2$:KCl:NaCl.

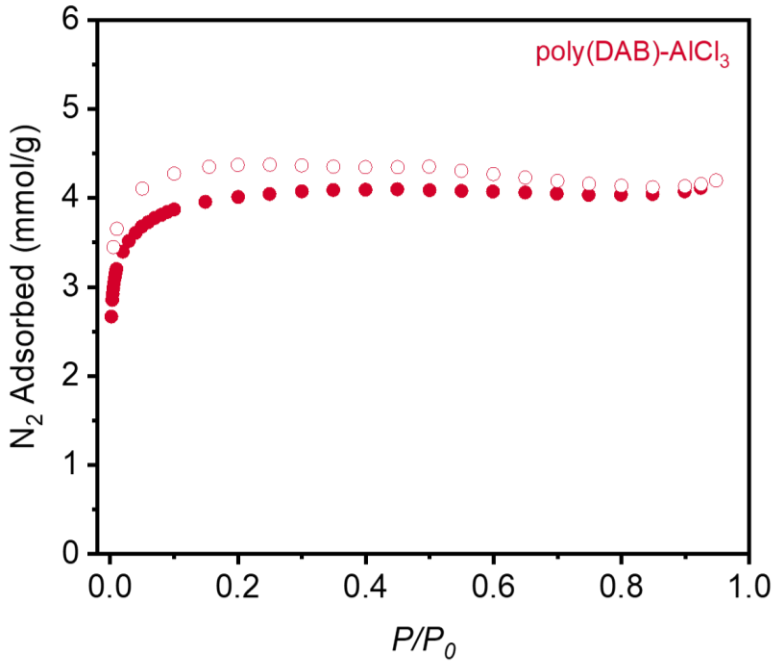

Figure S141. 77 K N_2 adsorption (filled circles) and desorption (open circles) isotherm for **poly(DAB)** synthesized with 10.0 equivalents of $AlCl_3$ for 72 h. The Brunauer-Emmett-Teller (BET) and Langmuir surface areas were determined to be 345 ± 2 m^2/g and 398 ± 2 m^2/g, respectively.

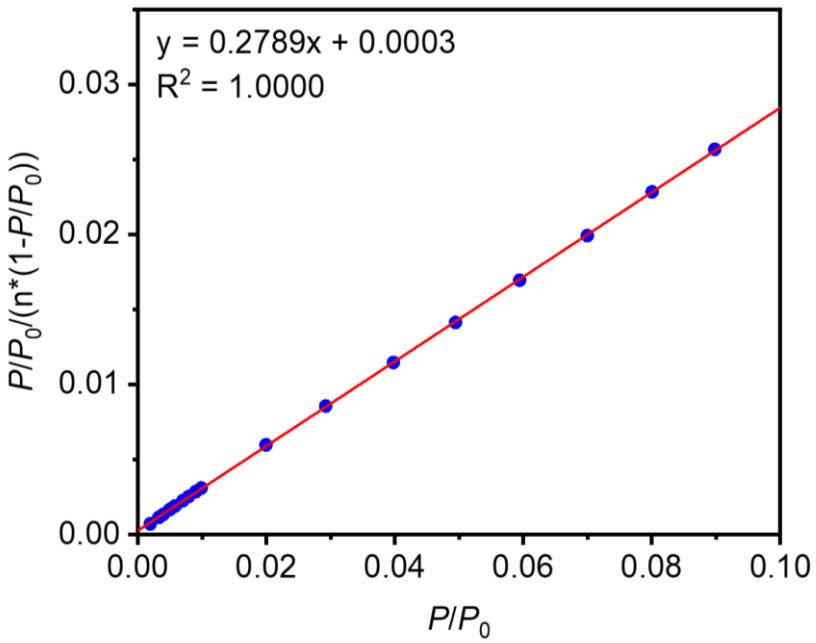

Figure S142. Linearized BET plot of **poly(DAB)** synthesized with 10.0 equivalents of $AlCl_3$ for 72 h.

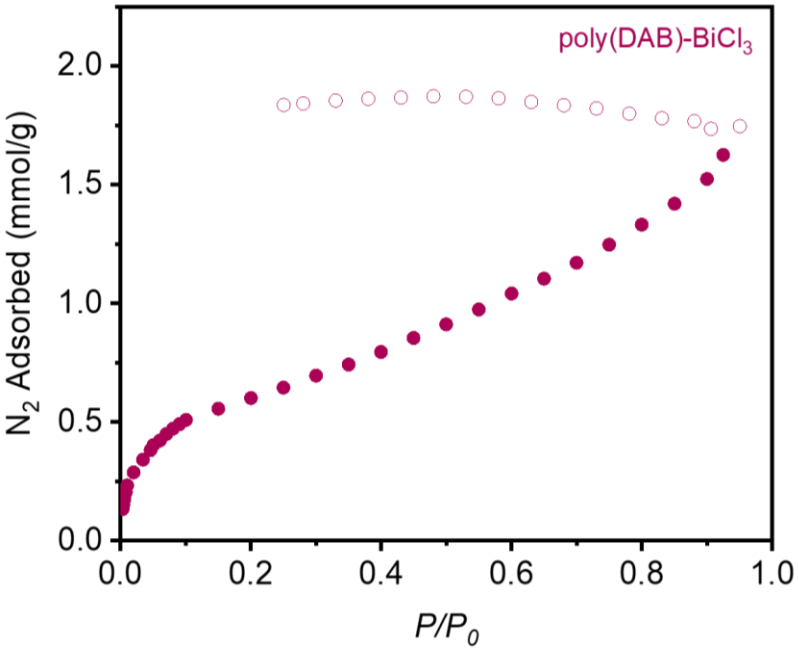

Figure S143. 77 K N_2 adsorption (filled circles) and desorption (open circles) isotherm for **poly(DAB)** synthesized with 10.0 equivalents of $BiCl_3$ for 72 h. The Brunauer-Emmett-Teller (BET) and Langmuir surface areas were determined to be 50 ± 1 m^2/g and 151 ± 10 m^2/g, respectively.

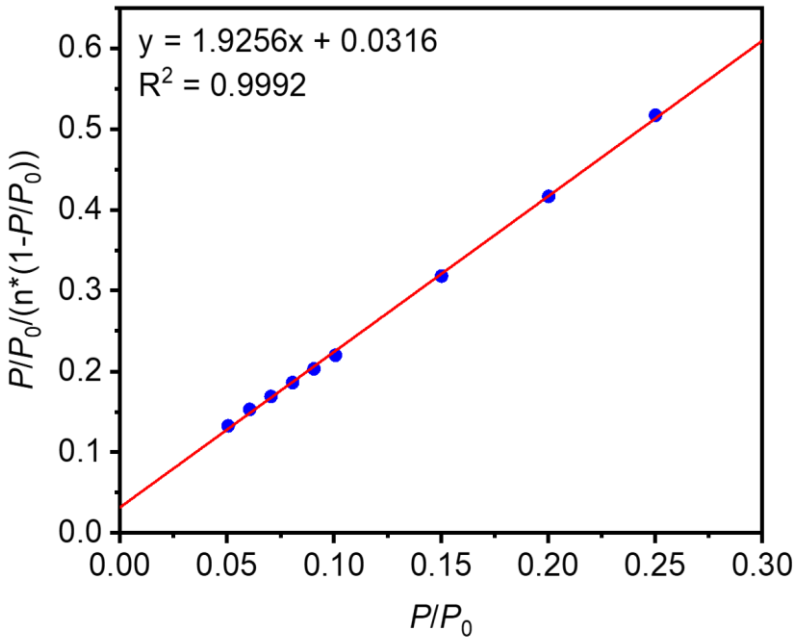

Figure S144. Linearized BET plot of **poly(DAB)** synthesized with 10.0 equivalents of $BiCl_3$ for 72 h.

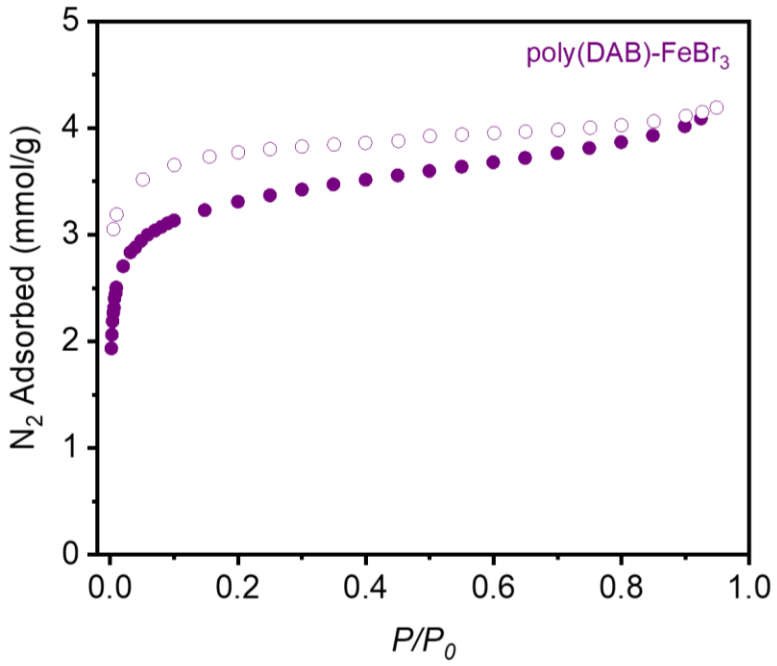

Figure S145. 77 K N_2 adsorption (filled circles) and desorption (open circles) isotherm for **poly(DAB)** synthesized with 10.0 equivalents of $FeBr_3$ for 72 h. The Brunauer-Emmett-Teller (BET) and Langmuir surface areas were determined to be 280 ± 1 m^2/g and 384 ± 3 m^2/g, respectively.

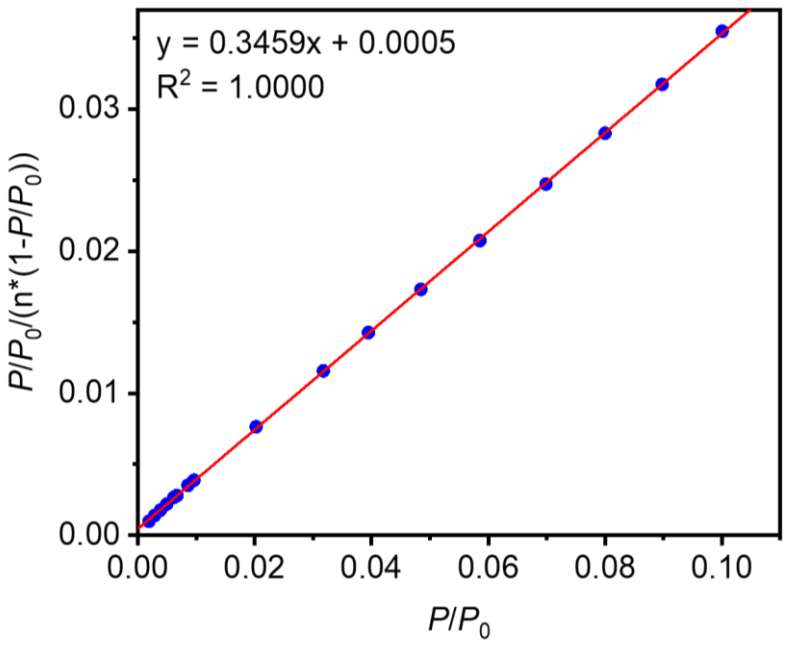

Figure S146. Linearized BET plot of **poly(DAB)** synthesized with 10.0 equivalents of $FeBr_3$ for 72 h.

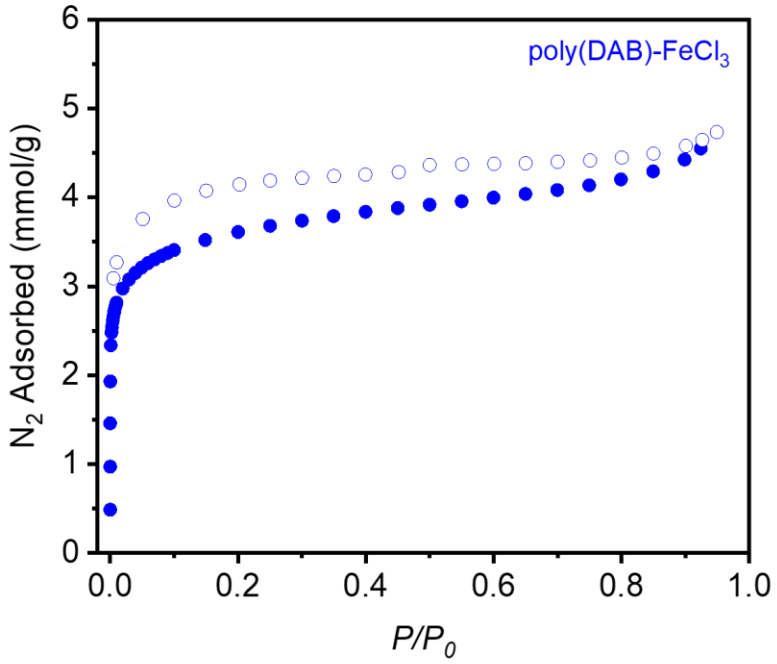

Figure S147. 77 K N_2 adsorption (filled circles) and desorption (open circles) isotherm for **poly(DAB)** synthesized with 10.0 equivalents of $FeCl_3$ for 72 h. The Brunauer-Emmett-Teller (BET) and Langmuir surface areas were determined to be 302 ± 1 m^2/g and 408 ± 2 m^2/g, respectively.

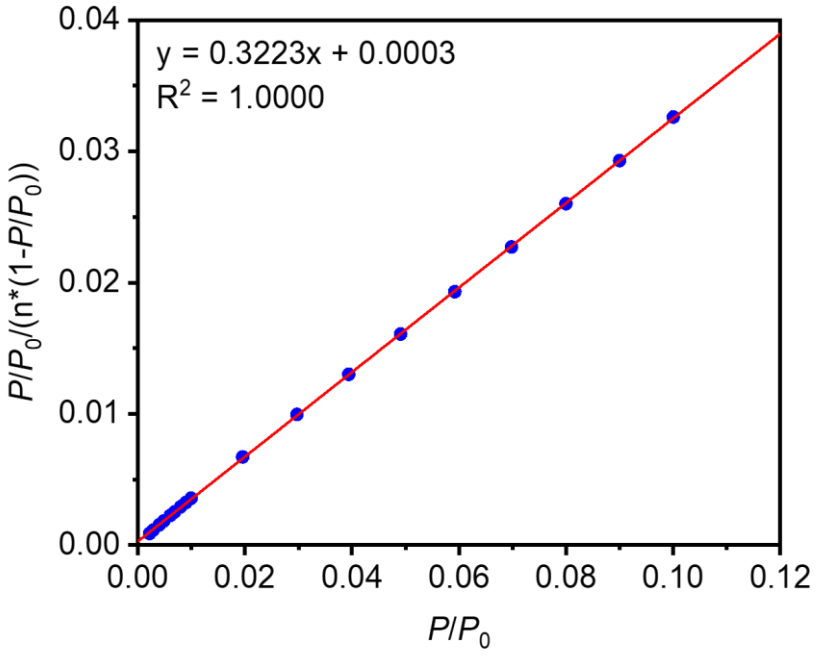

Figure S148. Linearized BET plot of **poly(DAB)** synthesized with 10.0 equivalents of $FeCl_3$ for 72 h.

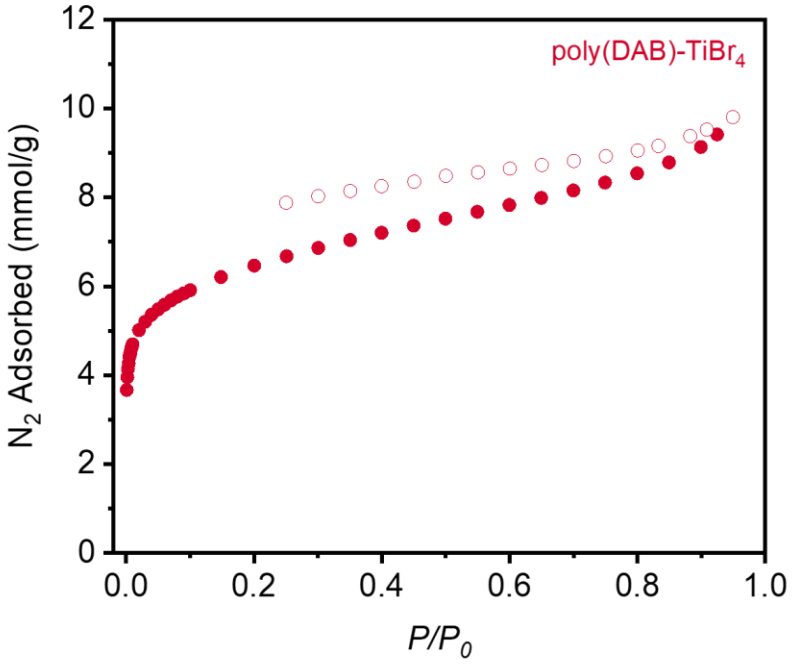

Figure S149. 77 K N_2 adsorption (filled circles) and desorption (open circles) isotherm for **poly(DAB)** synthesized with 10.0 equivalents of $TiBr_4$ for 72 h. The Brunauer-Emmett-Teller (BET) and Langmuir surface areas were determined to be 489 ± 7 m^2/g and 871 ± 20 m^2/g, respectively.

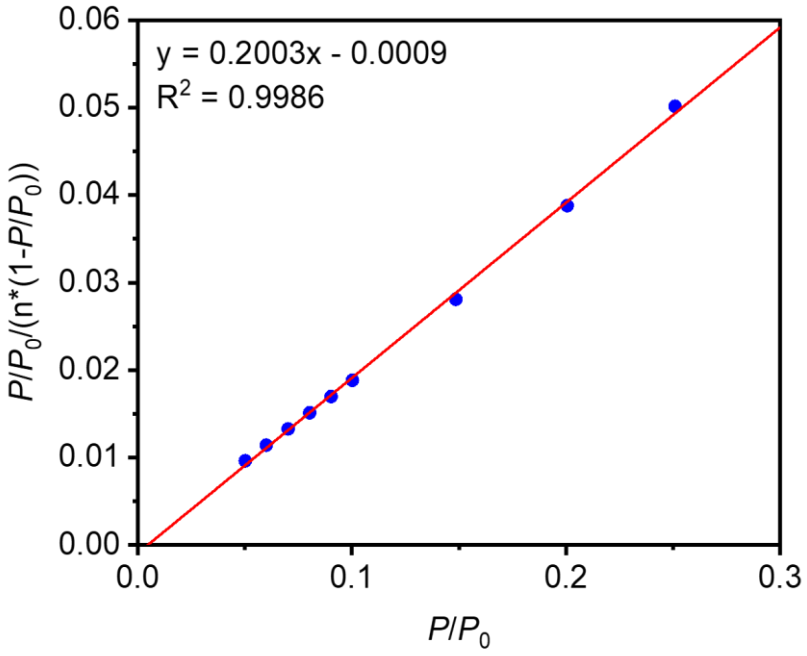

Figure S150. Linearized BET plot of **poly(DAB)** synthesized with 10.0 equivalents of $TiBr_4$ for 72 h.

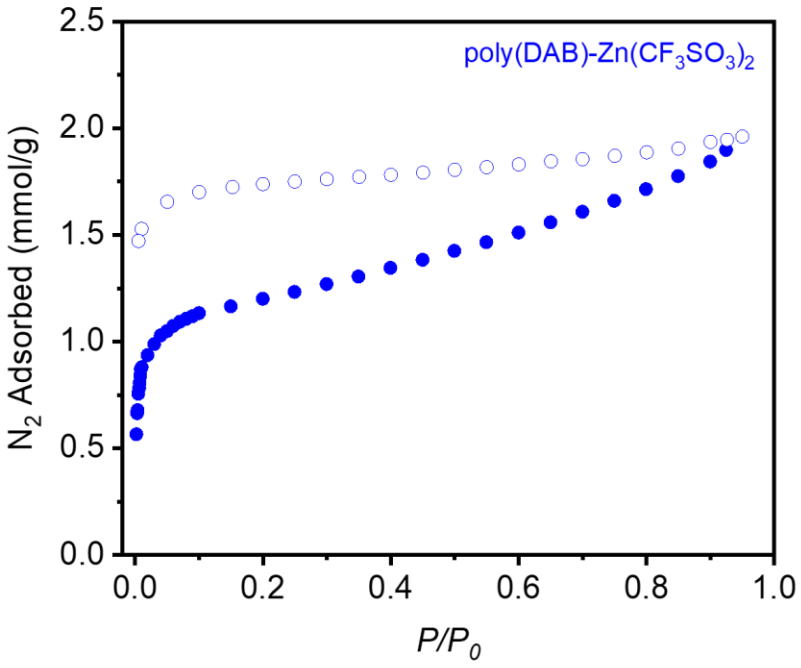

Figure S151. 77 K N_2 adsorption (filled circles) and desorption (open circles) isotherm for **poly(DAB)** synthesized with 10.0 equivalents of $Zn(CF_3SO_3)_2$ for 72 h. The Brunauer-Emmett-Teller (BET) and Langmuir surface areas were determined to be 101 ± 1 m^2/g and 154 ± 4 m^2/g, respectively.

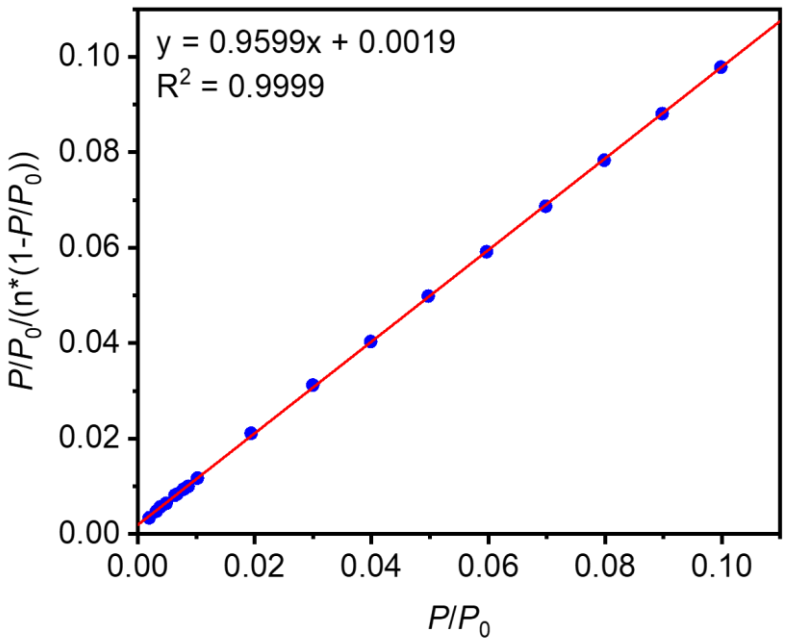

Figure S152. Linearized BET plot of **poly(DAB)** synthesized with 10.0 equivalents of $Zn(CF_3SO_3)_2$ for 72 h.

b. Brønsted acid mediators.

Table S21. List of conditions for the trimerization of **poly(DAB)** using different Brønsted acids.

Mediator	Total Mass of Mediator (mg)	Temperature (°C)	Yield (mg (%))[a]	BET Surface Area (m^2/g)[c]	pK_a
Py•HCl	866 (285 × 3)	160	9.9 (11)	not measured	5
$Ph_2P(O)OH$	1614 (538 × 3)	205	21.4 (23)	nonporous	2.3
$(PhSO_2)_2NH$	2200 (733 × 3)	168	79.2 (85)	nonporous	−1.1
$(MePhSO_2)_2NH$	2408 (803 × 3)	185	166.8 (179)	nonporous	−0.5
$PhSO_3H$	1172 (391 × 3)	75	63.4 (68)	nonporous	−2.5
$TsOH•H_2O$[b]	1407 (469 × 3)	110	107 (115)	900 ± 5	−2.8
AcOH[c]	445 (148 × 3)	108	0 (0)	not measured	4.7
CF_3CO_2H[c]	885 (295 × 3)	62	0 (0)	not measured	0.5
$(CF_3SO_2)_2NH$[c]	2127 (709 × 3)	66	0 (0)	not measured	−12
$(PhO)_2P(O)OH$[c]	1854 (618 × 3)	74	0 (0)	not measured	1.1

[a]Yields over 100% are indicative of contamination by decomposed mediator, even after soaking, and/or due to incomplete water elimination.
[b]Reported previously.[7]
[c]No insoluble solids were isolated.

Notably, every Brønsted acid attempted left significant residual carbonyl stretches in the isolated solids, indicative of incomplete cyclotrimerization (**Figure S153**).

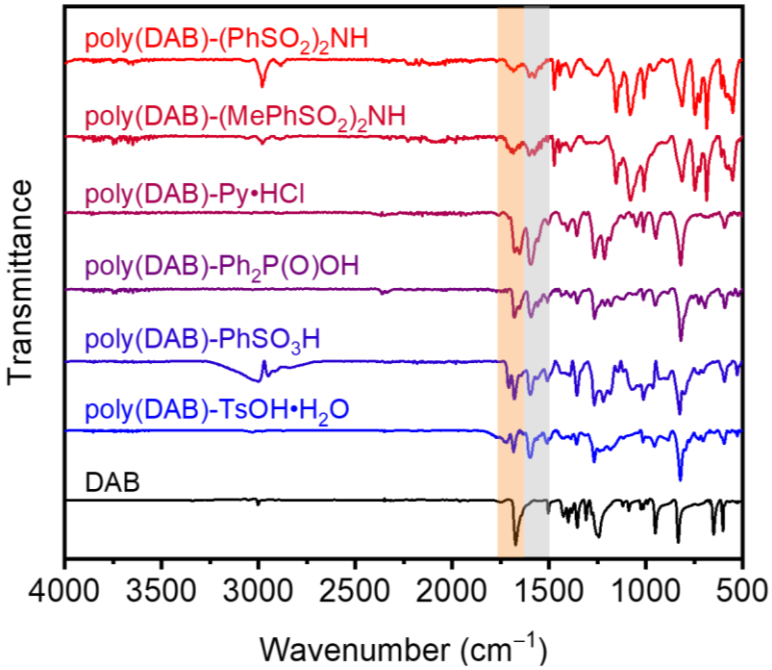

Figure S153. ATR-IR spectra of **DAB** and **poly(DAB)** synthesized with the Brønsted acids $(CF_3SO_2)_2NH$, $(PhSO_2)_2NH$, $(MePhSO_2)_2NH$, Py•HCl, PhP(O)OH, MsOH, $PhSO_3NH$, and $TsOH•H_2O$. The indicated peaks correspond to carbonyl C=O (orange) and aromatic C=C (gray) stretches.

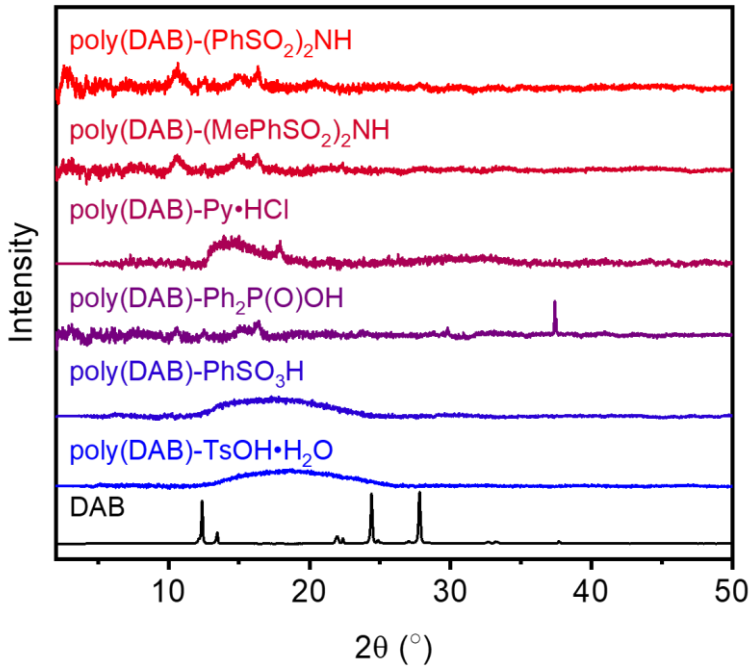

Figure S154. PXRD (λ = 1.5406 Å) patterns of **DAB** and **poly(DAB)** synthesized with the Brønsted acids $(CF_3SO_2)_2NH$, $(PhSO_2)_2NH$, $(MePhSO_2)_2NH$, Py•HCl, $(PhO)_2P(O)OH$, MsOH, $PhSO_3NH$, and $TsOH•H_2O$.

7. Calculated structural models of polymer materials.

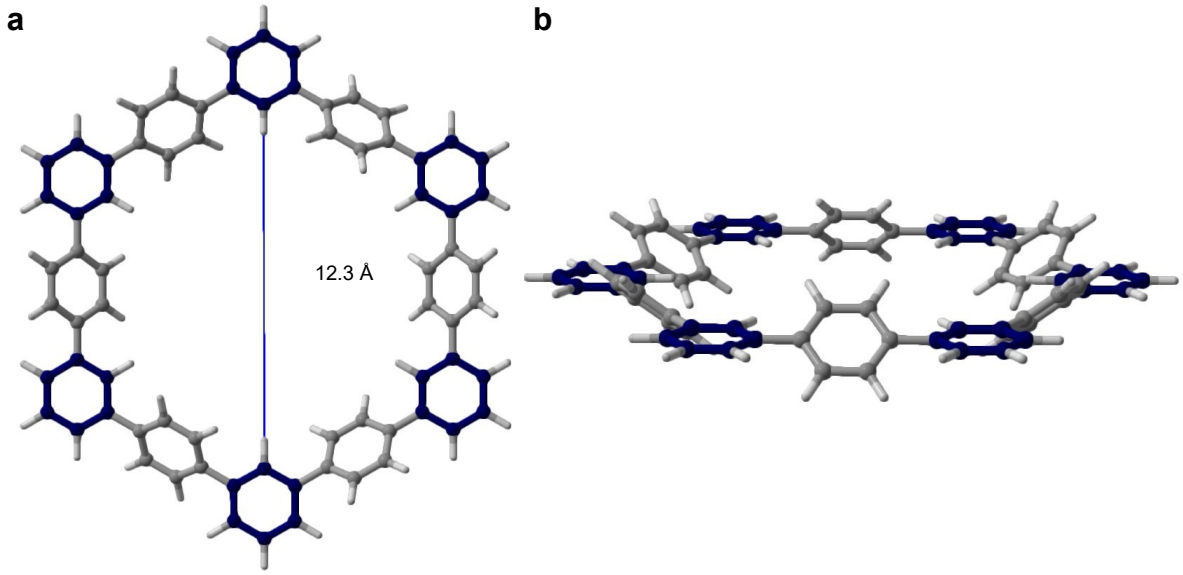

Figure S155. Predicted ideal, non-interpenetrated structural model of a single **DAB-CMP** pore (a) down the pore dimension and (b) parallel to the pore dimension. The navy colored atoms denote carbons originating from the acetyl groups in the starting monomer.

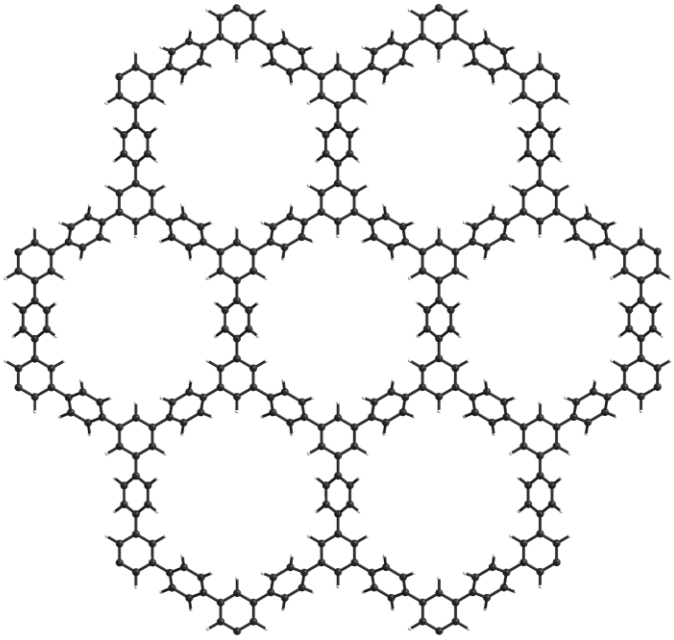

Figure S156. Predicted ideal, non-interpenetrated structural model of **DAB-CMP**, which has a calculated pore diameter of 12.2 Å.

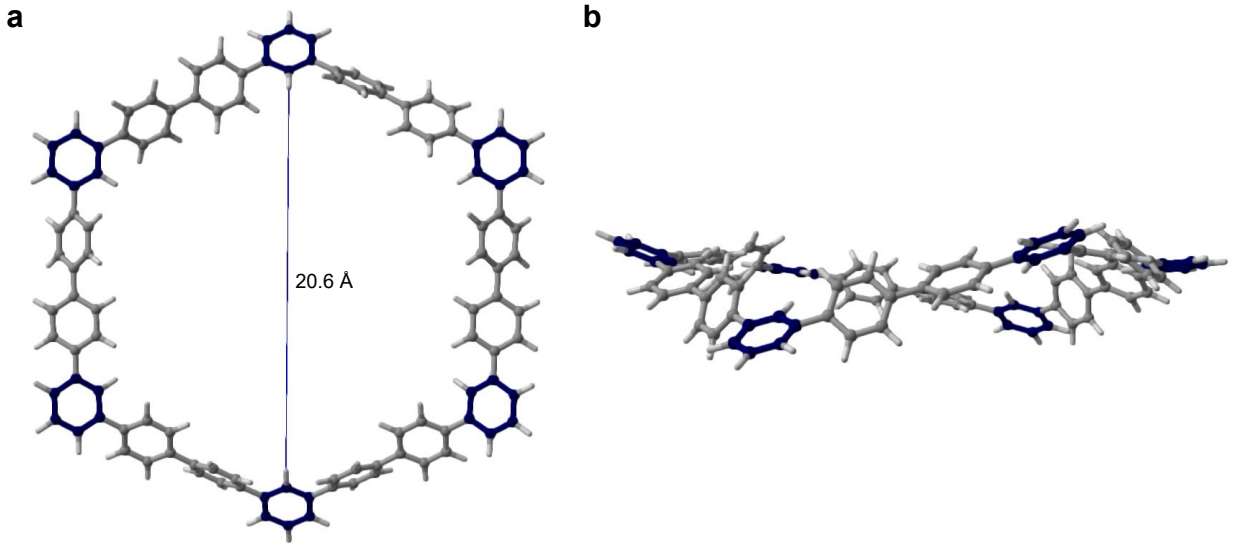

Figure S157. Predicted ideal, non-interpenetrated structural model of a single **DABP-CMP** pore (a) down the pore dimension and (b) parallel to the pore dimension. The navy colored atoms denote carbons originating from the acetyl groups in the starting monomer.

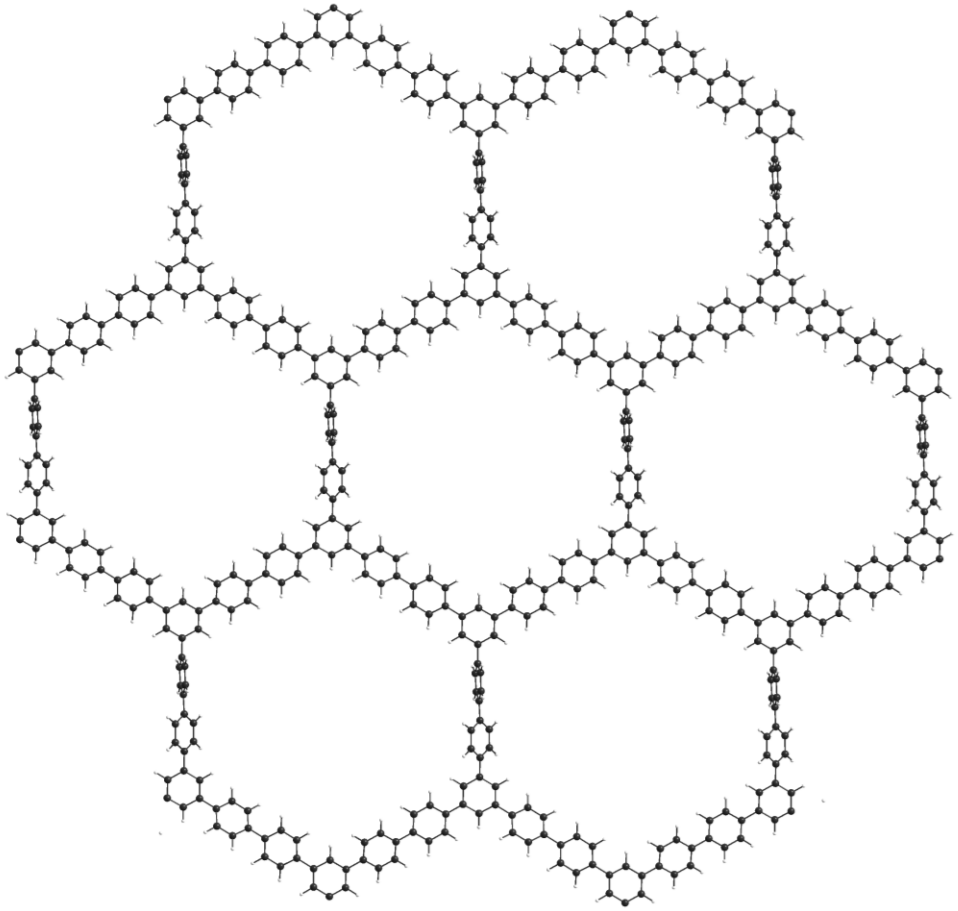

Figure S158. Predicted ideal, non-interpenetrated structural model of **DABP-CMP**, which has a calculated pore diameter of 20.2 Å.

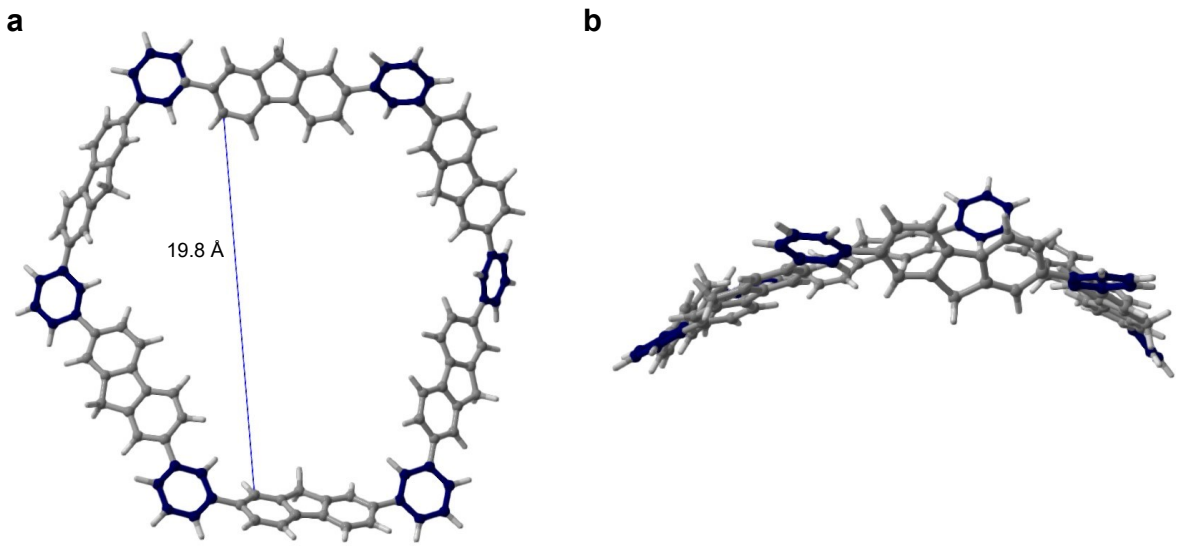

Figure S159. Predicted ideal, non-interpenetrated structural model of a single **DAF-CMP** pore (a) down the pore dimension and (b) parallel to the pore dimension. The navy colored atoms denote carbons originating from the acetyl groups in the starting monomer.

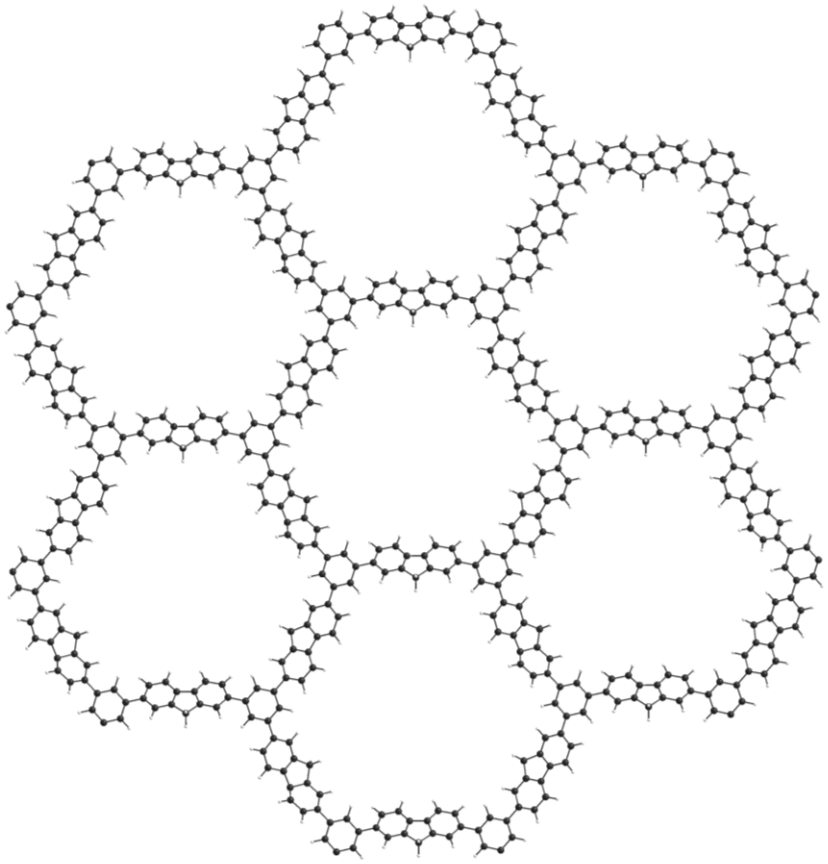

Figure S160. Predicted ideal, non-interpenetrated structural model of **DAF-CMP**, which has a calculated pore diameter of 18.8 Å.

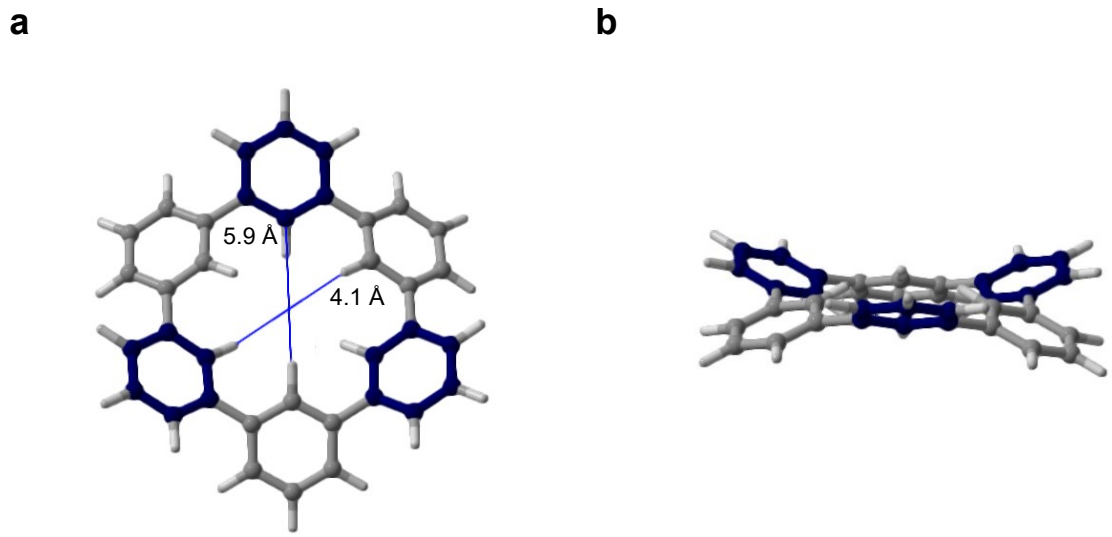

Figure S161. Predicted ideal, non-interpenetrated structural model of a single **TAB-CMP** pore (a) down the pore dimension and (b) parallel to the pore dimension. The navy colored atoms denote carbons originating from the acetyl groups in the starting monomer.

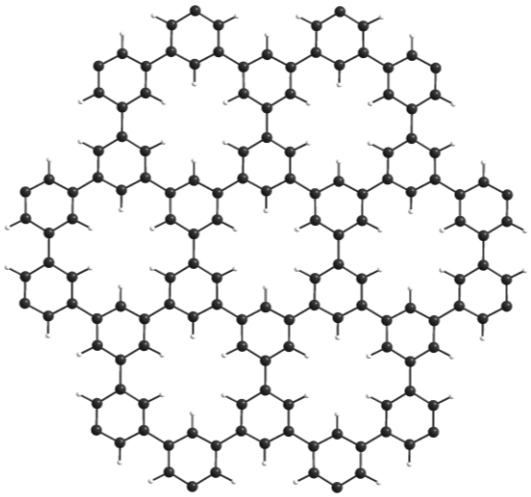

Figure S162. Predicted ideal, non-interpenetrated structural model of **TAB-CMP**, which has a calculated pore diameter of 5.9 Å.

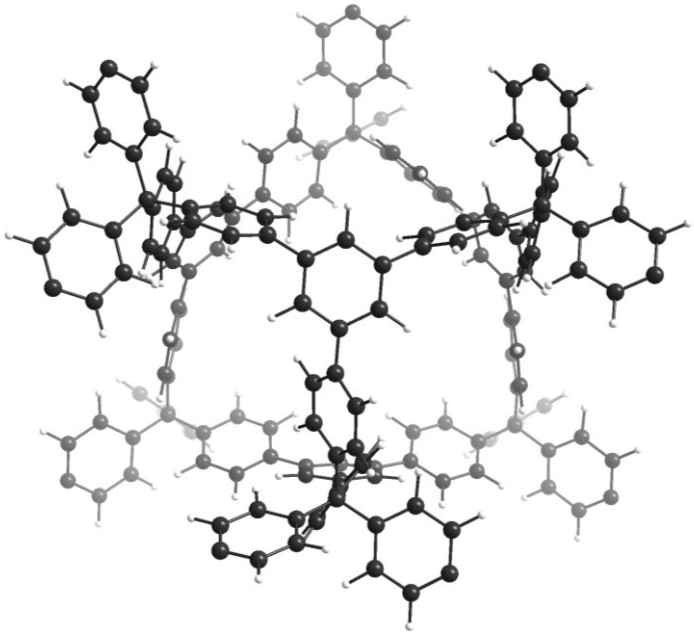

Figure S163. Predicted ideal, non-interpenetrated structural model of **TAPM-PAF**.

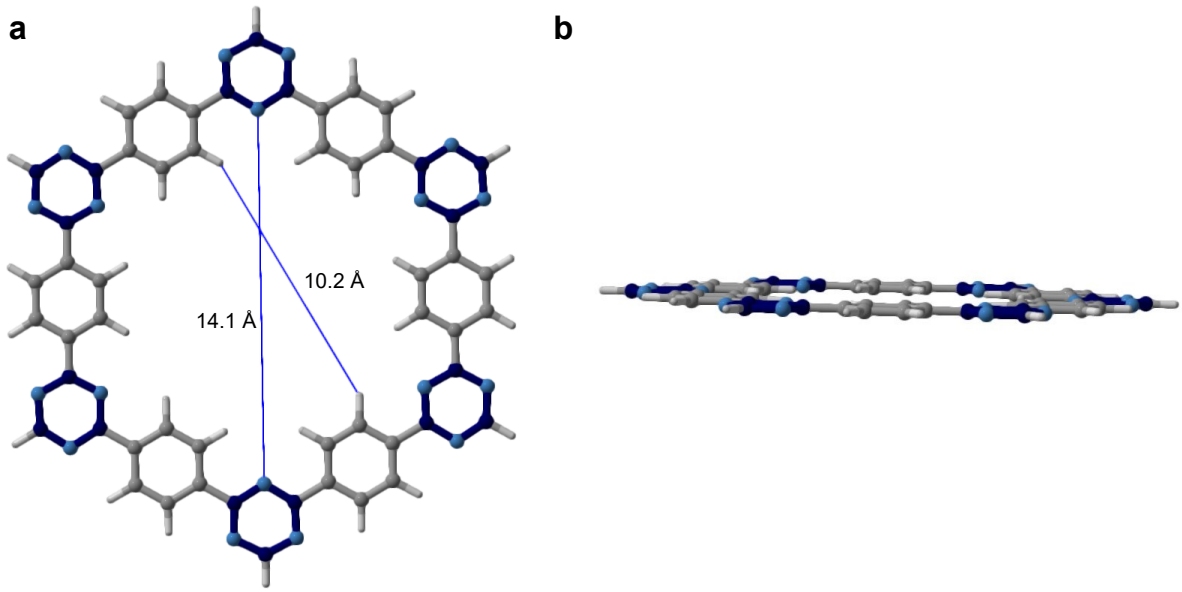

Figure S164. Predicted ideal, non-interpenetrated structural model of a single **DCNB-CTF** pore (a) down the pore dimension and (b) parallel to the pore dimension. The navy colored atoms denote carbon, and the aqua colored atoms denote nitrogen from the nitrile groups.

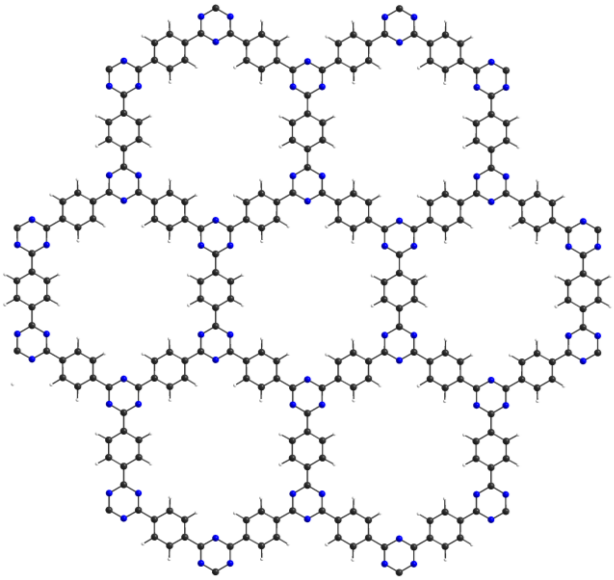

Figure S165. Predicted ideal, non-interpenetrated structural model of **DCNB-CTF**, which has a calculated pore diameter of 10.5 Å.

8. References.

1 J.-D. Chai and M. Head-Gordon, *J. Chem. Phys.*, 2008, **128**, 084106.

2 M. J. Frisch, G. W. Trucks, H. B. Schlegel, G. E. Scuseria, M. A. Robb, J. R. Cheeseman, G. Scalmani, V. Barone, G. a. Petersson, H. Nakatsuji, X. Li, M. Caricato, a. V. Marenich, J. Bloino, B. G. Janesko, R. Gomperts, B. Mennucci, H. P. Hratchian, J. V. Ortiz, a. F. Izmaylov, J. L. Sonnenberg, Williams, F. Ding, F. Lipparini, F. Egidi, J. Goings, B. Peng, A. Petrone, T. Henderson, D. Ranasinghe, V. G. Zakrzewski, J. Gao, N. Rega, G. Zheng, W. Liang, M. Hada, M. Ehara, K. Toyota, R. Fukuda, J. Hasegawa, M. Ishida, T. Nakajima, Y. Honda, O. Kitao, H. Nakai, T. Vreven, K. Throssell, J. a. Montgomery Jr., J. E. Peralta, F. Ogliaro, M. J. Bearpark, J. J. Heyd, E. N. Brothers, K. N. Kudin, V. N. Staroverov, T. a. Keith, R. Kobayashi, J. Normand, K. Raghavachari, a. P. Rendell, J. C. Burant, S. S. Iyengar, J. Tomasi, M. Cossi, J. M. Millam, M. Klene, C. Adamo, R. Cammi, J. W. Ochterski, R. L. Martin, K. Morokuma, O. Farkas, J. B. Foresman and D. J. Fox, Gaussian 16, Revision B.01, 2016.

3 F. Weigend and R. Ahlrichs, *Phys. Chem. Chem. Phys.*, 2005, **7**, 3297.

4 C. Y. Legault, *Université de Sherbrooke*, 2020.

5 O. Plietzsch, C. I. Schilling, M. Tolev, M. Nieger, C. Richert, T. Muller and S. Bräse, *Org. Biomol. Chem.*, 2009, **7**, 4734–4743.

6 T. J. Zimmermann, O. Freundel, R. Gompper and T. J. J. Müller, *Eur. J. Org. Chem.*, 2000, 3305–3312.

7 J. Kim, C. M. Moisanu, C. N. Gannett, A. Halder, J. J. Fuentes-Rivera, S. H. Majer, K. M. Lancaster, A. C. Forse, H. D. Abruña and P. J. Milner, *Chem. Mater.*, 2021, **33**, 8334–8342.

8 P. Kuhn, A. Forget, D. Su, A. A. Thomas, M. Antonietti, A. A. Thomas and D. Su, *J. Am. Chem. Soc.*, 2008, **130**, 13333–13337.

9 E. D. Boyes, *Adv. Mater.*, 1998, **10**, 1277–1280.

10 K. Wang, L.-M. Yang, X. Wang, L. Guo, G. Cheng, C. Zhang, S. Jin, B. Tan and A. Cooper, *Angew. Chem. Int. Ed.*, 2017, **56**, 14149–14153.

11 J. Lefebvre, F. Galli, C. L. Bianchi, G. S. Patience and D. C. Boffito, *Can. J. Chem. Eng.*, 2019, **97**, 2588–2593.

12 V. M. Rangaraj, K. S. K. Reddy and G. N. Karanikolos, *Chem. Eng. J.*, 2022, **429**, 132160.

13 J. Jia, Z. Chen, Y. Belmabkhout, K. Adil, P. M. Bhatt, V. A. Solovyeva, O. Shekhah and M. Eddaoudi, *J. Mater. Chem. A*, 2018, **6**, 15564–15568.

14 V. Cadierno, S. E. García-Garrido and J. Gimeno, *J. Am. Chem. Soc.*, 2006, **128**, 15094–15095.

15 C. Sreenivasulu, D. A. Thadathil, S. Pal and S. Gedu, *Synth. Commun.*, 2020, **50**, 112–122.

16 Ž. Antić, R. M. Krsmanović, M. G. Nikolić, M. Marinović-Cincović, M. Mitrić, S. Polizzi and M. D. Dramićanin, *Mater. Chem. Phys.*, 2012, **135**, 1064–1069.

17 H. Ijadpanah-Saravi, S. Dehestaniathar, A. Khodadadi-Darban, M. Zolfaghari and S. Saeedzadeh, *Desalin. Water Treat.*, 2016, **57**, 20503–20510.